



UNIVERSIDADE FEDERAL DE OURO PRETO  
ESCOLA DE MINAS  
DEPARTAMENTO DE ENGENHARIA CIVIL  
PROGRAMA DE PÓS-GRADUAÇÃO EM ENGENHARIA CIVIL



**STUDIES ON THE USE POTENTIAL OF IRON ORE TAILINGS AS ALTERNATIVE  
RAW MATERIAL IN MANUFACTURE OF CERAMIC AND HYDRAULIC TILES**

Wanna Carvalho Fontes

Ouro Preto

2018

UNIVERSIDADE FEDERAL DE OURO PRETO ESCOLA DE MINAS  
DEPARTAMENTO DE ENGENHARIA CIVIL  
PROGRAMA DE PÓS-GRADUAÇÃO EM ENGENHARIA CIVIL

**STUDIES ON THE USE POTENTIAL OF IRON ORE TAILINGS AS ALTERNATIVE  
RAW MATERIAL IN MANUFACTURE OF CERAMIC AND HYDRAULIC TILES**

*ESTUDO SOBRE O POTENCIAL DE USO DE REJEITOS DE MINÉRIO DE FERRO COMO  
MATÉRIA-PRIMA ALTERNATIVA NA PRODUÇÃO DE REVESTIMENTOS CERÂMICOS E HIDRÁULICOS*

Wanna Carvalho Fontes

**Advisor:** Prof. Dr. Ricardo André Fiorotti Peixoto

Thesis carried out under the supervision  
of the Federal University of Ouro Preto (UFOP)  
and presented as a requirement for obtaining the  
degree of Doctor of Philosophy in Engineering  
Sciences, area of concentration: Structures and  
Construction.

Ouro Preto

July, 2018.

F683e Fontes, Wanna Carvalho.

Studies on the use potential of iron ore tailings as alternative raw material in manufacture of ceramic and hydraulic tiles [manuscrito] / Wanna Carvalho Fontes. - 2018.

117f.: il.: color; grafs; tabs; mapas.

Orientador: Prof. Dr. Ricardo André Fiorotti Peixoto.

Tese (Doutorado) - Universidade Federal de Ouro Preto. Escola de Minas. Departamento de Engenharia Civil. Programa de Pós-Graduação em Engenharia Civil.

Área de Concentração: Estruturas e Construção.

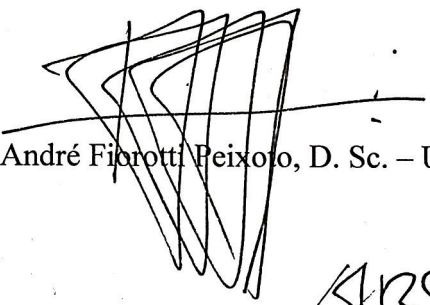
1. Sustentabilidade. 2. Rejeito de mineração. 3. Tecnologia de materiais. 4. Revestimento cerâmico. 5. Revestimento hidráulico. I. Peixoto, Ricardo André Fiorotti. II. Universidade Federal de Ouro Preto. III. Título.


CDU: 624.014

**ESTUDO SOBRE O POTENCIAL DE USO DE REJEITOS DE  
MINÉRIO DE FERRO COMO MATÉRIA-PRIMA ALTERNATIVA  
NA PRODUÇÃO DE REVESTIMENTOS CERÂMICOS E  
HIDRÁULICOS**

**AUTORA: WANNA CARVALHO FONTES**

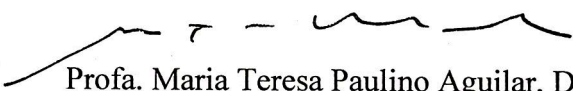
Esta tese foi apresentada em sessão pública e aprovada em 05 de julho de 2018, pela Banca Examinadora composta pelos seguintes membros:

  
Prof. Ricardo André Fiorotti Peixoto, D. Sc. – UFOP (Presidente)

  
Prof. Guilherme Jorge Brigolini Silva, D. Sc. – UFOP

  
Profa. Cláudia Maria Arcipreste, D. Sc. – UFOP

  
Prof. White José dos Santos, D. Sc. – UFMG

  
Profa. Maria Teresa Paulino Aguilar, D. Sc. – UFMG

This doctoral thesis was developed in cooperation between the Federal University of Ouro Preto (UFOP) of Brazil, in the Civil Construction Materials Laboratory (lmc<sup>2</sup>) of the Department of Civil Engineering (DECIV), by the Graduate Program in Civil Engineering (PROPEC) under the adviso of Prof. Dr. Ricardo André Fiorotti Peixoto, and the University of Aveiro (UA) of Portugal, at the Laboratory of Hybrid, Vitreous and Ceramic Materials of the Department of Materials and Ceramics Engineering (DEMaC), under the adviso of Profa. Dr. Ana Maria Bastos Costa Segadães, with funding from the Foundation for Research Support of the State of Minas Gerais (FAPEMIG).

I dedicate this work to everyone, without exception.

## ACKNOWLEDGEMENTS

Firstly, I would like my gratitude to God, for providing the strength and perseverance.

I would like to express my sincere gratitude to my advisor Prof. Dr. Ricardo Fiorotti for the continuous support of my Ph.D study and related research, for his patience, motivation, and immense knowledge. His guidance helped me in all the time of research of this thesis.

Besides my advisor, I would like to thank the rest of my thesis committee: Prof. Dr. White José dos Santos, Profa. Dra. Maria Teresa Paulino, Prof. Dr. Guilherme Brigolini, Profa. Dra. Cláudia Arcipreste and Profa. Dra. Regina Álvares, for their insightful comments and encouragement, but also for the hard question which incited me to widen my research from various perspectives.

My sincere thanks also goes to Profa. Dra. Ana Segadães who provided me an opportunity to join their team as intern, and who gave access to the laboratory and research facilities in UA. Without their precious support it would not be possible to conduct this research.

I thank the UFOP, PROPP and PROPEC for the opportunity to carry out this work and training.

I thank my fellow labmates lmc<sup>2</sup> in for the stimulating discussions, for the sleepless nights we were working together before deadlines, and for all the fun we have had in the last four years. Also I thank my friends in the following laboratories of the School of Mines - UFOP (Nanolab, Laboratory of Bio & Hydrometallurgy, Central of Chemical Analysis) and CICECO laboratories - UA.

I thank the FAPEMIG for the financial support and for granting me the BDSS scholarship.

I would like to thank the agencies that support research in Brazil (CAPES, CNPq and FAPEMIG).

Last but not the least, In a very special way to my husband for the unconditional, silent and loving support. I would like to thank my family: my parents and to my sister for supporting me spiritually throughout writing this thesis and my life in general.



*"Se em ti estiver apenas o cientista, não sentirás as penas do mundo.*

*Explicá-las-á, apenas".*

José Virgílio Gonçalves

# ABSTRACT

---

Iron ore mining is a very important economic activity to Brazil. The increase in tailings generation, as well as its inadequate waste disposal, has awakened concerns over the sustainability of its processes, mainly due to the environmental impacts and socioeconomic risks associated with tailing dams. On the other hand, the reuse of the tailings in building materials can contribute to the sustainable consumption of resources, mitigation of the negative environmental impacts, new market opportunities and the aggregation of values to the companies. This study aims assessment of the potential use of iron ore tailings as an alternative raw material in the production of ceramics and cement tiles. The materials were collected from four tailings-dams and an part was subjected to a dry separation procedure. Besides the iron ore, two other powder fractions were produced (“clay” and “sand” fractions). The clay, sand, and residual iron ore concentrate were characterized (particle size and morphology, chemical and mineralogical composition). The residual iron ore concentrate showed fine, crystalline, and dense particles, no toxic, suitable technically for use as addition and aggregate in the production of terracotta cement tiles. The sands showed the greatest uniformity (particle size and shape, mineralogy and chemical composition) which contributed to the compressive strength gains of the cement composites. The clay present adequate plasticity and dry strength, and develop mullite and glass upon firing. Despite the greatest firing shrinkage (between 22.59 and 26.51%), the resulting tiles show a appealing dark brown luster and are very compact (vitrified products, classified in groups BIa, BIb or BIIa), with high mechanical strength.

**Keywords:** Iron Ore Tailings, materials technology, ceramic tiles, cement tiles

## RESUMO

---

A mineração de ferro é uma atividade de suma importância econômica para o Brasil. O aumento da geração de rejeitos, bem como seu descarte inadequado, tem despertado reflexões acerca da sustentabilidade de seus processos, em virtude, principalmente, dos impactos ambientais e os riscos socioeconômicos associados às barragens de rejeitos. Por outro lado, o reaproveitamento desses rejeitos em elementos construtivos pode contribuir para o consumo sustentável de recursos, mitigação dos impactos ambientais negativos, novas oportunidades de mercado e agregação de valores aos empreendimentos. Assim, o presente estudo avaliou o potencial de uso dos rejeitos de minério de ferro como matéria-prima alternativa na produção de revestimentos, cerâmicos e hidráulicos. Os materiais foram coletados de quatro barragens de rejeitos e uma parte submetida a um procedimento de segregação a seco. Além do minério de ferro recuperado, foram produzidas duas outras frações em pó (frações "argila" e "areia"). A argila, a areia e o rejeito bruto foram caracterizados (tamanho de partículas e morfologia, composição química e mineralógica). O rejeito bruto apresentou partículas cristalinas e densas, sem toxicidade, adequadas tecnicamente para uso como adição e agregado na produção de revestimentos hidráulicos com tons terracota. As areias apresentaram maior uniformidade (tamanho e forma de partícula, composição química e mineralógica), o que contribuiu para ganhos de resistência à compressão dos compósitos de cimento. As argilas apresentam plasticidade e rigidez adequadas as placas verdes, e desenvolvem mulita e vidro ao queimar. Apesar da elevada retração (entre 22.59 and 26.51%), as cerâmicas resultantes mostram um brilho castanho escuro atraente e são muito compactas (produtos vitrificados, classificados em grupos BIa, BIb ou BIIa) e com alta resistência mecânica.

**Palavras-chave:** Rejeitos da mineração de ferro, tecnologia de materiais, revestimento cerâmico, revestimento hidráulico.

# **LIST OF ABBREVIATIONS**

---

Iron Ore Tailings - IOT

Ceramic Tile - CT

Hydraulic Tile - HT

Color Hydraulic Tile - CHT

Thermogravimetric Analysis - TGA

Portland Cement - PC

X-Ray Diffraction - XRD

Scanning Electron Microscopy - SEM

Sustainable Cement Tile - SCT

Use Value -  $V_u$

Esteem Value -  $V_e$

Cost Value -  $V_c$

Exchange Value -  $V_x$

# LIST OF FIGURES

---

## Chapter 1

Figure 1.1. Experimental design .....	7
---------------------------------------	---

## Chapter 2

Figure 2.1. Sampling points in the iron ore tailings-dams D1, D2 and D3 in the Complexo Itabirito (Google Maps, 2017a), and in the Vargem Grande dam (D4) (Google Maps, 2017b).....	15
Figure 2.2. Particle size distribution of the powder samples: (A) raw IOTs; (B) clay fractions; and (C) sand fractions.....	19
Figure 2.3. Photomicrographs (SEM) of the IOT powder samples (R denotes raw samples, C denotes clay fractions and S denotes sand fractions).....	20
Figure 2.4. Mineralogical composition of the IOT samples (crystalline phases as determined by XRD; R denotes raw samples, C denotes clay fractions and S denotes sand fractions).....	21
Figure 2.5. Phase equilibrium diagram of the ternary system $Al_2O_3-SiO_2-FeO.Fe_2O_3$ (Levin et al., 1974), showing the position of the various samples.....	24
Figure 2.6. Macroscopic appearance of fired CT-3 tiles, showing the typical dark brown lustre.....	27
Figure 2.7. Photomicrographs (SEM) of the fired samples (fracture surface).....	27
Figure 2.8. Mineralogical composition (crystalline phases as determined by XRD) of the fired clay samples	28
Figure 2.9. Water absorption, linear firing shrinkage and flexural strength (modulus of rupture) of fired samples.....	29
Figure 2.10. Density (true, apparent and bulk) of fired samples.....	29
Figure 2.11. Porosity (total, open and closed) of fired samples.....	30

## Chapter 3

Figure 3.1. Localization of the iron ore tailing dams in Brazil.....	43
Figure 3.2. Schematic of the resistance to deep abrasion test apparatus and geometric parameters.....	48
Figure 3.3. Thermogravimetry (TGA) of the raw IOT and IOT clay, highlighting (1) reduction of goethite into haematite and (2) de-hydroxylation of kaolinite.....	52
Figure 3.4. Mineralogical composition of the samples (crystalline phases as determined by XRD).....	52
Figure 3.5. Particle size distributions of the powder samples: (A) River sand and non-heat-treated IOT-based materials; (B) Reference and IOT pigments.....	53
Figure 3.6. Photomicrographs (SEM) of the reference river sand and raw IOT, IOT sand and IOT clay.....	55
Figure 3.7. Photomicrographs (SEM) of the reference and proposed IOT-based pigments.....	55
Figure 3.8. Physical characteristics of the hydraulic tiles samples.....	57
Figure 3.9. Dimensional variation of the hydraulic tiles samples, comprising measurements and comparisons under different conditions (oven-dried and water saturated).....	57
Figure 3.10. Micrographs (SEM) of the tiles CHT-1050R and HT-1050C.....	58
Figure 3.11. Flexural tensile strength of the hydraulic tiles samples.....	59
Figure 3.12. Resistance to deep abrasion of the hydraulic tiles samples.....	60

Fig 3.13. Standard deviations of the RGB colour histograms obtained from the crude IOT materials (Raw IOT and IOT clay) and studied pigments (Reference pigment, 1050R, 1150R, 1050C and 1150C).....	61
Figure 3.14. Standard deviations of the RGB histograms of the colours of the tiles produced without pigment (HT-REF, HT-R and HT-S) and tiles produced with pigments (CHT-REF, CHT-1050R, CHT-1150R, CHT-S-1150R, CHT-1050C, CHT-1150C and CHT-S-1150C).....	62
<b>Chapter 4</b>	
Fig. 4.1. Hierarchy of user’s needs for products .....	73
Fig. 4.2 Sample of the colour layer with IOT as aggregate, for pigment evaluation.....	80
Fig. 4.3 Particle Size Distribution of the Materials.....	83
Fig. 4.4. SEM of CP particles.....	84
Fig. 4.5. SEM of P-IOT particles .....	84
Fig. 4.6. SEM of IOT particles.....	85
Fig. 4.7. SEM of CWM particles.....	85
Fig. 4.8. SEM of River Sand particles.....	85
Fig. 4.9. DRX diffractogram of IOT.....	86
Fig. 4.10. Colour layer mixtures: T1, T2 and T3 comprise 0%, 25% and 50% of IOT as aggregate; in T4 and T5 use CP as pigment, T6 and T7, IOT and T8 and T9, P-IOT; finally, T10 and T11 present double colours with CP and P-IOT respectively.....	88
Fig. 4.11. Surface of mixtures T5 (left) and T7 (right), magnification 10x.....	89
Fig. 4.12. Empathy Map of a persona of a SCT consumer: end user.....	90
Fig. 4.13. Empathy Map of a persona of a SCT consumer: interior designer.....	90
Fig. 4.14. Surface design of the prototypes of the SCT, based on the value analysis and colour palette.....	91

# LIST OF EQUATIONS

---

## Chapter 3

Equation 3.1.....	48
Equation 3.2.....	48
Equation 3.3.....	48
Equation 3.4.....	48
Equation 3.5.....	48
Equation 3.6.....	48
Equation 3.7.....	49

## Chapter 4

Equation 4.1.....	72
Equation 4.2.....	72
Equation 4.3.....	72
Equation 4.4.....	81

# LIST OF TABLES

---

## Chapter 2

Table 2.1. Characteristics of the tailings-dams considered in this study (heightening method: upstream raised embankment).....	15
Table 2.2. Physical characteristics of the IOT samples (R denotes raw samples, C denotes clay fractions and S denotes sand fractions).....	18
Table 2.3. Chemical composition of the IOT samples (as obtained by XRF, expressed as wt.% oxides; R denotes raw samples, C denotes clay fractions and S denotes sand fractions).....	22
Table 2.4. Relative proportions of phases in equilibrium at first-melting, as calculated by the lever rule from the diagram in Figure 5.....	25

## Chapter 3

Table 3.1. Identification of the pigments produced in this study, including the material used, firing and grinding conditions.....	44
Table 3.2. Technological properties of the Portland cement used in this study.....	45
Table 3.3. Identification of the HTs produced, materials used and proportioning.....	46
Table 3.4. Physical characteristics of the samples (R denotes raw samples fired and C denotes clay fractions fired).....	50
Table 3.5. Chemical composition of the samples (XRF, expressed as wt.% oxides).....	51
Table 3.6. w/b ratios as a result of the fluidity test performed in the proposed mixtures.....	56
Table 3.7. $L^*a^*b^*$ and $\Delta E$ parameters of the IOT-based materials and produced tiles.....	63

## Chapter 4

Table 4.1. Mixtures developed for the colour layer.....	80
Table 4.2. Questions for developing the empathy map (Osterwalder & Pigneur (Business Model Generation, 2013)).....	82
Table 4.3. Characteristic dimensions of the materials.....	83
Table 4.4. Physical Characterization of the materials.....	85
Table 4.5. Chemical characterisation of the Materials.....	86
Table 4.6. Dissolution results for the raw IOT that exceeded the standard requirements.....	87



# SUMMARY

---

Abstract .....	IX
Resumo .....	X
List of figures .....	XII
List of equations .....	XIV
List of tables .....	XV

## Chapter 1

1. Introduction .....	4
1.1 . Introduction, Motivation and Originality .....	4
1.2 . Objectives and Contribution to Society .....	6
1.3 . Experimental Design .....	7
1.4 . Structure of this Thesis .....	8

## Chapter 2

2. Assessment of the use potential of iron ore tailings in the manufacture of ceramic tiles: from tailings-dams to “brown porcelain” .....	10
2.1. Introduction.....	11
2.2. Experimental .....	14
2.3. Results and discussion .....	18
2.3.1. Characterization of the powder samples .....	18
2.3.2. Characterization of the fired samples .....	23
2.4. Conclusions.....	31
2.5. Acknowledgements .....	32
2.6. References.....	33
Annex A. Archimedes’ water displacement method used on a ceramic porous body.....	37
Annex B. Mineralogical composition of the IOT samples (A, B and C); and mineralogical composition of the fired samples (D) (XRD; the actual X-ray diffraction patterns).....	38

## Chapter 3

3. Assessment of the use potential of use of iron ore tailings as fine aggregates and pigments in the manufacture of hydraulic tiles .....	40
3.1. Introduction.....	41
3.2. Materials and Methods .....	43
3.3. Results and Discussion.....	50
3.3.1. Characterisation of aggregates and pigments.....	50
3.4. Conclusion .....	64

3.5. Acknowledgments .....	64
3.6. References .....	65

#### **Chapter 4**

4. Iron ore tailings in the production of cement tiles: a value analysis on building sustainability .....	68
4.1. Introduction.....	69
4.1.1. Cement Tiles .....	70
4.1.3. Emotional/Esteem Value .....	73
4.1.4. Social Value .....	75
4.1.5. Environmental Value .....	75
4.2. Methodology .....	76
4.2.1. Technical Feasibility.....	76
4.2.2. Environmental Feasibility .....	78
4.2.3. Feasibility as Pigment .....	79
4.2.4. Value Analysis.....	81
4.2.4.1. Empathy Map .....	81
4.2.4.2. Surface Design .....	82
4.3. Results and discussion .....	83
4.3.1. Technical Feasibility.....	83
4.3.2. Environmental Feasibility .....	87
4.3.4. Feasibility as Pigment .....	87
4.3.4. Value Analysis.....	89
4.3.4.1. Empathy Map .....	89
4.3.4.2. Environmental, Social and Esteem Assessments.....	91
4.4. Conclusion .....	92
4.5. Acknowledgments .....	93
4.6. References .....	94

#### **Chapter 5**

5. Final considerations.....	99
5.1. Conclusions.....	99
5.2. recommendations for future research .....	101

# Chapter 1

---

## Introduction

Introduction, Motivation and Originality; Objectives and Contribution to Society;  
Experimental Design and Structure of this Thesis.

## **1. INTRODUCTION**

### **1.1 . INTRODUCTION, MOTIVATION AND ORIGINALITY**

This work comprises a study on the potential use of iron ore tailings (IOT) as an alternative raw material for the production of ceramic and hydraulic tiles, developed by exploratory and experimental methods with qualitative and quantitative approaches, respectively. This work intends to expand the knowledge on the possibilities of using IOT and to mitigate the negative impact of tailings dams without sacrificing the opportunities provided by the mining activity.

Iron ore mining is of great importance to the Brazilian economy, but the large amounts of tailings generated demand large volumes of reservoirs, related to environmental damage and risk to human lives in case of collapse. On the other hand, Brazil is currently one of the world leaders in the production and consumption of covering tiles, and this industrial sector also faces challenges in the search for more eco-friendly products. In this way, the use of IOT as raw material represent advantages for the tile covering industry compared to conventional natural resources, including reduction of the volume of material extracted from nature, reduction of costs, less pollutant emissions, maintenance of a healthy environment, and meeting of the expectations of a society more concerned with the environmental issue. In addition, new products and bussines can represent competitive advantages.

The use of raw IOT in constructive elements has already been studied by other researchers motivated by the environmental issue. The collapse of the Fundão dam in Mariana, MG, Brazil, highlighted the problem of safe disposal of industrial waste (G1, 2015). After this, the Brazilian Federal Public Prosecutor's Office, by the recommendation Ner.014/2016-MPF-GAB/FT, has motivated researchers to investigate the environmental damages and

propose safer disposal methods and prevention of future incidents. Previous studies have shown that the raw IOT, in low concentrations and in association with other conventional materials used in the manufacture of cement and ceramic elements, improves the mechanical performance and the durability of constructive elements (Chen et al.,2013; Das et al., 2012, Uchechukwu and Ezekiel,2014; Yellishetty et al., 2008). On the other hand, in high concentration can impair the performance due to the heterogeneity of its physico-chemical characteristics (Chen et al.,2013; Liu et al.,2012; Zhao et al., 2014). However, the beneficiation process of raw IOT may contribute to obtaining materials with homogeneous and adequate characteristics, allowing better reuse and higher consumption of IOTs in the production chain (Andrade, 2014).

Different from aforementioned works, this research comprises the use of raw IOT and segregated IOTs (i.e., materials obtained by a dry-route method), in the manufacture of covering tiles. Iron ore concentrate is obtained in this process and has well defined economic value. Other materials composed mainly by clayey and siliceous compounds are of interest to the construction industry and their productive and economic destinations are investigated. For this end, the process requirements were evaluated and adjusted in order to homogenize the physicochemical properties. From the separation of the residual iron ore concentrate, two other fractions with uniform particle sizes were separated. The coarser is called here “sand” for simplicity and is intended for use as fine aggregate in the production of cement tiles. The thinner is referred to here as “clay” and can be used in the production of ceramic tiles presenting plasticity and dry strength during processing and development of mullite and vitreous phase during firing. Therefore, a work that proposes the incorporation of large amounts of waste, obtained from a recycling and separation process of iron ore tailings, in the production of covering tiles for civil construction, is unprecedented and intends to be a valuable contribution in the current scenario.

## **1.2 . OBJECTIVES AND CONTRIBUTION TO SOCIETY**

The general objective of this work is to evaluate the potential use of iron ore tailings as alternative raw material in the production of ceramic and cement tiles.

The specific objectives of this research are summarized as follows:

- Obtain and evaluate the physical, chemical and mineralogical properties of the IOT (raw IOT, IOT clay fraction and IOT sand fraction), according to properties of interest for basic technological materials for the production of covering elements - *Imc<sup>2</sup>/DECIV/EM/UFOP e DEMaC/UA*;
- Evaluate compositions and mixture proportions for ceramic tiles and mortars for cement tiles - *Imc<sup>2</sup>/DECIV/EM/UFOP e DEMaC/UA*;
- Evaluate the physical and mechanical properties of the elements produced with iron ore tailings in comparison with the normative requirements - *Imc<sup>2</sup>/DECIV/EM/UFOP e DEMaC/UA*; and
- Contribute to the assignment of intangible values to the covering tiles through the use of IOT and provide greater encouragement in the adoption of sustainable production routes.

### 1.3 . EXPERIMENTAL DESIGN

In order to meet the objectives, the experimental design of the work was proposed with a linear structuring, but with cyclical possibilities of adjustments of parameters aiming at the technological improvement of the developed products, as shown in the Figure 1.1.

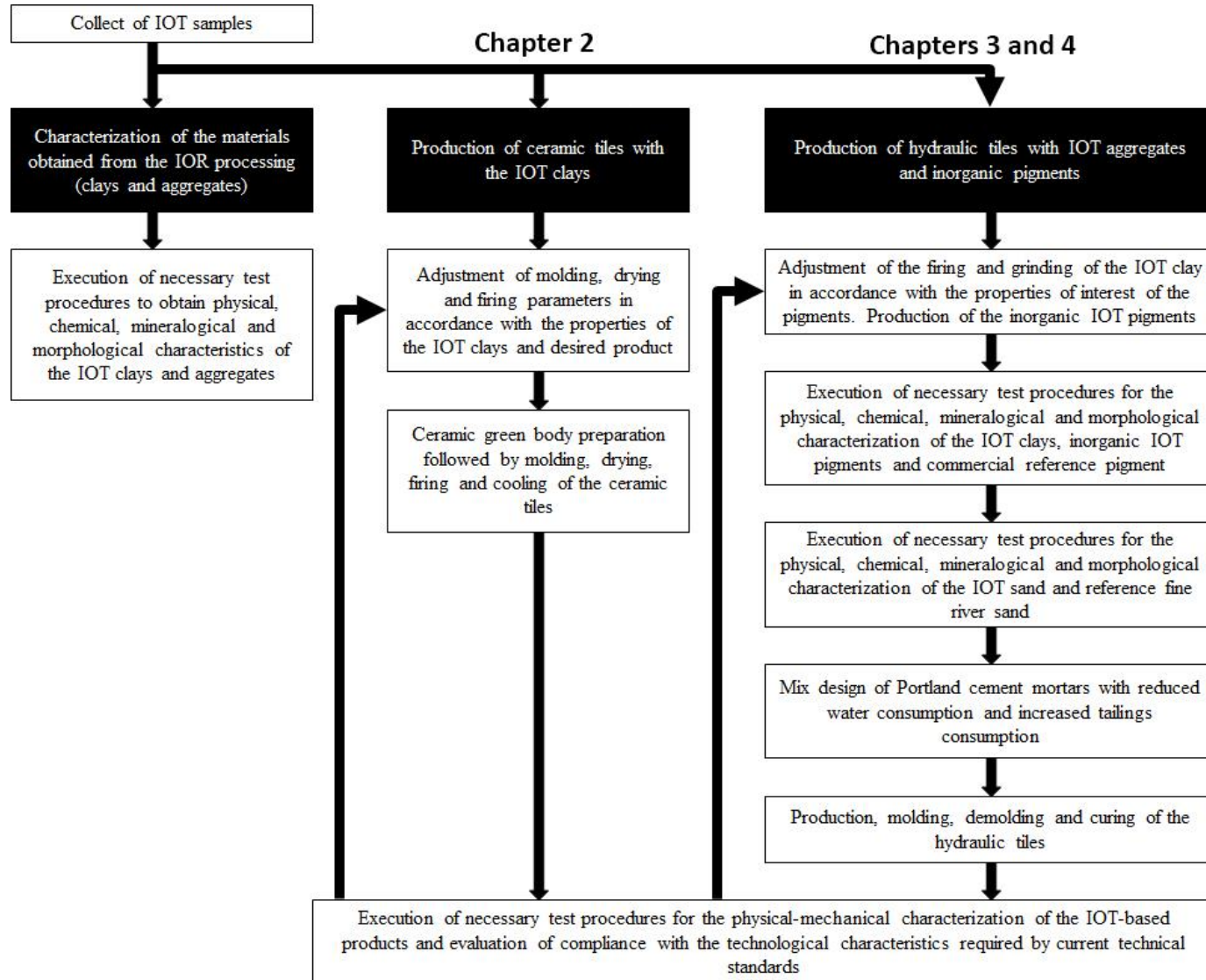


Figure 1.1. Experimental design

#### **1.4 . STRUCTURE OF THIS THESIS**

This work was structured in chapters:

The first chapter covers, in addition to the organization, the general introduction of the problem with the motivation and originality of the work; citing the objectives and the experimental plan.

The chapter 2, 3 and 4 have specific themes structured according to the the experimental design of the work. Each chapter consists of a complete manuscript with formatting in accordance with the norms of the journal chosen for publication, as well as its typical subdivisions (Introduction, Materials and Methods, Results and Discussion, Conclusion, Acknowledgments and Bibliographic References). However, to facilitate reading, the visual formatting of this work did not necessarily follow all the norms of the journals, for example, the figures and tables were included in the text. A consistent standard for citations and bibliographic references has also been established. The annexes are information or data complementary to the results presented in the chapters.

Different from the other chapters, the closing chapter draws together the main findings and establishes the significance of the work. In other words, the Final Considerations chapter presents a summary of the conclusions of the thesis as well as perspectives for future research.



# Chapter 2

---

**Assessment of the use potential of iron ore tailings in the manufacture of ceramic tiles: from tailings-dams to “brown porcelain”**

## **2. ASSESSMENT OF THE USE POTENTIAL OF IRON ORE TAILINGS IN THE MANUFACTURE OF CERAMIC TILES: FROM TAILINGS-DAMS TO “BROWN PORCELAIN”**

### **ABSTRACT**

Nearly half of the total iron ore volume extracted in mining operations is rejected as tailings and disposed of in containment dams that are liable for considerable environmental impact and human hazard in case of breaching. This work aims to expand the usage possibilities of iron ore tailings and help mitigate the negative impact of tailings-dams without sacrificing the opportunities provided by mining. Materials were collected from four tailings-dams, characterized (particle size and morphology, chemical and mineralogical composition) and subjected to a dry separation procedure. Besides the residual iron ore concentrate, two other powder fractions were produced (“clay” and “sand” fractions). The sands showed the greatest uniformity (particle size and shape, mineralogy and chemical composition) and can be used in the production of cement-based composites. The clays present adequate plasticity and dry strength, and develop mullite and glass upon firing, showing a rather amenable processing behaviour suitable for both artisanal and full-fledged industrial production. The resulting tiles are dimensionally homogeneous and very compact (vitrified products, classified in groups BIa, BIb or BIIa), with high mechanical strength. Either industrialised or artisanal, these materials can be used in the production of “brown porcelain” tiles and ware, showing a very appealing dark brown lustre.

**Keywords:** Iron ore tailings, Industrial waste, Recycling, Ceramic tiles.

## 2.1. INTRODUCTION

Iron ore mining is a very important economic activity in Brazil, as it corresponds to 87.7% of the exported primary goods and 4% of the Brazilian national GDP. The Brazilian reserves are mostly located in the States of Minas Gerais (72.5%), Mato Grosso do Sul and Pará, with an average iron content of 49.0%, and represent 11.9% of the world reserves (DNPM, 2016).

During processing, and depending on the concentration and market conditions, a large percentage of the total extracted ore volume is rejected (iron ore tailings) and disposed of as mud in containment dams with percolating water control (Fontes et al., 2016; Li et al., 2009; Yellishetty and Mudd, 2014). There are 672 tailings-dams in Brazil, 340 of which are located in the Minas Gerais State (SNISB, 2018). Tailings-dams reservoirs occupy large areas and originate considerable environmental impacts, from construction to closure. Besides visual impact throughout the entire lifespan, they are responsible for deforestation in the construction phase, surface and underground water pollution during operation and after mine closure, dust generation on the rejects beach, and severe environmental damage and human hazard in case of rupture (Edraki et al., 2014; Fontes et al., 2016; Kossoff et al., 2014). The tailings-dam breach that recently occurred in Bento Rodrigues–MG was considered one of the biggest environmental disasters in Brazil and in the world. Due to high production volumes and inadequate management, more than  $35 \times 10^6$  m<sup>3</sup> of mud were released into the environment. As a result, Bento Rodrigues district was completely devastated, 19 people died, and expressive impacts were inflicted on the ecosystems along 662 km downstream along the banks of the Doce River, affecting two Brazilian States and reaching the Atlantic Ocean (Garcia et al., 2017; IBAMA, 2015).

A considerable increase in the number of “severe” and “very serious” tailings-dams breaches was observed in recent years. Such trend is related to the risks associated with these structures and intensified by the exploitation of lower-grade ore deposits, thus generating an increasing amount of tailings. Currently, about 379,000 tons of iron ore tailings are generated daily (FEAM, 2015; IPEA, 2012), which need to be properly disposed of to prevent future dam failures with impacts on an enlarged scale.

In view of current strategies in the transition for more sustainable means of production (innovative and technological development and effective use of sustainable practices in the productive processes and supply chains), companies can play a crucial role in the integrated management of the territories (Gabaldón-Estevan et al., 2014; IBRAM, 2013). Finding a meaningful potential use for iron ore tailings (IOT) might mitigate part of the negative impact of tailings-dams without sacrificing the opportunities provided by mining, and promote the economic and social welfare of the communities neighboring the dams (Kumar et al., 2006).

It has been shown that IOT can be used as admixture or in substitution of natural aggregates or clay in constructive elements (Fontes et al., 2016; Yellishetty et al., 2008). It so happens that the construction industry is responsible for up to 50% of extracted natural resources and is also held accountable for various environmental impacts, from raw materials extraction process to the use and maintenance of buildings (Bianchini et al., 2005). On the other hand, the sector employs 7.4% of the labor force in Brazil, and 30% of the employment in the mineral processing industry are related to the production of building materials (DNPM, 2016). Together, these two sectors exert great influence in the socioeconomic and environmental dynamics and can be considered catalysts in sustainable development.

IOT is a fine, weighty, stable and crystalline material composed mainly by iron oxide, silica and alumina. When used as aggregate in partial substitution of natural ones in cement-based composites, it promotes mechanical strength (Uchechukwu and Ezekiel, 2014; Yellishetty et al., 2008) but 100% substitution of conventional aggregates can significantly reduce the workability and compressive strength of concrete (Liu et al., 2012; Zhao et al., 2014). Heterogeneity of physical-chemical characteristics, given the diversity of beneficiation processes and mineralogical composition might be the reasons for such behaviour. Additionally, higher iron contents (mostly in haematite form), associated with lower silica, explain the observed increase in density of the cement-based product.

On the other hand, if fired ceramic products are considered, although the chemical characteristics of IOT are generally similar to those of common ceramic raw materials, IOT usage has only been successful in combination with other materials (Chen et al., 2013; Das et al., 2012). The IOT's fluxing character was demonstrated, but so were the adverse implications of over usage. However, a suitable conditioning process might further improve the appealing characteristics of IOT for the production of high quality ceramic tiles (Dias et al., 2017; Kumar et al., 2006). Given the comparatively high processing temperatures, effective inertization of most potentially hazardous contaminants is guaranteed and the use of IOT as alternative ceramic raw material might be both technically and economically attractive.

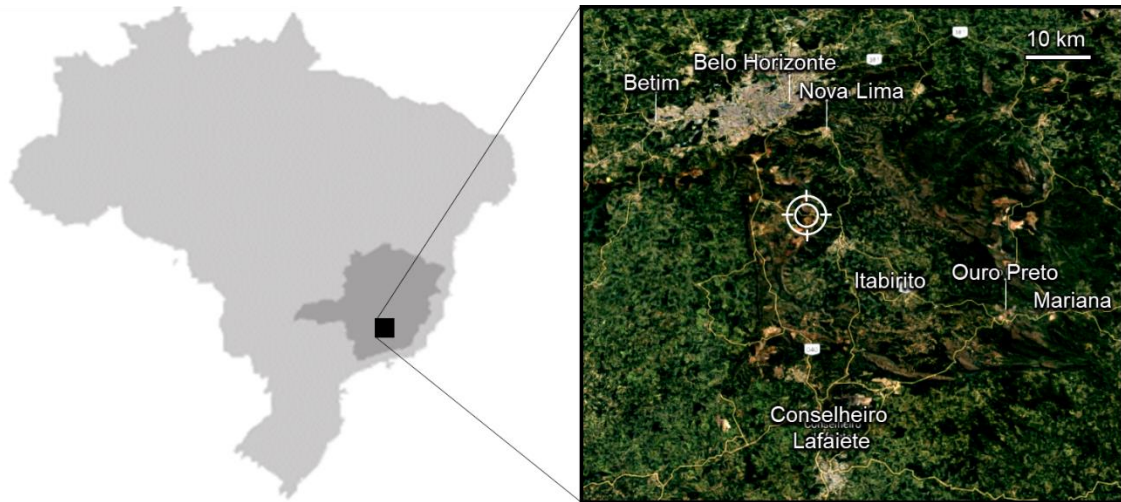
Brazil is the world's third largest producer and consumer of ceramic tiles (ACIMAC, 2017), the current challenges in the sector being continuous improvement of product quality, development of national design, implementation of marketing strategies for greater penetration of Brazilian brands in the international market, and minerals supply

on a sustainable basis (Cabral et al., 2010). The latter involves improvement and control of the quality of raw materials, as well as greater environmental control of mining projects for minimized impacts.

This work explores the usage possibilities of IOT in fired ceramic products. Processing requirements will first be assessed in order to adjust and improve the IOT interesting physicochemical characteristics, and then a possible application will be sought, ranging from artisanal to full fledged industrial production. Such approach should promote the economic and social welfare of the communities neighbouring the dams, as well as the efficient and effective introduction of innovation in the ceramics sector (Gabaldón-Estevan et al., 2014; Meyer-Stamer et al., 2004).

## **2.2. EXPERIMENTAL**

Four Class III high environmental risk IOT dams (COPAM, 2005) were selected, considering the associated potential social and environmental risks, as well as economic relevance based on the dams inventory of the Minas Gerais State (FEAM, 2017). Those were (Figure 2.1): three dams (D1, D2 and D3) from the Complexo Itabirito (Google Maps, 2017a) and the Vargem Grande dam (D4) (Google Maps, 2017b). All are located near important urban areas (Conselheiro Lafaiete, Ouro Preto, Mariana, Itabirito and Belo Horizonte). The D1, D2 and D3 dams are in the hydrographic basin of Velhas River and receive tailings from beneficiation of itabirite. The D4 dam is in the hydrographical basin of the Vargem Grande River and receives haematite tailings. Table 2.1 presents the main characteristics of those dams.



**Figure 2.1. Sampling points in the iron ore tailings-dams D1, D2 and D3 in the Complexo Itabirito (Google Maps, 2017a), and in the Vargem Grande dam (D4) (Google Maps, 2017b)**

**Table 2.1. Characteristics of the tailings-dams considered in this study (heightening method: upstream raised embankment).**

<b>Tailings-dam reference</b>	<b>Height (m)</b>	<b>Area (m<sup>2</sup>)</b>	<b>Reservoir volume (m<sup>3</sup>)</b>
<b>D1, D2</b>	88	863,707	24,000,000
<b>D3</b>	77	880,000	18,200,000
<b>D4</b>	35	667,500	9,500,000

From each IOT sample, a portion was kept as collected (raw IOT) and the rest was separated (dry segregation: drying, milling, gravity segregation and magnetic separation) into three fractions, namely iron ore concentrate and two particle size fractions (fine and coarse), totalling 36 samples. Details on the dry segregation procedure can be found elsewhere (Peixoto et al., 2013). The iron ore concentrates have well defined commercial

value, outside the scope of this work, and were considered no further. As for the remainder 32 fractions, the equivalent fractions from the same dam were mixed and homogenized. Thus, a total of 12 samples were produced, i.e. 4 samples of raw IOT (R-D1, R-D2, R-D3 and R-D4), 4 samples of IOT clays (C-D1, C-D2, C-D3 and C-D4) and 4 samples of IOT sands (S-D1, S-D2, S-D3 and S-D4). These 12 samples were oven dried (105 °C, 24 h) and characterized.

Chemical composition was determined by X-ray fluorescence (XRF, Shimadzu,  $\mu$ EDX 1300). Mineralogical characterization was carried out by X-ray diffraction (DRX, Shimadzu 7000), using the  $\text{CuK}\alpha$  radiation ( $\lambda = 1.54060 \text{ \AA}$ ) at 40 kV and 30 mA. The identification of mineral phases was carried out using the X Powder 12 software and the ICDD PDF2+ database (International Centre for Diffraction Data). Phase quantification was carried out by Rietveld refinement with Fullprof software. Fluorite was used as internal standard. For these analyses, the samples were milled in a high efficiency planetary ball mill (Retsch PM 100, 5 min, 300 rpm), using Y-ZrO<sub>2</sub> 250 cm<sup>3</sup> jar and balls (80 cm<sup>3</sup>).

The physical characterization included the determination of particle size distribution (by laser diffraction, Bettersize 2000), apparent density, bulk density and moisture content, as specified by the Brazilian standards NBR NM 52 (ABNT, 2009), NBR NM 45 (ABNT, 2006) and NBR 9939 (ABNT, 2011).

Particle morphology was observed by scanning electron microscopy (SEM, HITACHI S-410) after carbon coating.

For the manufacture of ceramic test-pieces, the appropriate amount of powder was weighted and hand-mixed with 10 wt.% water for 15 minutes, after which the mixture was kept in a sealed plastic bag for 24 h to ensure moisture uniformity. From each



mixture, seven  $50 \times 50 \times 5$  mm<sup>3</sup> plates were uniaxially pressed at ~10 MPa (100 kgf/cm<sup>2</sup>) in a steel die using a laboratory hydraulic press. The plates were oven dried (110 °C, 24 h) and fired at 1200 °C for 2 h inside an electric Termolab furnace (10 °C/min heating rate, natural furnace cooling).

After firing, the crystalline phases formed in the samples were identified by XRD and the usual technological properties were evaluated as specified in the relevant Standards, namely linear firing shrinkage (LFS) and three-point-bending mechanical strength (modulus of rupture, MoR, Shimadzu AG-X/E universal testing machine, with a 20 kN load cell). Water absorption (WA, refers to open porosity), apparent solid density (AD, excludes open porosity) and bulk solid density (BD, includes open and closed porosity) were calculated from the dry, saturated and immersed weights of test-pieces fragments using the water displacement Archimedes method, and the solid true density (RD) by Helium gas pycnometry (Quantachrome Multipycnometer). The final results were taken as the average of measurements carried out on at least five different test-piece fragments. From the results obtained for those properties, open porosity ( $OP = WA \times BD$ ), total porosity ( $TP = (1 - BD/RD) \times 100$ ) and closed porosity ( $CP = TP - OP$ ) were calculated. A summary of the description of the various properties as used in the present work and the relationships among them can be found in Annex A.

Based on the results of the technological characterization, the microstructure of some of the produced ceramic tiles was observed by SEM on fracture surfaces after carbon coating.

## 2.3. RESULTS AND DISCUSSION

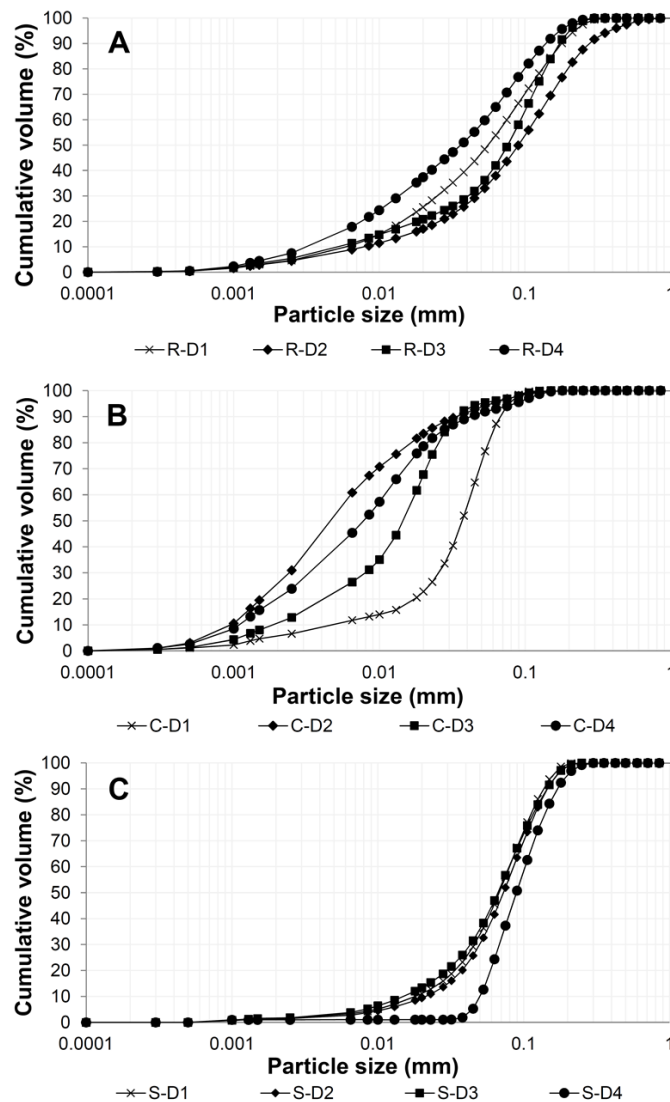
### 2.3.1. CHARACTERIZATION OF THE POWDER SAMPLES

Apart from the iron ore concentrate, the dry segregation procedure essentially results in the separation into powder fractions of uniform particle sizes. As is customary in Civil Engineering or in Sedimentology for granular solids (Verruijt, 2001), the finest particle sizes, below 2  $\mu\text{m}$ , are referred to as clay, whereas sand refers to particle sizes between 63  $\mu\text{m}$  and 2 mm. Silt is the designation for the class with sizes between 2 and 63  $\mu\text{m}$ . In what follows, and for the sake of simplicity, the finer particles will be described as the “clay” fraction, whereas “sand” fraction will refer to the coarser particles. Table 2.2 gathers information about real (true) density, bulk density and moisture content of the materials, as well as their characteristic particle sizes D10, D50 and D90 (DN is the sieve mesh opening through which passes N% of the material). It can be seen that the raw IOTs are denser than any of the corresponding clay and sand fractions, due to the presence of residual iron ore. As expected, moisture contents are higher in the clay fractions, which also show the largest difference between real and bulk densities (worse particle packing). Both findings are attributable to clay minerals crystallography and particle morphology and size.

**Table 2.2. Physical characteristics of the IOT samples (R denotes raw samples, C denotes clay fractions and S denotes sand fractions).**

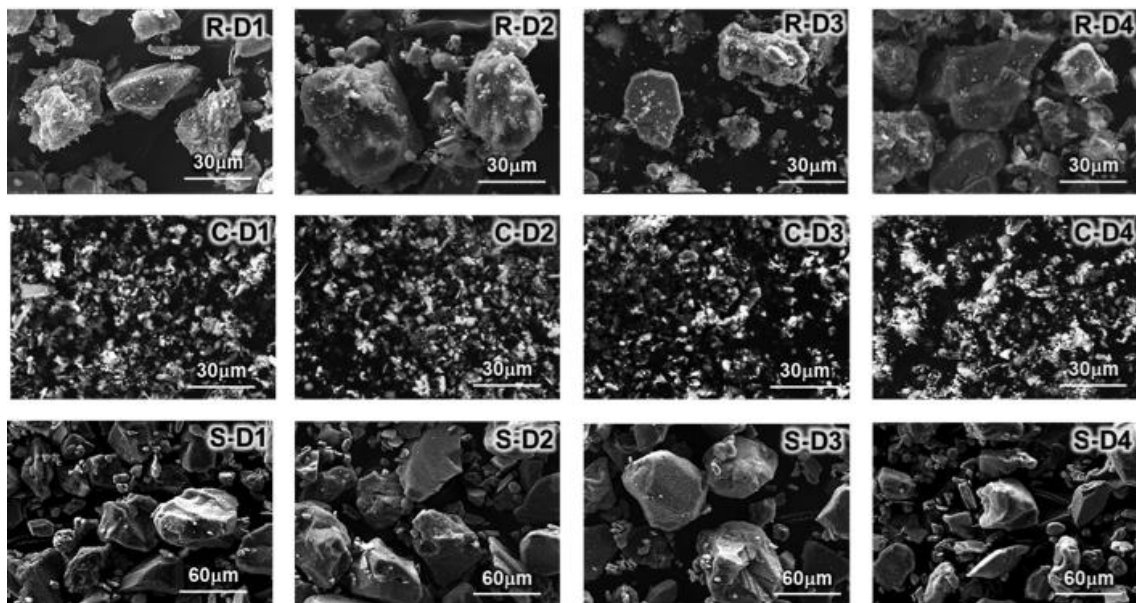
Sample	True density ( $\text{g}/\text{cm}^3$ )	Bulk density ( $\text{g}/\text{cm}^3$ )	Moisture content (%)	D <sub>10</sub> ( $\mu\text{m}$ )	D <sub>50</sub> ( $\mu\text{m}$ )	D <sub>90</sub> ( $\mu\text{m}$ )
R-D1	3.68	1.94	0.20	6	60	180
R-D2	3.61	1.79	0.20	8	90	280
R-D3	3.34	1.42	0.14	5	80	170
R-D4	3.78	1.89	0.22	3	40	140
C-D1	4.52	0.60	1.97	4	40	70
C-D2	3.88	0.51	1.04	1	5	30
C-D3	3.37	0.53	1.74	2	10	30
C-D4	4.48	0.86	1.14	1	8	40
S-D1	2.96	1.57	0.14	20	70	140
S-D2	2.92	1.61	0.16	20	70	140
S-D3	3.03	1.62	0.30	20	70	140
S-D4	2.83	1.55	0.10	50	90	170

Figure 2.2-A shows that the raw IOTs present broad particle size distributions with an average particle size in the range of 40–90  $\mu\text{m}$ , as already seen in Table 2.2. They contain higher amounts of coarser particles (larger than 100  $\mu\text{m}$ ) and present lower contents of particles finer than 5  $\mu\text{m}$ . After the separation process, the resulting fractions show narrower distributions, the clays (Figure 2-B) with an average particle size in the range of 5–40  $\mu\text{m}$ , whereas that of the sands (Figure 2-C) is in the range of 70–90  $\mu\text{m}$ . Thus, after removal of the iron ore, coarser particles are concentrated in the sand fractions (90% of particles smaller than 140–170  $\mu\text{m}$ ) while finer particles are concentrated in the clay fractions (90% of particles smaller than 30–70  $\mu\text{m}$ ).



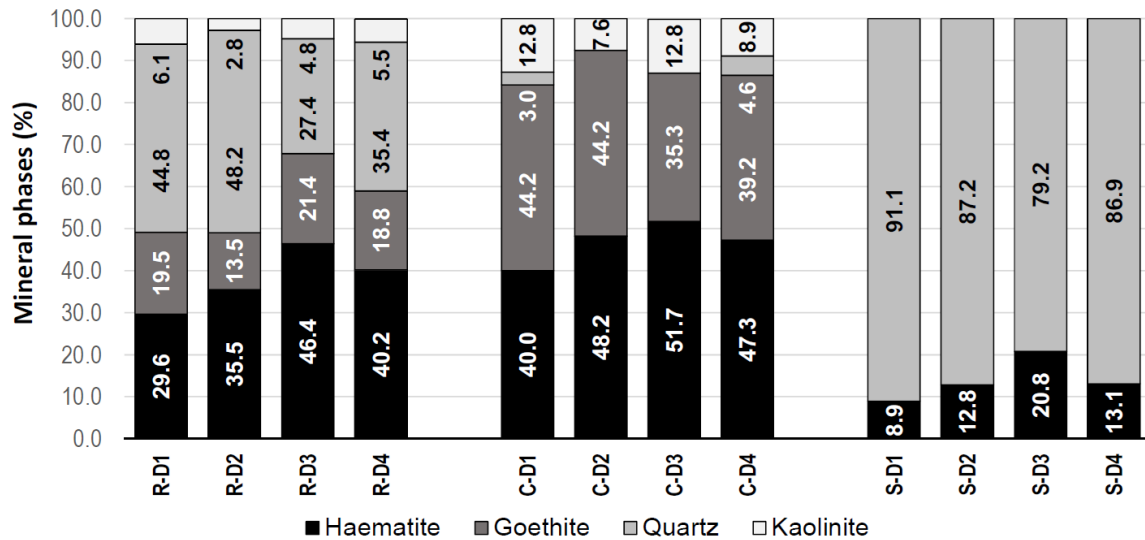
**Figure 2.2. Particle size distribution of the powder samples: (A) raw IOTs; (B) clay fractions; and (C) sand fractions.**

Figure 2.3 corroborates this and further illustrates the morphology of the particles. The larger particles observed tend to be sub-rounded and angular, and are likely quartz grains. Other smaller particles are also present, some of which tabular, and a rather thin material can be seen adhered onto larger particles, which is characteristic of clay minerals. The greater uniformity of particle sizes and shapes upon separation is clearly noticeable in the micrographs of both clay and sand fractions.



**Figure 2.3. Photomicrographs (SEM) of the IOT powder samples (R denotes raw samples, C denotes clay fractions and S denotes sand fractions).**

The mineralogical composition (XRD; the actual X-ray diffraction patterns can be found in Annex B.) shows that the main minerals present are quartz, haematite, goethite and kaolinite (Figure 2.4), all raw IOTs presenting important iron ore contents. Figure 2.4 also evidences the efficiency of the size segregation procedure. Upon separation, quartz is clearly dominant in the sand fractions, whereas the clay fractions concentrate the finer particles, those being clay minerals but also iron oxides and hydroxides.



**Figure 2.4. Mineralogical composition of the IOT samples (crystalline phases as determined by XRD; R denotes raw samples, C denotes clay fractions and S denotes sand fractions).**

The chemical composition of the various IOT samples (raw, clays and sands) is shown in Table 2.3. In good agreement with the XRD results, the major constituents in all samples are iron, silicon and aluminium oxides. It should be noted that no chlorine, vanadium or zirconium were detected in any of the samples. Also noteworthy is the near absence of alkalis and alkaline earth metal oxides ( $\text{Na}_2\text{O}$ ,  $\text{K}_2\text{O}$ ,  $\text{CaO}$ ,  $\text{MgO}$ ). Given that those are the common fluxing oxides in the production of fired ceramics, some densification difficulties might be anticipated. On the other hand, the same absence of alkalis, particularly in the sand fractions, suggests good durability performance in cement-based composites (Cheng et al., 2016; Kuranchie et al., 2015). The IOT sands showed the greatest uniformity, both in particle size (Figure 2.2-C) and shape (Figure 2.3), as well as in mineralogy (Figure 2.4) and chemical composition (Table 2.3). Such uniformity is of great importance for industrial scale use. As seen in Figure 2.4, data in Table 2.3 confirm that the separation process was very effective in the separation of iron oxide from quartz (all sand fractions with iron oxide contents generally below 10%) and show that, in global terms, S-D1 is the less contaminated sand fraction.

**Table 2.3. Chemical composition of the IOT samples (as obtained by XRF, expressed as wt.% oxides; R denotes raw samples, C denotes clay fractions and S denotes sand fractions).**

Oxide	R-D1	R-D2	R-D3	R-D4	C-D1	C-D2	C-D3	C-D4	S-D1	S-D2	S-D3	S-D4
<b>Al<sub>2</sub>O<sub>3</sub></b>	5.49	5.63	5.00	3.45	15.28	17.59	18.81	13.19	2.16	2.14	3.13	2.07
<b>SiO<sub>2</sub></b>	44.48	59.96	58.13	36.10	16.99	20.45	20.04	15.78	90.34	89.04	79.20	89.60
<b>P<sub>2</sub>O<sub>5</sub></b>	-	-	-	-	-	0.66	0.60	0.59	-	-	-	-
<b>K<sub>2</sub>O</b>	-	-	0.07	0.08	0.24	0.21	0.28	0.24	-	0.05	0.05	-
<b>CaO</b>	0.14	0.06	0.16	0.39	0.34	0.29	0.30	1.18	0.03	0.07	0.11	0.04
<b>Fe<sub>2</sub>O<sub>3</sub></b>	49.49	33.92	36.27	59.04	65.35	58.82	57.32	67.44	7.29	8.38	16.79	7.92
<b>MnO</b>	0.14	0.37	0.30	0.93	1.49	1.98	2.62	1.56	0.11	0.05	0.06	0.02
<b>Other</b>	0.26	0.06	0.07	0.01	0.31	-	0.03	0.02	0.07	0.27	0.66	0.35
<b>LoI*</b>	2.6	2.2	2.4	2.5	8.9	9.4	9.4	7.3	1.2	1.0	1.1	1.6

\* Loss on ignition

As expected from the XRD results (Figure 2.4), IOT clays have higher Al<sub>2</sub>O<sub>3</sub> contents and the majority of fluxing oxides (K<sub>2</sub>O, CaO), which are related to the presence of clay minerals (Dias et al., 2017; Zhang et al., 2006). The silica/alumina weight ratios in all clay fractions are quite similar and close to its theoretical value in kaolinite (1.18), confirming that clay minerals were concentrated in these fractions. The observed loss on ignition (LoI) is also consistent with the dehydroxylation of kaolinite. However, these clay fractions also retained a significant amount of fine iron ore particles, which results in unusually high Fe<sub>2</sub>O<sub>3</sub> contents (the presence of goethite further contributes to the LoI values). This, as well as the presence of manganese oxide, will certainly have a strong bearing in the final products colour. Although present in low quantity, the minor oxides can have, depending on temperature, an important fluxing effect during firing of ceramics. If the firing temperature is high enough (~1200°C), particularly if the firing atmosphere

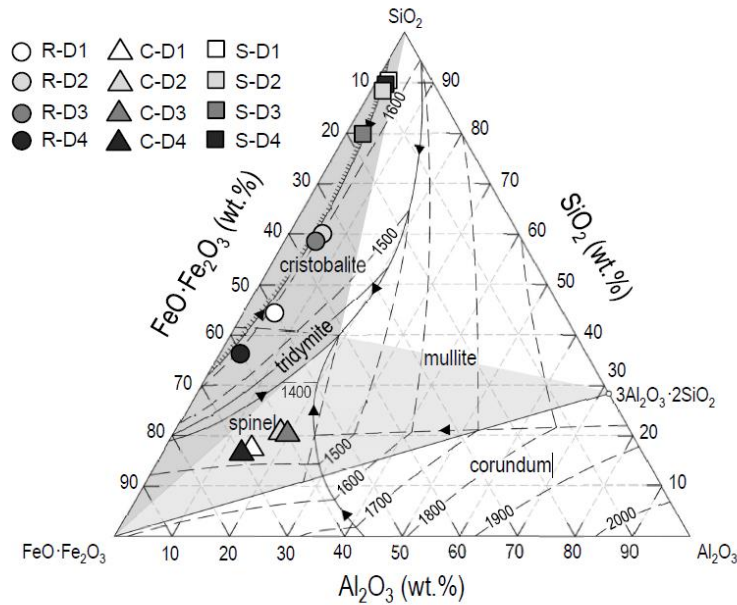
is slightly reducing, the iron oxide will also have a strong fluxing effect. This and the low particle size (i.e. high specific surface area) are expected to result in improved sinterability of these powders (Carty and Senapati, 1998; Lecomte-Nana et al., 2013). On the other hand, the presence of free quartz (Figure 2.4), with lower reactivity, should enable the adjustment of the thermal expansion coefficient and contribute to the dimensional stability of fired ceramic tiles. In terms of product formability, the kaolinite present is expected to improve plasticity, although fine particle powders are generally amenable in this respect.

### *2.3.2. CHARACTERIZATION OF THE FIRED SAMPLES*

Having in mind the possible use in the industrial production of ceramic tiles, it is appropriate to recall the classifications set forward by the ISO 13006 (ISO, 2012) and NBR 13818 (ABNT, 1997) Standards for pressed ceramic tiles. Those are based on the water absorption value (wt.%) and define five tile types: BIa–porcelain ( $WA \leq 0.5$ ), BIb–vitrified ( $0.5 < WA \leq 3$ ), BIIa–semi vitrified ( $3 < WA \leq 6$ ), BIIb– semi porous ( $6 < WA \leq 10$ ) and BIII–porous ( $WA > 10$ ). The choice of water absorption as controlling property derives from its direct relationship with open porosity, which, in turn, strongly affects the physical and chemical performance of the fired product (Carty and Senapati, 1998).

Open porosity is a clear indicator of the production process, as it implicitly measures green-body compaction and the experienced densification. During firing, densification mechanisms commonly rely on the presence of a liquid phase that promotes diffusion processes and ultimately leads to pore closure (Carty and Senapati, 1998). Although in normal conditions of industrial operation the thermodynamic equilibrium is generally not achieved, the phase equilibrium diagram of the relevant system can be used to predict the amount of liquid formed at the firing temperature and the reactions trends (Segadães,

2006). In the present case, based on the chemical composition (Table 2.3), the obvious choice of phase diagram is that of the  $\text{Al}_2\text{O}_3\text{-SiO}_2\text{-FeO.Fe}_2\text{O}_3$  system, in air (Lecomte-Nana et al., 2013; Levin et al., 1974). Also, given their fluxing effect, the joint content of  $(\text{CaO} + \text{K}_2\text{O} + \text{Fe}_2\text{O}_3)$  should be considered as “equivalent  $\text{Fe}_2\text{O}_3$ ” in the mixtures. Figure 2.5 shows the location of the various samples in the phase diagram.



**Figure 2.5. Phase equilibrium diagram of the ternary system  $\text{Al}_2\text{O}_3\text{-SiO}_2\text{-FeO.Fe}_2\text{O}_3$  (Levin et al., 1974), showing the position of the various samples.**

As expected from the results in Figure 2.4 and Table 2.3, the sand fractions are not adequate, on their own, for the production of ceramic tiles. They can be put to better use in the production of cement-based composites (e.g. mortar, concrete) and will be considered no further. Figure 2.5 shows that all raw IOTs and clays lie in the mullite-spinel-silica compatibility triangle, in which melting starts at  $\sim 1400$  °C (it should be reminded that in the actual multicomponent system, melting will start at a significantly lower temperature). Figure 2.5 also shows that in this representation the clay fractions remain nearly aligned along the same silica/alumina constant weight ratio, which validates the use of the “equivalent  $\text{Fe}_2\text{O}_3$ ” content concept.



Although the liquid phase formed at first-melting is the same, raw IOTs and clays lie in two different first-melting tie-triangles, meaning that in all clay fractions (spinel-mullite-liquid tie-triangle) silica will dissolve first in the first-melting liquid phase and that, after firing, samples should contain some mullite. On the contrary, in all the raw IOTs (silica-spinel-liquid tie-triangle) mullite will be the first solid to dissolve.

The amounts of liquid phase at first-melting will also be different and those can be estimated by the use of the lever rule applied to the corresponding liquid–solids tie–lines (for clarity, only those for R-D3 and C-D3 are shown in the diagram in Figure 2.5), as summarized in Table 2.4. In practice, the nature and amounts of solid phases are expected to be substantially affected by the slow reaction kinetics and the firing atmosphere (non-equilibrium residual phases are likely to be detected) and, thus, may differ from those predicted by the phase equilibrium diagram. Nevertheless, given the chemical-mineralogical similarity among samples, the deviations are expected to be also similar.

**Table 2.4. Relative proportions of phases in equilibrium at first-melting, as calculated by the lever rule from the diagram in Figure 2.5.**

<b>Sample</b>	<b>Liquid phase formed at first-melting (wt.%)</b>	<b>Compatible solids (wt.%)</b>
<b>R-D1</b>	28.0	Spinel (38.0) + silica (34.0)
<b>R-D2</b>	30.0	Spinel (21.5) + silica (48.5)
<b>R-D3</b>	25.7	Spinel (26.2) + silica (48.1)
<b>R-D4</b>	18.2	Spinel (51.9) + silica (29.9)
<b>C-D1</b>	33.3	Spinel (52.9) + mullite (13.8)
<b>C-D2</b>	41.2	Spinel (45.8) + mullite (13.0)
<b>C-D3</b>	39.6	Spinel (43.1) + mullite (17.3)
<b>C-D4</b>	32.8	Spinel (60.5) + mullite (6.7)

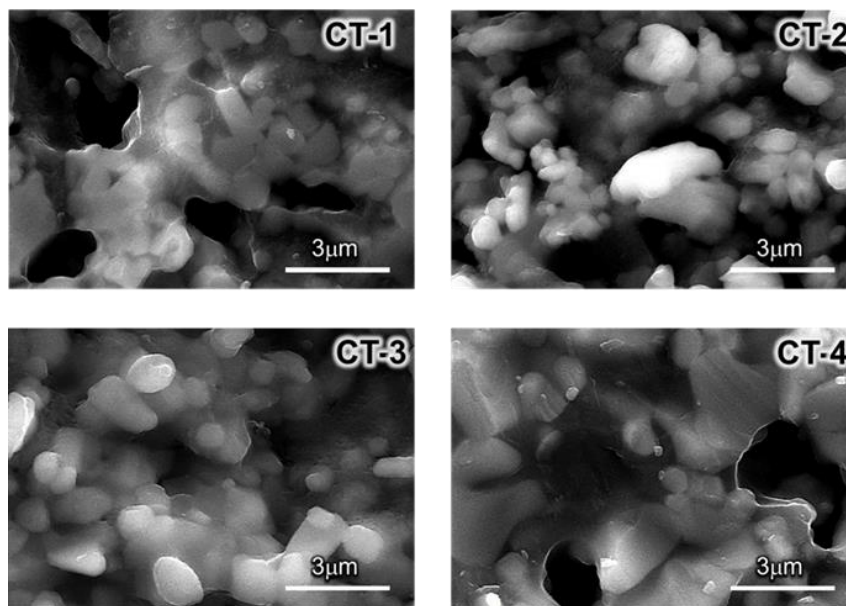
Figure 2.5 and Table 2.4 show that despite the modest mullite content, the clay fractions have a privileged location in terms of liquid phase formation, and their amount of liquid at first-melting is expected to be higher than that of the corresponding IOT. There is another major difference between raw IOTs and clays, which is particle sizes (Figures 2.2-A and 2.2-B). Such difference is expected to negatively affect green forming (plasticity) of raw IOTs to begin with, and then densification and the iron-oxygen equilibrium during firing. Also, particle size directly affects the pore size in the green and fired ceramic body (Sánchez et al., 1998). Indeed, and as anticipated, trial runs showed that cohesive green test-pieces were much harder to produce with the coarser raw IOTs under the low compaction pressure used. And, even then, the successful ones showed little densification under the same firing conditions, a clear suggestion of a prevailing oxidizing atmosphere (Karamanov et al., 2000) and the presence of a minor liquid phase. Considering that mullite is generally regarded as the key crystalline phase in fired ceramics (Aras, 2004; Carty and Senapati, 1998; Iqbal and Lee, 2000; Sánchez et al., 2009), the fact that mullite is not expected to be present in the fired IOT samples is also a strong deterrent against their use. Therefore, raw IOTs will be considered no further.

On the contrary, test-pieces produced with the clay fractions (CT-1, CT-2, CT-3 and CT-4, produced with the C-D1, C-D2, C-D3 and C-D4, respectively) were easier to obtain, even under the low compacting pressure used (compatible with more artisanal production processes) and densified as expected, showing a dark brown lustre after firing (Figure 2.6), as is typical of a prevailing reducing atmosphere and the presence of an abundant liquid phase. Their characterization will now be presented and discussed.



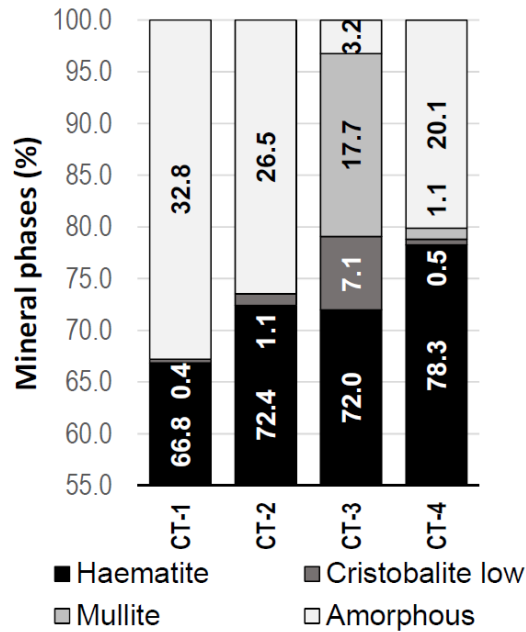
**Figure 2.6. Macroscopic appearance of fired CT-3 tiles, showing the typical dark brown luster.**

The microstructure of the fired samples (fracture surface) can be observed in Figure 2.7. The presence of an abundant glassy (liquid) phase is evident in all samples (under a slightly reducing atmosphere the fluxing effect of the iron oxides will be even stronger).



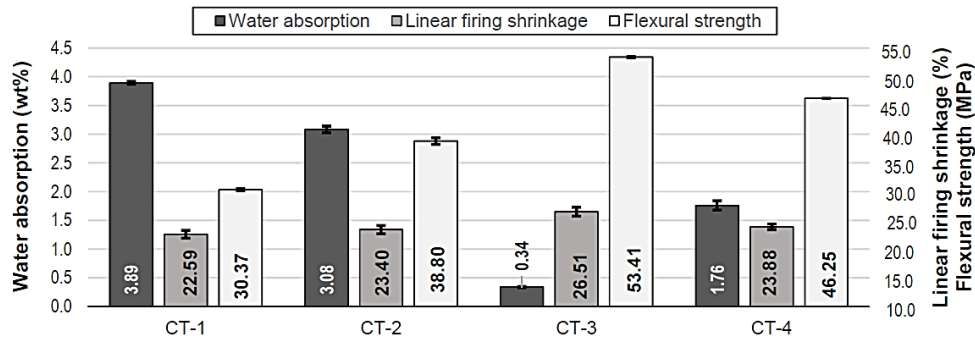
**Figure 2.7. Photomicrographs (SEM) of the fired samples (fracture surface).**

Figure 2.8 shows the relative amounts of crystalline phases and confirms the expected phase transformation during firing (Table 2.4), namely cristobalite and mullite, in line with the estimates from the phase diagram (Aras, 2004; Imanaka et al., 1995; Iqbal and Lee, 2000). The quartz present should mostly be unreacted (residual) quartz. The original iron compounds (Figure 2.4) resulted in the formation of haematite, whose presence, rather than that of spinel, hints at the sensitivity to the firing atmosphere.



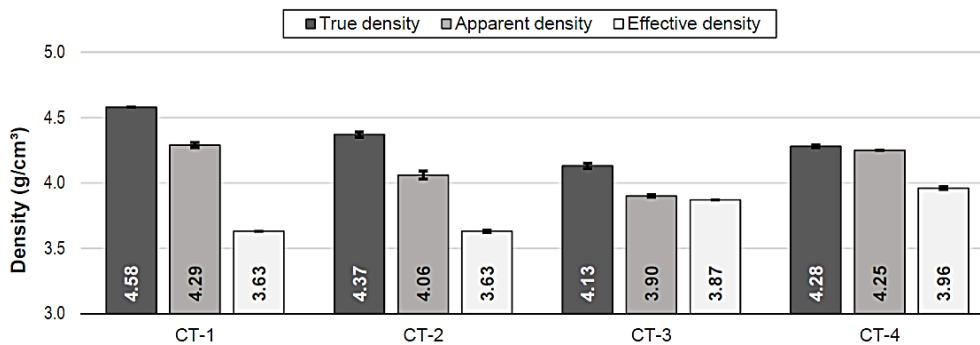
**Figure 2.8. Mineralogical composition (crystalline phases as determined by XRD) of the fired clay samples.**

Given the low compacting pressure used, it is no surprise (Figure 2.9) that all samples showed an impressive firing shrinkage (~24%), particularly so the CT-3 sample, which combines a high content of finer particles (Table 2.2 and Figure 2.2-B) and of kaolinite (Figure 2.4). The resulting green sample likely was comparatively better packed and the liquid phase formed during firing promoted the observed shrinkage and pore closure. Water absorption (i.e. open pores) was found to be lowest for this sample, which presented the highest flexural strength. Despite the high shrinkage, all fired samples were dimensionally homogeneous and hardly warped, with no obvious cracks either. This is an indication of a rather amenable processing behaviour, even though such high shrinkage cannot be credibly managed in industrial production. In the latter case, higher compaction pressures would no doubt be applied, resulting in lower shrinkage and enabling the use of shorter firing times, or even lower firing temperatures, towards the same end result.

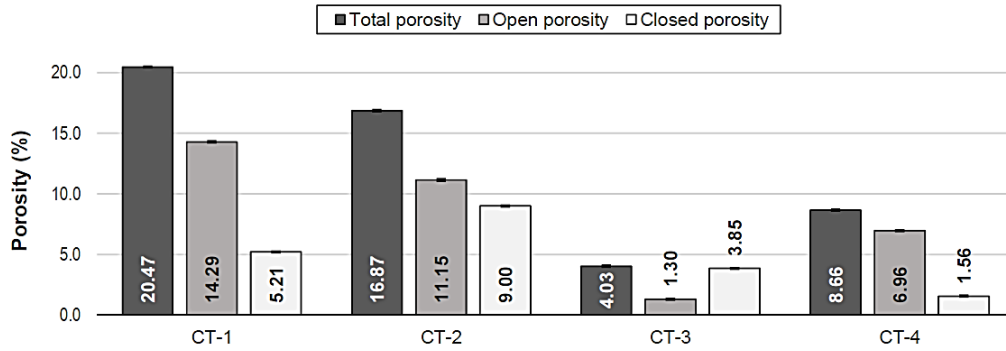


**Figure 2.9. Water absorption, linear firing shrinkage and flexural strength (modulus of rupture) of fired samples.**

The density results (Figure 2.10) confirm the above and reflect the high iron oxide contents. True density values are consistently high (highest for CT-1, with the highest iron oxide content), closely followed by apparent and bulk densities only for CT-3 and CT-4, which are less porous. For CT-3, apparent and bulk densities are identical and translate into a rather low water absorption value (Figure 2.9). Figure 11 further details the differences in porosity, based on which the flexural strength results (Figure 2.9) come as no surprise: CT-3 has the best mechanical strength and CT-4 is second best. Following the same reasoning, CT-1 tiles are heavier (Figure 2.10) due to the higher iron oxide content (Table 2.3 and Figure 2.4), but their lower kaolinite content and coarser particles (Table 2.2 and Figure 2.2-B), as well as the lower amount of liquid formed at first-melt (Table 2.4), result in higher porosity (Figure 2.11) and lower linear shrinkage and, consequently, lower mechanical strength (Figure 2.9).



**Figure 2.10. Density (true, apparent and bulk) of fired samples.**



**Figure 2.11. Porosity (total, open and closed) of fired samples.**

Bearing in mind the Standards requirements for the typology of pressed ceramic tiles, based on the water absorption values, CT-3 can already be classified in group BIa (pressed tiles with absorption below 0.5 wt.%), i.e. as porcelain. The CT-2 and CT-4 tiles will be classified as vitrified tiles (group BIb, pressed tiles, with water absorption between 0.5 and 3 wt.%) and CT-1 as semi-vitrified tiles (Group BIIa, pressed tiles with water absorption between 3 and 6 wt.%). When subjected to an industrial fabrication process, using an adequately higher compaction pressure, such tiles are expected to exhibit even better properties, have good chemical and abrasion resistance (easy to clean, adequate to highly trafficked and industrial areas) and be resistant to frost (could be used in outdoor floors and walls in cold climates). In such applications, the dark brown colour should pose no drawbacks and might even be considered advantageous. At the same time, the rather amenable processing behaviour enables the use of these materials by local artisans to produce smaller series of higher artistic value “brown porcelain” tiles and ware.

Today, due to scarcity and high transportation costs, as well as lower homogeneity of some of the conventional raw materials, the possibility of using waste materials in the production of high quality products with high added value is highly desirable and provides greater encouragement in the adoption of sustainable production routes.

## 2.4. CONCLUSIONS

This work was aimed at finding a meaningful potential use for iron ore tailings (IOT) that might mitigate part of the negative impact of tailings-dams without sacrificing the opportunities provided by mining, and promote the economic and social welfare of the communities neighbouring the dams. A dry segregation procedure was implemented, which resulted in the separation into residual iron ore concentrate, with well defined commercial value, outside the scope of this work, and two other powder fractions of uniform particle sizes, classified as “clay” and “sand” as is generally used in Sedimentology and Civil Engineering for fine and medium sized powders, respectively. Quartz is clearly dominant in the sand fractions, whereas the clay minerals are concentrated in the clay fractions. The IOT sands showed the greatest uniformity, both in particle size and shape, as well as in mineralogy and chemical composition. Such uniformity is of great importance for industrial scale use. These sand fractions are not adequate, on their own, to the production of fired ceramic tiles and can be put to better use in the production of cement-based composites (e.g. mortar, concrete, hydraulic tiles).

The direct use of the raw IOTs in the production of fired ceramic tiles requires special care and needs to be further investigated given that their coarser particles negatively affect green forming (plasticity) to begin with, and then densification and the iron-oxygen equilibrium during firing. The expected absence of mullite after firing is also a strong deterrent against their use in the production of ceramics.

The IOT clays can be used in the ceramic tile production process, as they present adequate plasticity and dry strength during processing, and develop mullite and a glass phase upon firing. Despite the impressive firing shrinkage, a direct consequence of the used low compaction pressure, a rather amenable processing behaviour was observed, resulting in

dimensionally homogeneous, nor cracked neither warped pieces. The resulting ceramic tiles show a rather appealing dark brown lustre and are very compact, with very low porosity (vitrified products, classified in groups BIa, BIb or BIIa) and high mechanical strength. These same materials can be used by local artisans in the production of smaller series of higher artistic value “brown porcelain” tiles and ware.

When comparing the behaviour during firing under the same conditions, it can also be concluded that, although the four IOT clays contain the same minerals, the differences in grain sizes, associated with the differences in proportions of phases, play a major role and directly affect the final properties of the products, as they control porosity, density and mechanical strength.

The possibility of using waste materials in the production of tiles with high added value is highly desirable and provides greater encouragement in the adoption of sustainable production routes. There is a more stringent end-market environmental regulation and increased concern among companies regarding reputation and operational legitimacy as the key drivers of adoption of corporate-based environmental standards. When inserting the IOT clays in the ceramic tile production process can be group different agents and different sub-strategies, to form an umbrella organization able to produce ecological innovations.

## **2.5. ACKNOWLEDGEMENTS**

Authors acknowledge the financial support provided by CAPES, FAPEMIG, CNPq, UFOP, UFV and Fundação Gorceix. Equipment and technical support provided by CEFET-MG (Laboratory of Non-Destructive Testing), UFOP Escola de Minas laboratories (Laboratory of Electronic Microscopy NANOLAB–Redemat and Laboratory of Construction Materials Department of Civil Engineering) and UA laboratories from



the Department of Materials and Ceramic Engineering (CICECO), is gratefully appreciated. Thanks are also due to the Research Group on Solid Wastes RECICLOS–CNPq for infrastructure use and collaboration.

## 2.6. REFERENCES

ABNT, 1997. *NBR 13818: Ceramic tiles – Specification and test methods*. Rio de Janeiro: Associação Brasileira de Normas Técnicas - ABNT (in Portuguese).

ABNT, 2004. *NBR 1007: Sampling of solid waste*. Rio de Janeiro: Associação Brasileira de Normas Técnicas - ABNT (in Portuguese).

ABNT, 2006. *NBR NM 45: Aggregates – Determination of the unit weight and air-void contents*. Rio de Janeiro: Associação Brasileira de Normas Técnicas - ABNT (in Portuguese).

ABNT, 2009. *NBR NM 52: Fine aggregate – Determination of the bulk specific gravity and apparent specific gravity*. Rio de Janeiro: Associação Brasileira de Normas Técnicas - ABNT (in Portuguese).

ABNT, 2011. *NBR 9939: Coarse aggregate – Determination of total moisture content – Test method*. Rio de Janeiro: Associação Brasileira de Normas Técnicas - ABNT (in Portuguese).

Andrade, L.C.R., 2014. *Caracterização de rejeitos de mineração, in natura e segregados, para aplicação como material de construção civil*. Doctoral dissertation, Federal University of Viçosa, Brazil (in Portuguese).

ACIMAC, 2017. *World production and consumption of ceramic tiles*. [http://www.mec-studies.com/filealbum/655\\_0.pdf](http://www.mec-studies.com/filealbum/655_0.pdf) (accessed 18.12.03).

Aras, A., 2004. *The change of phase composition in kaolinite- and illite-rich clay-based ceramic bodies*. *Applied Clay Science* 24, 257–269. DOI: 10.1016/j.clay.2003.08.012

Bianchini, G., Marrocchino, E., Tassinari, R., Vaccaro, C., 2005. *Recycling of construction and demolition waste materials: a chemical–mineralogical appraisal*. *Waste Management* 25, 149–159. DOI: 10.1016/j.wasman.2004.09.005.

Cabral Jr, M., Boschi, A.O., Motta, J.F.M., Tanno, L.C., Sintoni, A., Coelho, J.M., Caridade, M., 2010. *Panorama e perspectivas da indústria de revestimentos cerâmicos no Brasil*. *Cerâmica Industrial* 15, 7–18 (in Portuguese).

Carty, W.M., Senapati, U., 1998. *Porcelain – raw materials, processing, phase evolution and mechanical behavior*. *Journal of the American Ceramic Society* 81, 3–20. DOI: 10.1111/j.1151-2916.1998.tb02290.x

Chen, Y., Zhang, Y., Chen T., Liu, T., Huang, J. *Preparation and characterization of red porcelain tiles with hematite tailings*. *Construction and Building Materials* 38, 1083–1088. DOI: 10.1016/j.conbuildmat.2012.06.056

Cheng, Y., Huang, F., Li, W., Liu, R., Li, G., Wei, J., 2016. *Test research on the effects of mechanochemically activated iron tailings on the compressive strength of concrete*. Construction and Building Materials 118, 164–170. DOI: 10.1016/j.conbuildmat.2016.05.020

COPAM, 2005. *Normative resolution nº 87, 17 June: Classification criteria for tailings and residues containing dams and water reservoirs in industrial and mining enterprises in Minas Gerais State*. Belo Horizonte: Conselho Estadual de Política Ambiental - COPAM (in Portuguese).

Das, S.K., Ghosh, J., Mandal, A.K., Singh, N., Gupta, S., 2012. *Iron Ore Tailing: A Waste Material used in Ceramic Tile Compositions as Alternative Source of Raw Materials*. Transactions of the Indian Ceramic Society 71, 21–24. DOI: 10.1080/0371750X.2012.689507

Dias, F.G., Segadães, A.M., Perottoni, C.A., Cruz, R.C.D., 2017. *Assessment of the fluxing potential of igneous rocks in the traditional ceramics industry*. Ceramics International 43, 16149–16158. DOI: 10.1016/j.ceramint.2017.08.190).

DNPM, 2016. *Mineral summary 2015*. Brasília: Departamento Nacional de Produção Mineral - DNPM (in Portuguese).

Edraki, M., Baumgartl, T., Manlapig, E., Bradshaw, D., Franks, D.M., Moran, C.J., 2014. *Designing mine tailings for better environmental, social and economic outcomes: a review of alternative approaches*. Journal of Cleaner Production 84, 411–420. DOI: 10.1016/j.jclepro.2014.04.079.

FEAM, 2015. *Dams management 2014*. Belo Horizonte: Fundação Estadual do Meio Ambiente - FEAM (in Portuguese).

FEAM, 2017. *Dams inventory of Minas Gerais State*. Belo Horizonte: Fundação Estadual do Meio Ambiente - FEAM (in Portuguese).

Fontes, W.C., Mendes, J.C., Silva, S.N., Peixoto, R.A.F., 2016. *Mortars for laying and coating produced with iron ore tailings from tailing dams*. Construction and Building Materials 112, 988–995. DOI: 10.1016/j.conbuildmat.2016.03.027

Gabaldón-Estevan, D., Criado, E., Monfort, E., 2014. *The Green Factor in European Manufacturing: A case study of the Spanish ceramic tile industry*. Journal of Cleaner Production 70, 242–250. DOI: 10.1016/j.jclepro.2014.02.018

Garcia, L.C., Ribeiro, D.B., Roque, F.O., Ochoa-Quintero, J.M., Laurance, W.F., 2017. *Brazil's worst mining disaster: Corporations must be compelled to pay the actual environmental costs*. Ecological Applications 27, 5–9. DOI: 10.1002/eap.1461.

Google Maps, 2017a. Complexo Itabirito. <https://www.google.com.br/maps/place/Itabirito,+MG,+35450-000/@-20.4106247,-43.8519887,3801m/data=!3m1!1e3!4m5!3m4!1s0xa6a9f68df75965:0xf0d14225d3467064!8m2!3d-20.2530617!4d-43.8030567> (accessed 17.09.12).

Google Maps, 2017b. Vargem Grande. <https://www.google.com.br/maps/search/vargem+grande+itabirito/@-20.1758077,-43.8703848,2811m/data=!3m1!1e3> (accessed 17.09.12).

IBAMA, 2015. *Preliminary technical report – Environmental impacts arising from the disaster involving the rupture of the Fundão dam, in Mariana, MG*. Brasília: Instituto Brasileiro do Meio Ambiente e dos Recursos Naturais Renováveis - IBAMA (in Portuguese).

IBRAM, 2013. *Management for the sustainability in mining – 20 years of history*. Brasília: Instituto Brasileiro de Mineração - IBRAM (in Portuguese).

Imanaka, Y., Aoki, S., Kamehara, N., Niwa, K., 1995. *Cristobalite phase formation in glass/ceramic composites*. Journal of the American Ceramic Society 78, 1265–1271. DOI: 10.1111/j.1151-2916.1995.tb08480.x

IPEA, 2012. *Diagnosis of the solid wastes of the mining activity of non-energetic substances*. Brasília: Instituto de Pesquisa Econômica Aplicada - IPEA (in Portuguese).

Iqbal, Y., Lee, W.E., 2000. *Microstructural Evolution in Triaxial Porcelain*. Journal of the American Ceramic Society 83, 3121–3127. DOI: 10.1111/j.1151-2916.2000.tb01692.x

ISO, 2012. *ISO 13006:2012: Ceramic tiles — Definitions, classification, characteristics and marking*. Geneva: International Organization for Standardization - ISO.

Karamanov, A., Pisciella, P., Cantalini, C., Pelino, M., 2000. *Influence of Fe<sup>3+</sup>/Fe<sup>2+</sup> ratio on the crystallization of iron-rich glasses made with industrial wastes*. Journal of the American Ceramic Society 83, 3153–3157. DOI: 10.1111/j.1151-2916.2000.tb01697.x

Kossoff, D., Dubbin, W.E., Alfredsson, M., Edwards, S.J., Macklin, M.G., Hudson-Edwards, K.A., 2014. *Mine tailings dams: Characteristics, failure, environmental impacts, and remediation*. Applied Geochemistry 51, 229–245. DOI: 10.1016/j.apgeochem.2014.09.010.

Kumar, S., Kumar, R., Bandopadhyay, A., 2006. *Innovative methodologies for the utilisation of wastes from metallurgical and allied industries*. Resources, Conservation and Recycling 48, 301–314. DOI: 10.1016/j.resconrec.2006.03.003

Kuranchie, F.A., Shukla, S.K., Habibi, D., Mohyeddin, A., 2015. *Utilisation of iron ore tailings as aggregates in concrete*. Cogent Engineering 2, 1083137. DOI: 10.1080/23311916.2015.1083137

Lecomte-Nana, G., Bonnet, J.P., Soro, N., 2013. *Influence of iron on the occurrence of primary mullite in kaolin based materials: A semi-quantitative X-ray diffraction study*. Journal of the European Ceramic Society 33, 669–677. DOI: 10.1016/j.jeurceramsoc.2012.10.033

Levin, E.M., Robbins, C.R., McMurdie, H.F., 1974. Phase Diagrams for Ceramists, in: M.K. Reser (Ed), American Ceramic Society, Columbus, Figure 767.

Li, C., Sun, H., Bai, J., Li, L., 2009. *Innovative methodology for comprehensive utilization of iron ore tailings: Part I*. The recovery of iron from iron ore tailings using magnetic separation after magnetizing roasting. Journal of Hazardous Materials 174, 71–77. DOI: 10.1016/j.jhazmat.2009.09.018.

Liu, W.Y., Xu, X.L., An, Y.Y., 2012. *Study on the sprayed concrete with iron tailings*. Advanced Materials Research, 347–353, 1939–1943. DOI: 10.4028/www.scientific.net/AMR.347-353.1939

Meyer-Stamer, J., Maggi, C., Seibel, S., 2004. *Upgrading in the tile industry of Italy, Spain, and Brazil: insights from cluster and value chain analysis*, in: H. Schmitz (Ed), Local enterprises in the global

economy: issues of governance and upgrading. Edward Elgar Pub., Cheltenham, UK, Chapter 7, pp 174-199. ISBN: 978 1 84542 192 2

Peixoto, R.A.F., Oliveira, J.R., Barros, J.B., 2013. *Process for segregation of iron ore contained in rejects from mining and processing of iron ore*. Brasil, Patent No. BR 10 2012 008758 8 A2 (in Portuguese).

SNISB, 2018. *Dams Registered in the System*. Brasília: Sistema Nacional de Informações sobre Segurança da Barragens - SNISB (in Portuguese).

Sánchez, E., García-Ten, J., Barba, A., Beltran, V., 1998. *Estimation of packing density of raw material mixtures used in tile manufacture*. British Ceramic Transactions 97, 149–154.

Sánchez, E., García-Ten, J., Sanz, V., Moreno, A., 2009. *Porcelain tile: Almost 30 years of steady scientific-technological evolution*. Ceramics International 36, 831–845. DOI: 10.1016/j.ceramint.2009.11.016

Segadães, A.M., 2006. *Use of Phase Diagrams to Guide Ceramic Production from Wastes*. Advances in applied ceramics 105, 46–54. DOI: 10.1179/174329006X82927

Uchechukwu, E.A., Ezekiel, M.J., 2014. *Evaluation of the iron ore tailings from Itakpe in Nigeria as concrete material*. Advances in Materials 3, 27–32. DOI: 10.11648/j.am.20140304.12

Verruijt, A., 2001. Soil Mechanics, Delft University of Technology, 2001.

Yellishetty, M., Karpe, V., Reddy, E.H., Subhash, K.N., Ranjith, P.G., 2008. *Reuse of iron ore mineral wastes in civil engineering constructions: A case study*. Resources, Conservation and Recycling 52, 1283–1289. DOI: 10.1016/j.resconrec.2008.07.007

Yellishetty, M., Mudd, G.M., 2014. *Substance flow analysis of steel and long term sustainability of iron ore resources in Australia, Brazil, China and India*. Journal of Cleaner Production 84, 400–410. DOI: 10.1016/j.jclepro.2014.02.046.

Zhang, S., Xue, X., Liu, X., Duan, P., Yang, H., Jiang, T., Wang, D., Liu, R., 2006. *Current situation and comprehensive utilization of iron ore tailing resources*. Journal of Mining Science 42, 403–408. DOI: 10.1007/s10913-006-0069-9.

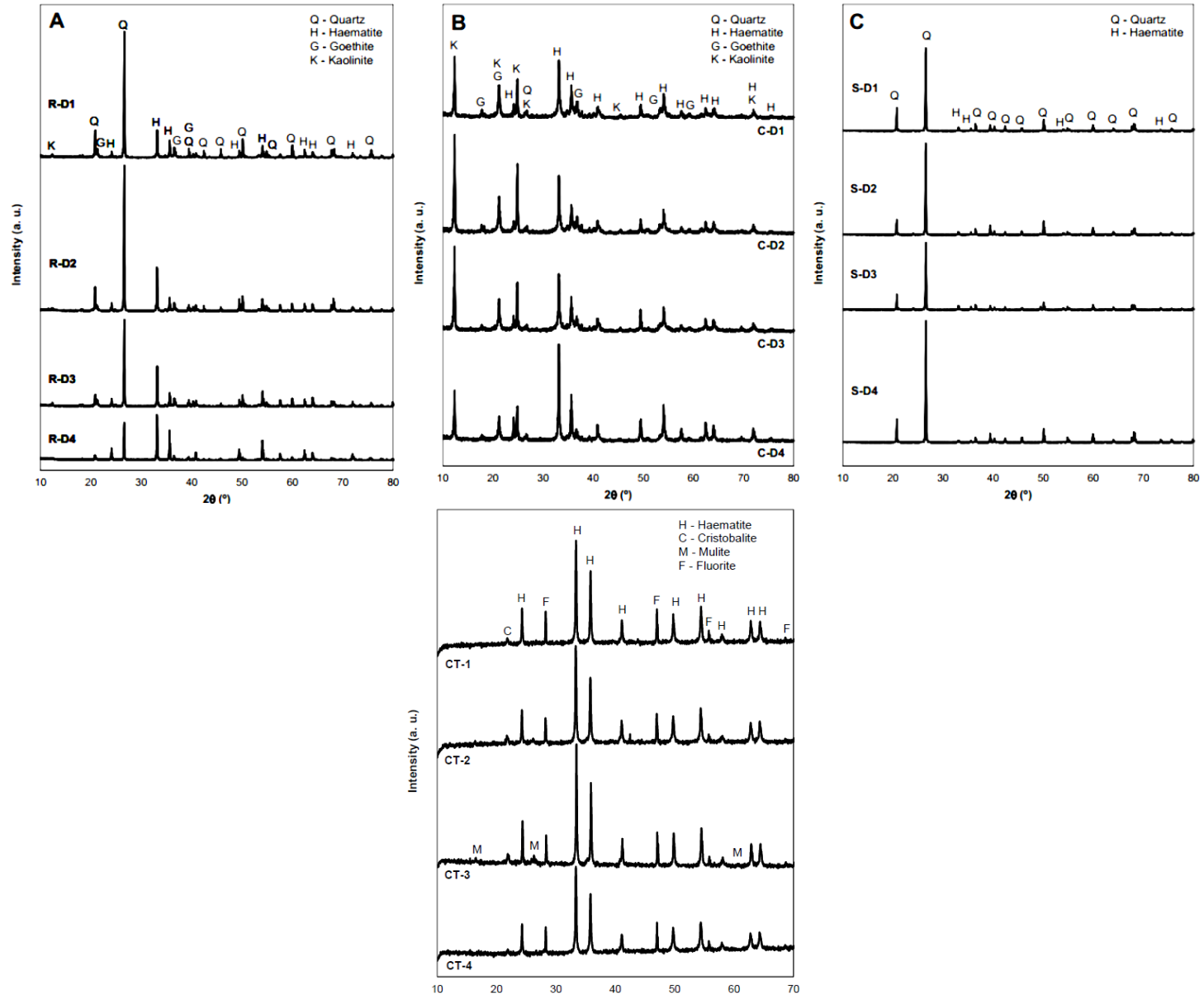
Zhao, S., Fan, J., Sun, W., 2014. *Utilization of iron ore tailings as fine aggregate in ultra-high performance concrete*. Construction and Building Materials 50, 540–548. DOI: 10.1016/j.conbuildmat.2013.10.019

ANNEX A. ARCHIMEDES' WATER DISPLACEMENT METHOD USED ON A CERAMIC POROUS BODY

Body = bulk solid = (real solid + closed pores) + open pores	Apparent solid = real solid + closed pores	
Bulk (total) volume, $V_B$ = Volume of real solid, $V_R$ + Volume of closed pores, $V_{CP}$ + Volume of open pores, $V_{OP}$	Apparent volume, $V_A$ = Volume of real solid, $V_R$ + Volume of closed pores, $V_{CP}$ Total pore volume, $V_{TP}$ = Volume of closed pores, $V_{CP}$ + Volume of open pores, $V_{OP}$	$V_B = V_R + V_{CP} + V_{OP}$ $V_B = V_A + V_{OP}$ $V_B = V_R + V_{TP}$ $V_{CP} = V_{TP} - V_{OP}$ ; $V_{TP} = V_B - V_R$
Solid dry weight, $W_d$		
Solid saturated weight, $W_s = W_d$ + weight of water in open pores	$W_s = W_d + V_{OP} \times \rho_w$	$V_{OP} = (W_s - W_d) / \rho_w$
Solid immersed weight, $W_i = W_d$ - weight of displaced water	$W_i = W_d - V_A \times \rho_w$	$V_A = (W_d - W_i) / \rho_w$ $V_B = (W_d - W_i) / \rho_w + (W_s - W_d) / \rho_w$ $\rho_w = (W_s - W_i) / \rho_w$
Real solid density (true density), $RD = W_d / V_R$	as determined by pycnometry	$V_R = W_d / RD$
Bulk solid density (effective density), $BD = W_d / V_B$	$BD = [W_d / (W_s - W_i)] \times \rho_w$	$V_B = W_d / BD$
Apparent solid density, $AD = W_d / V_A$	$AD = [W_d / (W_d - W_i)] \times \rho_w$	$V_A = W_d / AD$
Open porosity (vol.%), $OP = (V_{OP} / V_B) \times 100$	$OP = [(W_s - W_d) / (W_s - W_i)] \times 100$	
Water absorption (wt.%), $WA = (\text{weight of water in open pores} / \text{weight of solid}) \times 100$	$WA = [(W_s - W_d) / W_d] \times 100$	$WA = OP / BD$
Total porosity (vol.%), $TP = (V_{TP} / V_B) \times 100$	$TP = [(V_B - V_R) / V_B] \times 100 = (1 - V_R / V_B) \times 100$	$TP = (1 - BD / RD) \times 100$
Closed porosity (vol.%), $CP = (V_{CP} / V_B) \times 100$	$CP = [(V_{TP} - V_{OP}) / V_B] \times 100$	$CP = TP - OP$

ANNEX B. MINERALOGICAL COMPOSITION OF THE IOT SAMPLES (A, B AND C); AND MINERALOGICAL COMPOSITION OF THE FIRED SAMPLES

(D) (XRD; THE ACTUAL X-RAY DIFFRACTION PATTERNS).



# Chapter 3

---

**Experimental studies on the use of iron ore tailings as fine aggregates  
and pigments in the manufacture of hydraulic tiles**

### **3. ASSESSMENT OF THE USE POTENTIAL OF USE OF IRON ORE TAILINGS AS FINE AGGREGATES AND PIGMENTS IN THE MANUFACTURE OF HYDRAULIC TILES**

#### **ABSTRACT**

Considering the growing ecological awareness of the consumer market, the construction market has sought strategies to promote a greater insertion of waste in the production chain, contributing to the technological improvement of processes and products, and to mitigation of social and environmental impacts. In this sense, the present experimental study using iron ore tailings (IOT) in the production of hydraulic tiles represents a strategic alternative of technological implementation while at the same time conferring intangible value to the product. The physical, chemical and mineralogical characterization of the raw materials indicated the potential use of IOT as pigment, aggregate and supplementary cementing material. The segregation process proved to be efficient in obtaining high quality siliceous aggregate and Fe-rich clay for use as pigment, and the calcination and grind of this last improved the pigmentation and cementing potential of this last. The hydraulic tiles obtained with the tested IOT-based materials confirmed the expectations and products with satisfactory appearance and physical-mechanical performance were obtained.

**Key Words:** Iron ore tailings from tailing dams; recycled aggregates; sustainable mineral binder; sustainable mortars.



### 3.1. INTRODUCTION

In the recent era of intangible-assets, it is well known that the insertion of waste in the productive chain can contribute for the technological improvement of processes and products, and to the mitigation of social and environmental impacts. But the sense of pleasure, welfare and satisfaction provided by an ecofriendly product is strategic and represents new market opportunities. Both for the mineral extraction industry and for the construction industry, the multidisciplinary system and cross-cutting nature of the strategic design contribute for the development of such intangible assets. In this sense, the use of iron ore tailings (IOT) from tailing-dams in the production of hydraulic tiles (HT) represents a strategic alternative of technological implementation and intangibility that meets expectations and encourages an environmentally co-responsible society.

Only in Brazil about 379,000 tons of IOT are generated and disposed daily as sludge in percolating-water-controlled containment dams (FEAM 2015a; IPEA 2012). There are 663 dams in the country, of which 445 are located in the State of Minas Gerais, and many of them classified as class III dams (high environmental risk) (FEAM 2015b). The growing generation of IOTs and their inadequate disposal has raised concern due to social, environmental and economic problems related to the risk of collapse of these structures. Recently, all these damages were actually observed in the collapse of the Fundão dam, in the city of Mariana, in the State of Minas Gerais, in what is classified as the largest environmental disaster in Brazil and perhaps one of the worst in the world (Garcia et al. 2017; IBAMA 2015).

On the other hand, the IOT is a fine, dense, stable and crystalline material, composed of iron oxides, silica and alumina, and its use in substitution of conventional aggregates in cement-based composites have been proven to be suitable, promoting mechanical

strength and differentiated coloration (Shettima, et al., 2016; Fontes, et al., 2016; Yellishetty, et al., 2008). Furthermore, IOT sands obtained by a dry-route separation-process present homogeneous characteristics (morphology, mineralogic composition and particle-size distribution), suitable for use in cement-based composites (Peixoto, Oliveira & Barros 2012; Andrade 2014)

The Brazilian specification NBR 9457 (ABNT 2013) describes HT as high-strength concrete tiles due to its mechanical performance. This material, however, is composed of one or more layers of mortars, produced with Portland cement and aggregates, and may contain pigments or other powders, and rarely, admixtures. The pigments used in the production of the HT mortars are inert powdery materials, among them iron oxide, also present in the raw IOT (Fontes et al. 2016). These materials present high specific surface area, which increases the water/cement ratio for the same workability. The consequent reduction in mechanical strength is commonly compensated by the increase in cement consumption, which is also related to the increase in shrinkage and risk of resulting cracks (Tango 2000).

The Portland cement matrices used in the production of the HT have heterogeneous nature, with a wide composition spectrum. This feature allows the presence of residual materials, even in significant percentages (Marques 2012). Additionally, from an anthropologic and sociocultural perspective, the HT is a building material that brings within itself an architectural memory and cultural baggage, evident in its surface design, materials, colors and process of artisan production. These symbolic values when associated with sustainability provided by use of IOT materials increase the perception of value of the product (Fontes et al. 2018). For this purpose, experimental studies were

carried out with the objective of evaluating the potential of using raw and processed IOT in the production of HTs.

In this respect, on emerging market trends, the increasing environmental attractiveness of pigments obtained from sustainable materials is reaching consumers looking for green products (even at a more expensive cost) and those that meet current environmental regulations and standards (Freedonia 2017).

### 3.2. MATERIALS AND METHODS

The tailings were collected from a dam located in the state of Minas Gerais, Brazil (Figure 3.1), in accordance with normative instruction NBR 10007 (ABNT 2004). The IOT samples were air-dried, crushed in a jaw crusher (BB200, Retsch), sieved (150 $\mu$ m) and mixed to obtain a homogeneous raw IOT sample, which was stored in hermetically sealed plastic bags (Andrade 2014). One part of this sample was submitted to the dry-route segregation process proposed by Peixoto et al. (2012) in order to obtain iron ore concentrate, sand and clay.



**Figure 3.1. Localization of the iron ore tailing dams in Brazil.**

Iron ore concentrate has commercial value and defined destination, for this reason it was not used in this study. The IOT sand and raw IOT were used in substitution to the conventional fine aggregates (particles smaller than 300  $\mu\text{m}$ ) in the production of the HTs. The IOT clay and raw IOT were also used in the production of the pigments employed in substitution of the conventional ones. Table 3.1 shows the identifications of the tested pigments and the details of their production, including material used, firing and grinding conditions. Based on previous observations, the firing temperatures used in this study were 1050 °C and 1150°C. The firing procedures were carried out in a muffle furnace (JB3013, Jung) and the grinding process in a high-efficiency planetary ball mill (PM 100, Retsch), using zirconia balls (100  $\varnothing$ 10mm, 200  $\varnothing$ 5mm) and jar (250mL).

**Table 3.1. Identification of the pigments produced in this study, including the material used, firing and grinding conditions.**

<b>Pigment id.</b>	<b>Material</b>	<b>Firing temp. (°C)</b>	<b>Firing time (min.)</b>	<b>Grinding rotational speed (rpm)</b>	<b>Grinding time (min.)</b>
1050R	Raw IOT	1050	120	400	50
1150R	Raw IOT	1150	120	400	50
1050C	IOT clay	1050	120	400	10
1150C	IOT clay	1150	120	400	10

The binder used in this study was a high-early strength type III Portland cement (PC), specified in Brazil as CP-V (NBR 5735, ABNT 1991). This cement was chosen considering its reduced content of supplementary cementing materials (90-95% clinker, 0-5% limestone filler, 5% gypsum), and its high reactivity that favors the production of hydraulic tiles. The main technological properties of the cement were provided by the manufacturer and are shown in Table 3.2. A water-soluble synthetic polycarboxylate-based superplasticizer was used (SP, Powerflow4000 Mc Bauchemie – 0.2 wt.% by cement weight added in the mixing water). A river quartz sand and a commercial pigment

was used as reference materials. The river sand was obtained from a supplier from the city of Ponte Nova, in the state of Minas Gerais, and only the fraction passing through the sieve #50 (300 $\mu$ m) was used. The commercial pigment is a powder material, based on Fe<sub>2</sub>O<sub>3</sub>.

**Table 3.2. Technological properties of the Portland cement used in this study.**

Property	Result	Requirement (NBR 5735, ABNT 1991)
Insoluble residue (%)	0.97	≤ 1.0
Loss on ignition (%)	3.30	≤ 4.5
MgO content (%)	1.46	≤ 6.5
SO <sub>2</sub> content (%)	2.99	≤ 4.5
CO <sub>2</sub> content (%)	2.42	≤ 3.0
Blaine specific surface area (cm <sup>2</sup> /g)	4.74	≥ 3.0
Retained on #200 sieve (75 $\mu$ m) (%)	0.24	≤ 6.0
Initial setting time	130	≥ 60
Final setting time	183	≤ 600
Expansibility (Le Chatelier needle) (mm)	0.00	≤ 5.0
Compressive strength (1 days) (MPa)	27.0	≥ 14.0
Compressive strength (3 days) (MPa)	42.3	≥ 24.0
Compressive strength (7 days) (MPa)	46.4	≥ 34.0

A basic characterization work was carried out in the studied aggregates and pigments. Chemical composition was determined by X-ray fluorescence (Rayny EDX720, Shimadzu). Mineralogical characterization was carried out by X-ray diffraction (diffractometer D2 phaser Brucker, CuK $\alpha$  radiation, 20kV, 30mA, 2 $\theta$  range 5-75°, step size 0.01°, 1°/min). For this purpose, the ICDD PDF4+ v2016 crystallographic database and the software X'pert High-Score Plus V3 (Panalytical) were used. For these analyzes, samples with particle size smaller than 75 $\mu$ m were prepared by grinding in a planetary high-efficiency ball mill (PM 100 Retsch, zirconia balls and jar, 300 rpm, 5 min.). The physical characterization comprised particle size distributions by laser diffraction

(Bettersize 2000); real density by water pycnometry (NBR NM 52, ABNT 2006); bulk density by weighing known volumes of granular material (NBR NM 45, ABNT 2006); and moisture content by weighing and oven-drying (NBR 9939, ABNT 2011). The morphological aspects were observed using images obtained by scanning electron microscopy (SEM, S-4100 Hitachi).

Thermogravimetric analysis (TGA) was also performed on the raw IOT and IOT clay in order to obtain information on the weight changes of the materials (subjected to temperature variation in a controlled atmosphere) and information on physical phenomena such as oxidation/reduction, hydration/dehydration, among others. A STARE System Metler Toledo equipment was used and the tests were carried out in an inert atmosphere of N<sub>2</sub> (25mL/min.), with a temperature range of 50 - 1000°C and a heating rate of 10°C/min.

The HT are composed of a high flow mortar, which materials were proportioned obeying the ratio 1 : 2 (PC : aggregate), or 1 : 2 : 0.1 (PC : aggregate : admixture). Table 3.3 shows the identification of the HTs produced, materials used and proportioning.

**Table 3.3. Identification of the HTs produced, materials used and proportioning.**

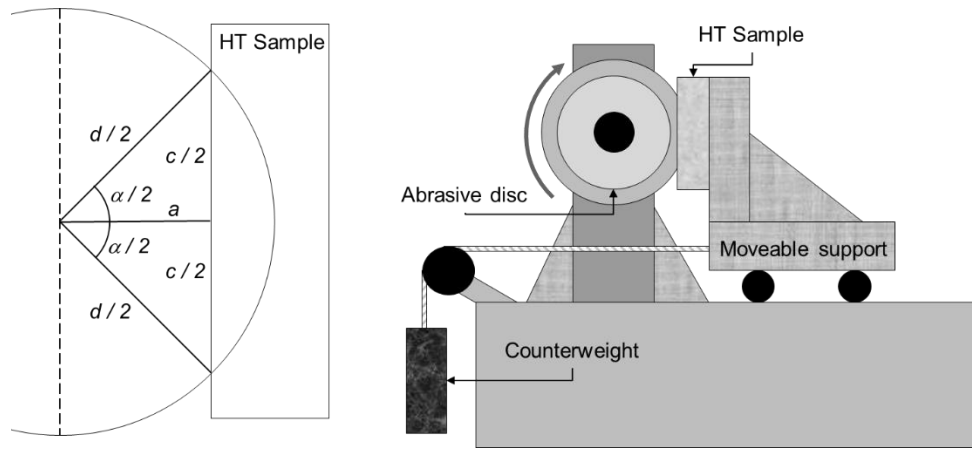
HT id.	Proportion	Materials
HT-REF	1 : 2	PC : river sand
HT-R	1 : 2	PC : raw IOT
HT-S	1 : 2	PC : IOT sand
CHT-REF	1 : 2 : 0.1	PC : river sand : commercial pigment
CHT-1050R	1 : 2 : 0.1	PC : river sand : 1050R
CHT-1150R	1 : 2 : 0.1	PC : river sand : 1150R
CHT-S-1150R	1 : 2 : 0.1	PC : IOT sand : 1150R
CHT-1050C	1 : 2 : 0.1	PC : river sand : 1050C
CHT-1150C	1 : 2 : 0.1	PC : river sand : 1150C
CHT-S-1150C	1 : 2 : 0.1	PC : IOT sand : 1150C

The kinematic viscosity of the mortars was set at 213.32 mm<sup>2</sup>/s and the water and SP contents for each mixture were provided and verified using a Ford viscosity cup (stainless steel cup, 105.7 cm<sup>3</sup> volume, Ø6 mm<sup>2</sup> brass orifice, 21s flow time, 25±1°C without airflow). Three determinations were performed within a time interval of 4 minutes after mechanical mixing (5 minutes mixing time, mixer Philips RI1342/02 300W). The HTs were then produced with the fresh mortars in a single layer using a carbon steel formwork with acetate-coated base in order to provide a smooth and luster surface. The tiles were demolded after 8h and the wet curing were performed in a wet chamber for 7 days (25°C, 90% relative humidity).

The characterization of the produced HTs comprised: (a) water absorption, void index and real density by oven-dried weighing, saturated surface dry weighing and immerse weighing NBR 9778 (ABNT 2005); (b) three-point flexural tensile strength in an EMIC DL 20000 universal test machine with a load cell of 200kN and load application rate of 50 N/s [NBR 13818 (ABNT 1997)]; (c) analysis of dimensional variation comprising measurements and comparisons under different conditions (oven drying at 110°C until mass stabilization and water saturation for 72h of immersion); and (d) resistance to deep abrasion.

The resistance to deep abrasion test consisted of an adaptation of the Brazilian standard NBR13818 (ABNT 1997) using a diamond saw replacing the standard steel disc and abrasive granular material. An illustrative schematic of the apparatus is shown in Figure 3.2 and consists of a circular diamond saw (Ø107.1mm and 2mm thick) assembled in an angle grinder securely attached to a support (9557HNG Makita / 11,000 rpm). A 186.55g counterweight was used in order to ensure constant pressure of the tiles against the saw.

The test time was set in 10s and two determinations were performed in each tile. Five tiles were used in the test comprising 10 determinations for each tested mixture. The test result consists of the volume of material removed from the tile calculated by Equations 3.1 to 3.6, where C is the average length of the cavity (mm); d is the disc diameter (mm); h is the disc thickness (mm); a is the height of the triangle (mm);  $\alpha$  is the cavity angle (rad);  $A_t$  is the area of the triangle (mm<sup>2</sup>);  $A_s$  is the area of the sector of the circle with angle  $\alpha$  (mm<sup>2</sup>);  $A_c$  is the cavity area (mm<sup>2</sup>); and V is the cavity volume (mm<sup>3</sup>).



**Figure 3.2 – Schematic of the resistance to deep abrasion test apparatus and geometric parameters.**

**Equation 3.1**

$$\text{sen} \frac{\alpha}{2} = \frac{C}{d}$$

**Equation 3.2**

$$a = \sqrt{\frac{d^2 - C^2}{4}}$$

**Equation 3.3**

$$A_t = \frac{C \times a}{2}$$

**Equation 3.4**

$$A_s = \frac{\alpha \times d^2}{8}$$

**Equation 3.5**

$$A_c = A_s - A_t$$

**Equation 3.6**

$$V = (A_s - A_t) \times h$$

SEM images were used to observe the microstructure of the produced HTs. A TESCAN Vega3 microscope was used for generate the images from gold coated fragments of the samples.



A Colour variability test allowed to evaluate the performance of the obtained pigments and effectiveness of the proposed processes in improve their pigmentation properties. The tests comprised the evaluation of standard deviations of the RGB histograms of the colours reproduced in an electronic device from the pigments and from polished sections of the tiles. The lower the standard deviation, the lower the colour variability. The tests were applied in portions corresponding to an area of 10 x 5 mm<sup>2</sup> from images obtained from tiles measuring 30 x 10 mm<sup>2</sup>. The images were obtained using a high-resolution scanner (Scanjet G4050 hp, 1200dpi) and the final value were calculated by averaging the standard deviations of red, green and blue colours identified by an image processing software.

The colour differences between the pigments and tiles were evaluated using the DE (or Delta-E) method (Galvão et al. 2018). The method consists in obtaining a quantitative difference between two colours in the system RGB. The DE is a value between 0 and 100 representing as Euclidian distance between the spectra red, green and blue from two RGB systems. This is the method adopted by the International Comission on Illumination (CIE) because better represent the human perception of colour. A value below 2 is considered sensitively equivalent. The DE values were calculated according to Equation 3.7, and the conversion of RGB values into CIELAB color space L\*ab were performed using the ColorMine colour conversion (ColorMine.org 2018).

**Equation 3.7** 
$$\Delta E = \sqrt{(L_2^* - L_1^*)^2 + (a_2^* - a_1^*)^2 + (b_2^* - b_1^*)^2}$$

### 3.3. RESULTS AND DISCUSSION

#### 3.3.1. CHARACTERISATION OF AGGREGATES AND PIGMENTS

Table 3.4 gathers information about real (true) density, bulk density and moisture content of the materials, as well as their characteristic particle sizes D10, D50 and D90 (DN is the sieve mesh opening through which passes N% of the material). Raw IOT is the densest material due to the presence of larger amounts of residual iron ore. On the one hand, it indicates a promising pigmentation potential but, on the other hand, in larger amounts (e.g. use as aggregate), it will increase the density of the composite. In this sense, the IOT clay also presented almost similar density, indicating also large amounts of iron oxide, making it a promising pigment, but its use as aggregate is not reasonable given its fineness. In contrast, IOT sand has the lowest density among the IOT products, indicating low iron oxide content. For this reason, pigment potential is poor, but its use as aggregate is promising and low impact on the density of composites is expected.

**Table 3.4. Physical characteristics of the samples (R denotes raw samples fired and C denotes clay fractions fired).**

Sample	Real density (g/cm <sup>3</sup> )	Bulk density (g/cm <sup>3</sup> )	Moisture content (%)	D <sub>10</sub> (µm)	D <sub>50</sub> (µm)	D <sub>90</sub> (µm)
River sand	2.69	1.54	0.06	20	100	200
Raw IOT	3.37	1.42	0.14	5	80	170
IOT sand	3.03	1.62	0.30	20	70	140
IOT clay	3.34	0.53	1.74	2	10	30
Ref. pigment	4.26	0.56	0.31	0.6	1.8	7.2
1050R	3.12	0.95	0.31	0.8	2.9	24
1150R	3.04	0.78	0.45	0.7	2.3	18
1050C	3.87	1,13	0.20	0.7	3.3	59
1150C	4.04	1,00	0.22	0.8	2.5	13

The chemical composition given by the XRF analysis (Table 3.5) confirms the high amounts of iron oxide in both raw IOT (36.3%) and IOT clay (57.3%), as well as the

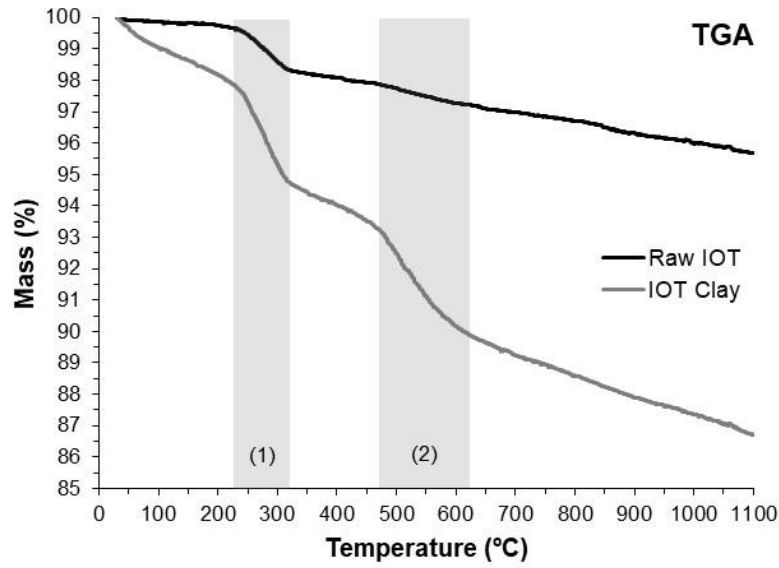
reduced Fe content in IOT sand. Si was the other major constituent present in small amounts in IOT clay (20.0%) and in large amount in the IOT sand (79.2%). A considerable amount of Al was observed in the IOT clay (18.8%), confirming its clayey nature. The results also indicate that the proposed segregation method (Peixoto, Oliveira & Barros 2012) proved to be highly effective as a chemical-mineralogical separator in the obtention of a high-purity quartz sand and a Fe-rich clay from the raw IOT.

**Table 3.5. Chemical composition of the samples (XRF, expressed as wt.% oxides).**

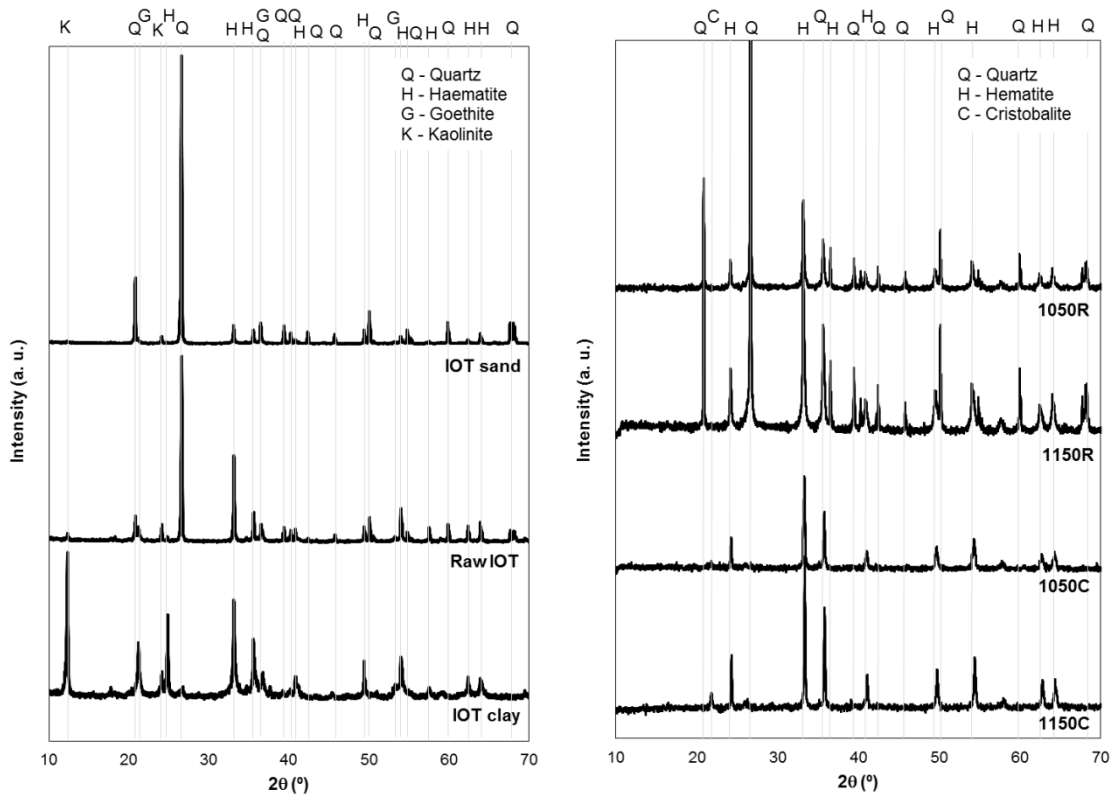
Sample	Al <sub>2</sub> O <sub>3</sub>	SiO <sub>2</sub>	P <sub>2</sub> O <sub>5</sub>	K <sub>2</sub> O	CaO	Fe <sub>2</sub> O <sub>3</sub>	MnO	Other	LoI*
River sand	31.3	59.6	0.0	1.7	0.5	5.8	0.1	1.1	0.3
Raw IOT	5.0	58.1	0.0	0.1	0.2	36.3	0.3	0.1	2.4
IOT sand	3.1	79.2	0.0	0.1	0.1	16.8	0.1	0.7	1.1
IOT clay	18.8	20.0	0.6	0.3	0.3	57.3	2.6	0.0	9.4
Ref. pigment	0.0	0.0	0.0	0.0	4.3	92.1	2.5	1.1	0.0
1050R	3.2	52.4	0.2	0.0	0.0	43.8	0.2	0.2	0.0
1150R	3.4	52.3	0.7	0.0	0.0	41.3	0.2	2.1	0.0
1050C	10.1	13.9	0.14	0.0	0.2	74.1	1.4	0.1	0.0
1150C	10.0	13.4	0.34	0.0	0.1	74.6	1.4	0.1	0.0

\*Loss on ignition (1000°C)

Firing produced reduced changes in density for the raw IOT samples (-7.4% and -9.8% for 1050R and 1150R, respectively) but significant increases were observed for IOT clays (+15.9% and +21.0% for 1050C and 1150C). It indicates formation of denser crystalline phases during firing for IOT clays. In this sense, calcined samples of IOT clay showed higher intensities in de-hydroxylation of kaolinite (~450-600°C) and reduction of goethite into haematite (~230-330°C), as shown by the weight losses in the thermalgravimetric analysis curves presented in Figure 3.3 (Ferreira et al. 2012). These observations are confirmed by the diffractograms of the studied materials (Figure 3.4), which also show the appearance of the peak of cristobalite in sample 1150C.



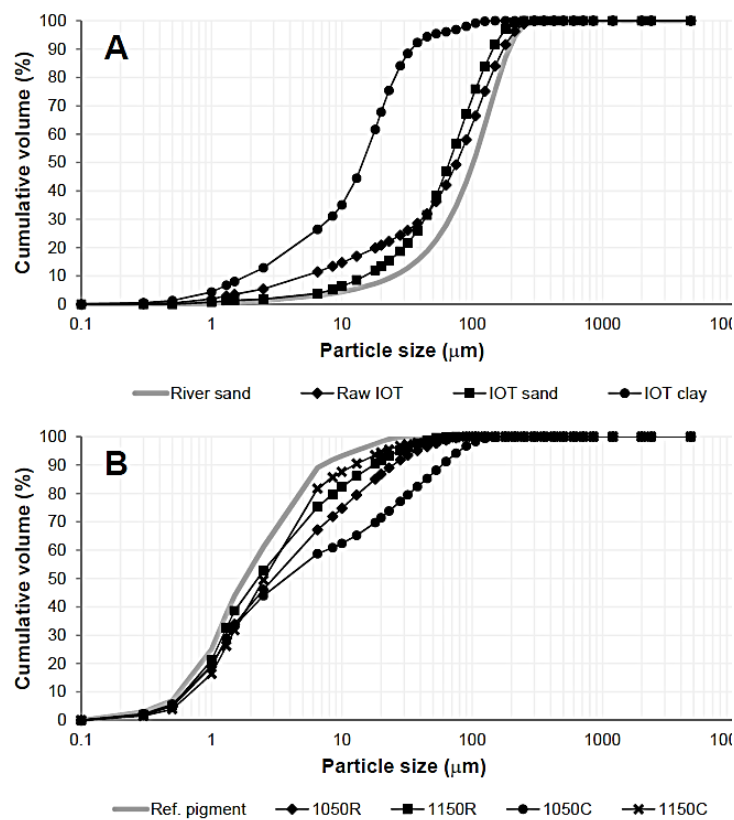
**Figure 3.3. Thermogravimetry (TGA) of the raw IOT and IOT clay, highlighting (1) reduction of goethite into haematite and (2) de-hydroxylation of kaolinite.**



**Figure 3.4. Mineralogical composition of the samples (crystalline phases as determined by XRD).**

The moisture content was higher in the IOT clay, which also showed the greater difference between real and bulk densities (worse particle packing). Both observations

are attributable to the clay minerals crystallography, and particle size and morphology. In addition, the proposed grinding programs were effective in promoting greater homogeneity and particle size distributions close to that presented by the commercial pigment (Figure 3.5). However, the raw IOT required a 5x longer grinding time compared to the IOT clay (Table 3.1), which is an economic and environmental disadvantage given the higher energy consumption. The temperature influenced the grindability, since better performances were observed in the IOT pigments burned at 1150°C [Figure 3.5 (B) and Table 3.4]. Figure 3.5 (A) also shows that the Raw IOT and IOT sand presented a wider particle size distribution, similar to that of the river sand and different from the IOT clay curve. The broad aspect of the particle size curve indicates a good particle-packing performance of the granular materials in the LH matrix, fundamental for a lower voids index and, consequently, better performance of the product.

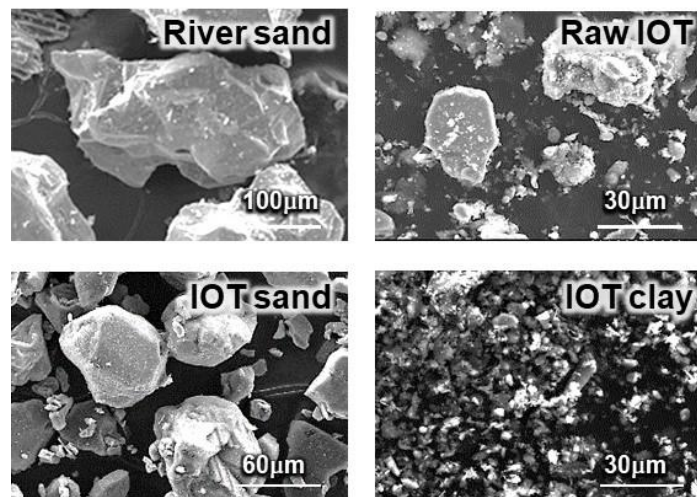


**Figure 3.5. Particle size distributions of the powder samples: (A) River sand and non-heat-treated IOT-based materials; (B) Reference and IOT pigments.**

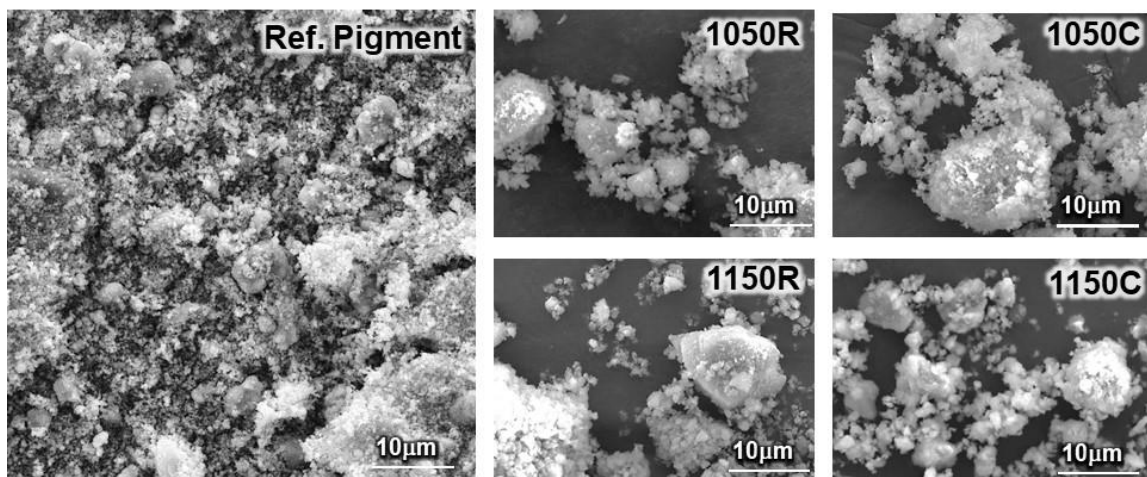
The particle size distribution also plays an important role in influencing the reaction kinetics of pigment-forming compounds, whereby finer materials are always indicated for use as pigment (particle size < 50 µm) (Barros et al. 2005). In this sense, the grinding process of the burned samples made them sufficiently thin, which contributes for a better dispersion of the material in the matrix and the higher specific surface area contributes to the hue. However, the particles that constitute the tailings present an irregular morphological aspect that can impair the dispersion (Figure 3.6).

The Raw IOT comprises larger and predominantly volumetric quartz particles with moderate roughness and sharp edges. A great number of small particles consisting of clay minerals are also observed (some of them adhered into larger quartz particles). Is noticeable a clear separation of these two categories in the SEM images of IOT sand and IOT clay, and the XRF results (Table 3.5) confirm the different mineralogical nature of these two materials. The worst particle shape of the IOT clay is evidenced by its bulk density and is observed in the SEM images. Calcination and grinding improved the particle shape, making them more volumetric with smoothed edges, as observed in the SEM images of the IOT pigments (Figure 3.7). This is a promising result, once a favorable particle shape is critical for a good flow performance and ability to fill voids between coarse particles.

The good particle-packing performance of the IOT pigments is confirmed by the better results of bulk density. Among the pigments, the worst particle shape was presented by the commercial reference material, as observed in the micrographs and confirmed by the reduced bulk density, which explains its worst particle-packing performance (Table 3.4).



**Figure 3.6 - Photomicrographs (SEM) of the reference river sand and raw IOT, IOT sand and IOT clay**



**Figure 3.7 - Photomicrographs (SEM) of the reference and proposed IOT-based pigments**

### **3.3.2. PHYSICAL AND MECHANICAL PERFORMANCE OF CEMENT TILES WITH THE STUDIED AGGREGATES AND PIGMENTS**

Table 3.6 presents the results of fluidity test and shows that the lowest water demand among all tested mixtures (for the required flow) was observed for the HT-REF (w/b = 0.5), which is expected, considering the reduced fines content and the favourable shape

of the river sand. The mixtures without pigment, but with IOT sand and raw IOT presented a significant increase in w/b ratio (+20%) due to their less favourable particle shape (angular with sharp edges) and higher specific surface area (increased fineness). By adding the powdery pigment, the specific surface area increases and the water demand increased as expected (+8% for 1050R, 1150R and 1050C; +12% for 1150C; and 14% for the reference pigment). In this sense, a very good agreement with the fineness is observed. Finally, combining the IOT sand with the pigments, the water demand increased considerably reaching the highest value in the mixture CHT-S-1150C (a/c = 0.78).

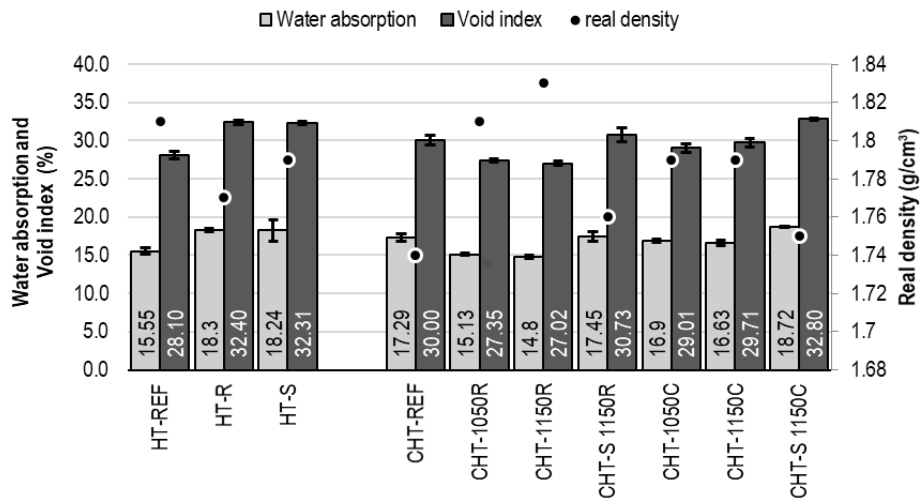
**Table 3.6. w/b ratios as a result of the fluidity test performed in the proposed mixtures.**

<b>HT</b>	<b>W/B RATIO (WEIGHT)</b>
<b>HT-REF</b>	<b>0.50</b>
<b>HT-R</b>	<b>0.60</b>
<b>HT-S</b>	<b>0.60</b>
<b>CHT-REF</b>	<b>0.57</b>
<b>CHT-1050R</b>	<b>0.54</b>
<b>CHT-1150R</b>	<b>0.54</b>
<b>CHT-S-1150R</b>	<b>0.63</b>
<b>CHT-1050C</b>	<b>0.54</b>
<b>CHT-1150C</b>	<b>0.56</b>
<b>CHT-S-1150C</b>	<b>0.78</b>

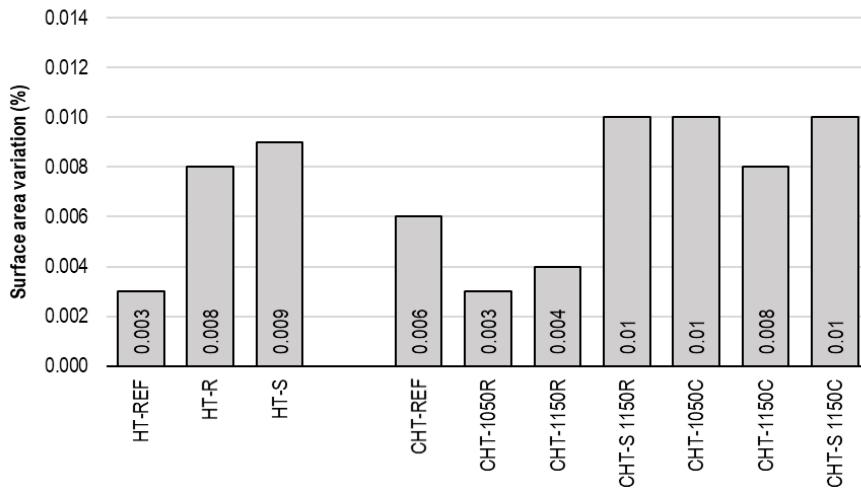
The results of water absorption and void index of the hardened HTs are in good agreement with the w/b ratios observed (Figure 3.8). In fact, for higher w/b ratios, more porosity is expected. The relative proximity of the void index results of the mixtures HT-REF, CHT-1050R (-3%), CHT-1150-R (-4%), CHT-1050C (+4%) and CHT-1150C (+6%) evidence this, but the slightly reduced values for the water absorption observed in the tile CHT-1150R (-5%) in association with its higher density among all tested tiles (1.826 g/cm<sup>3</sup>,



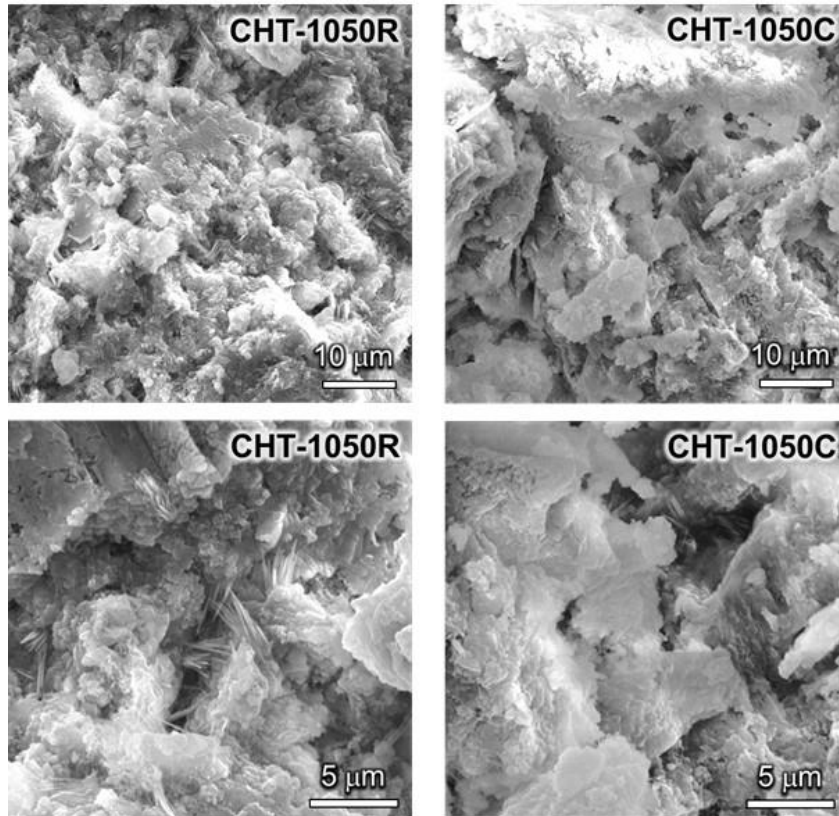
1.7% higher than HT-REF) indicates an increase in the hydration degree, compensating the higher w/b ratio compared to HT-REF (+8%). All these observations had implications in the surface area variation by water absorption, which results are closely related (Figure 3.9). In addition, comparing the micrographs of the CHT-1050R and CHT-1050C, it was possible to observe a denser and less porous structure in the first one (Figure 3.10).



**Figure 3.8. Physical characteristics of the hydraulic tiles samples.**



**Figure 3.9. Dimensional variation of the hydraulic tiles samples, comprising measurements and comparisons under different conditions (oven-dried and water saturated).**

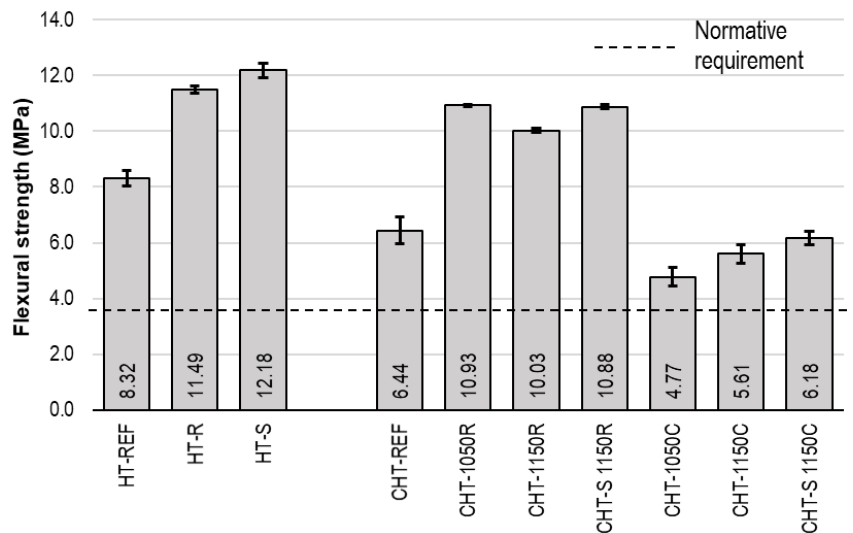


**Figure 3.10. Micrographs (SEM) of the tiles CHT-1050R and HT-1050C.**

In the most of the cases, the incorporation of IOT in the cement matrices increased the porosity, which is evidenced by the absorption values and void indices (i.e. a measure of the accessible voids), but mainly by the reduction in the density values (that is an indication of increase in the volume of inaccessible voids). This fact is even more evident considering the high density of IOT and the Fe-based commercial pigment. In this sense, their air-entraining properties and ability in induce formation of inaccessible voids are shown.

Further evidences of increasing in the hydration degree is provided by the mechanical results observed for HT-R, HT-S, CHT-1050R, CHT-1150R and CHT-S-1150R (Figure 3.11). Despite their increased w/b ratios compared to HT-REF, all of them reached superior tensile strength. In this sense, the results presented by the HT-R (+38%), HT-S

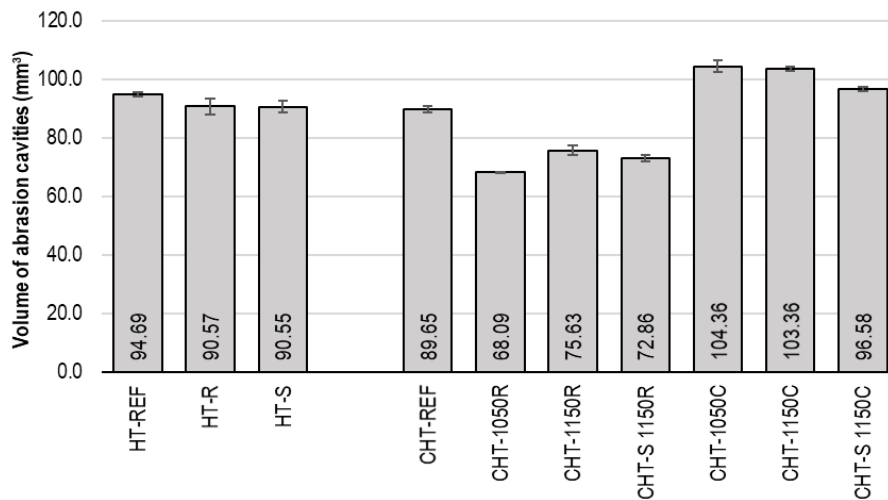
(+46%) and CHT-S-1150R (+31%) deserve to be highlighted, since they show the good performance of the IOT sand (and even the raw IOT) as fine aggregate in cement-based composites. The pigments produced from raw IOT presented the best mechanical performance in the tested matrices, with results even better compared to HT-REF, suggesting an interesting action as supplementary cementing material (+31% for CHT-1050R; +21% for CHT-1150R; and +31% for CHT-S-1150R). On the other hand, the pigments obtained from clay IOT did not presented the same performance, on the contrary, they showed the worst mechanical results (-43% for CHT-1050C; -33% for CHT-1150C; and -26% for CHT-S-1150C), which are not so different from that observed for the commercial pigment (-23%). Although, all tested samples presented flexural strength higher than the minimal requested for HTs [3.5 MPa according to NBR13818 (ABNT 1997)].



**Figure 3.11. Flexural tensile strength of the hydraulic tiles samples.**

Finally, the results of resistance to deep abrasion presented in Figure 3.12 are in good agreement with the results of flexural strength and void index. However, the IOT-free and pigment-free sample HT-REF presented a result comparable to the worst results, observed




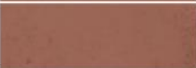
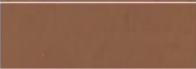


for CHT-1050C (+10.2%), CHT-1150C (+9.2%) and CHT-S-1150C (+2%). In this sense, the contribution of the burned IOT clay with the abrasion resistance was null. In fact, the reduced mechanical competence of the burned IOT clay was already demonstrated by its grindability. Better results, but also almost similar, were observed for HT-R (-4.3%), HT-S (-4.4%) and CHT-REF (-5.3%). In these cases, the increase in porosity was compensated by the presence of more mechanically competent aggregates (HT-S and HT-R) and powders (HT-R and reference pigment). The best performances observed in the CHT-1050R (-28.1%), CHT-1150R (-20.1%), and CHT-S-1150R (-23.1%) are result of the good mechanical performance of the mortars, low porosity and mechanical competence of the IOT powders and aggregates.



**Figure 3.12. Resistance to deep abrasion of the hydraulic tiles samples.**

### 3.3.3 PIGMENTATION PERFORMANCE EVALUATION

All the pigments presented brown coloration, but the IOT pigments showed different shades between them and in comparison with the reference pigment, according the results of RGB colour histogram analysis (Figure 3.13).

Materials id.	Colour	R	G	B	M.S. Dev.
Ref. pigment		105	80	72	3.9
Raw IOT		162	117	85	1.0
1050R		156	101	81	0.8
1150R		154	101	85	1.9
Clay IOT		139	97	73	1.3
1050C		103	77	69	2.0
1150C		89	77	77	1.7

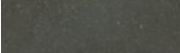


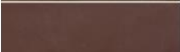



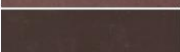

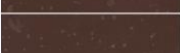
**Fig 3.13. Standard deviations of the RGB colour histograms obtained from the crude IOT materials (Raw IOT and IOT clay) and studied pigments (Reference pigment, 1050R, 1150R, 1050C and 1150C).**

The predominance of earth metallic oxides contributed for their characteristic ochre coloration. A change from original brown-yellow-ochre shade of the Raw IOT and IOT clay to a brown-red-ochre shade was observed. The cause is probably the conversion of goethite into haematite for the thermal de-hydroxylation. The Raw-IOT pigments showed less intense shades due to their greater amount of impurities (quartz). Regarding color variability, the tailing pigments were more homogeneous than the commercial pigment, since all of them presented reduced RGB averages standard deviations in comparison to the reference pigment.

Furthermore, the burning process, besides changing the original colour of the tailings, contributes to the chemical inertization of the produced pigments, improving their resistance to light, air and moisture, or combinations of these agents. On the other hand, the burning process in high temperatures (above 1000°C) causes sintering and consequent

increase in the average particle sizes. In this sense, grinding is necessary to enable the application of these materials as pigment in cement-based composites ( $D_{50} < 5\mu\text{m}$ ).

Regarding the tiles, the results presented in Figure 3.14 show that those produced without pigments presented great colour variability, since they are produced with different types of aggregates. The samples produced with river sand (HT-REF) presented considerable colour heterogeneity (average standard deviation of 1.3), due to the heterogeneity of the river sand. HT-R presented an intermediate colour variability (average standard deviation of 1.8) and a darker brown coloration in relation to HT-S, due the increased Fe content. Reduced color variability was observed in HT-S (0.9), as a result of the high quartz content of the IOT sand.

HT id.	Colour	R	G	B	M.S. Dev.
HT-REF		78	80	71	1.3
HT-R		86	74	64	1.8
HT-S		105	89	71	0.9
CHT-REF		94	66	59	1.4
CHT-1050R		112	72	68	2.0
CHT-1150R		115	75	75	3.0
CHT-S 1150R		114	82	78	1.1
CHT-1050C		72	56	52	1,3
CHT-1150C		77	52	45	1.1
CHT-S 1150C		77	53	45	0.6

**Figure 3.14. Standard deviations of the RGB histograms of the colours of the tiles produced without pigment (HT-REF, HT-R and HT-S) and tiles produced with pigments (CHT-REF, CHT-1050R, CHT-1150R, CHT-S-1150R, CHT-1050C, CHT-1150C and CHT-S-1150C).**

Table 3.7 shows that the burning process contributed to the greatest difference between the shades of Clay IOT and 1050C ( $\Delta E = 15.6$ ), while the color difference was lower between the raw and burnt IOT ( $\Delta E = 8.8$ ). The increase in firing temperature played an important role in the color change of the IOT clay ( $\Delta E$  of 8.7 between 1050C and 1150C), but lower influence was observed for the Raw IOT ( $\Delta E$  of 2.7 between 1050R and 1150R).

**Table 3.7.  $L^*a^*b^*$  and  $\Delta E$  parameters of the IOT-based materials and produced tiles.**

Id	$L^*$	$a^*$	$b^*$	$\Delta E$
RAW IOT	53.0	13.7	24.6	8.8
1050R	48.2	19.8	20.4	
1050R	48.2	19.8	20.4	2.7
1150R	48.0	19.4	17.8	
Clay IOT	45.0	14.0	20.5	15.6
1050C	35.2	9.7	9.0	
1050C	35.2	9.7	9.0	8.7
1150C	33.9	5.0	1.8	
CHT 1050R	35.0	16.6	9.4	2.8
CHT 1150R	36.3	17.0	7.0	
CHT 1150R	36.3	17.0	7.0	4.6
CHT S 1150R	38.1	12.8	7.6	
CHT 1050C	25.1	6.4	5.2	5.4
CHT 1150C	24.4	10.2	8.9	
CHT 1150C	24.4	10.2	8.9	0.8
CHT S 1150C	24.7	9.6	9.3	

\* RGB converted into CIELAB  $L^*ab$  colour space values (ColorMine.org 2018).

CHT-1050R and CHT-1150R presented a low color difference ( $\Delta E = 2.8$ ), as also observed for the corresponding pigments ( $\Delta E = 2.7$ ). In this sense, the increase in the firing temperature was not effective. On the contrary, considerable differences were observed for the pigments 1050C and 1150C ( $\Delta E = 8.7$ ), as well as for their corresponding tiles ( $\Delta E = 5.4$ ). The pigment 1150C presented the best dispersion and colour stability, as

indicated by the observed colour equivalence of its corresponding tiles CHT-1150C and CHT-S-1150C ( $\Delta E = 0.8$ ), even with the significant differences of their aggregates.

### **3.4. CONCLUSION**

The results of this study demonstrate that IOT is a strategic material for use as aggregate and pigment in cement-based composites, as well as in hydraulic tiles, once the produced tiles using IOT presented satisfactory physical and mechanical performances.

The Fe-rich raw IOT used in high amounts (e.g., as aggregate) make the composite denser and with a colour brown-ochre similar to composites produced with commercial pigment. The higher specific surface area and its particle shape (tabular and angular with sharp edges) impairs the fluidity, requiring an increased water consumption. However, it did not compromise the mechanical performance given its fineness and particle composition, favouring the composite hydration. In addition, subjected to firing and grinding, the raw IOT developed improved pigmentation potential, and promising properties for use as supplementary cementing material.

The used dry-route segregation method proved to be highly effective as chemical-mineralogical separator in obtaining high-purity quartz sand and Fe-rich clay from raw IOT. When fired and grinded, the IOT clay developed improved pigmentation properties, but presented the worst mechanical performances when used as addition in the composites. These results, however, are not so different from that observed for the reference commercial pigment. In addition, all tested samples presented flexural tensile strength higher than the minimum required (3.5 MPa).



### 3.5. ACKNOWLEDGMENTS

We gratefully acknowledge the agencies FAPEMIG, CNPq, CAPES, UFOP and Fundação Gorceix for providing financial support. We are also grateful for the infrastructure and collaboration of the Research Group on Solid Wastes - RECICLOS - CNPq.

The authors would like to acknowledge the Nanolab Electronic Microscopy Laboratory, at the Redemat, UFOP and the Department of Materials and Ceramic Engineering, CICECO, from Universidade de Aveiro.

### 3.6. REFERENCES

ABNT, 2006. *NBR NM 45: Aggregates – Determination of the unit weight and air-void contents*. Rio de Janeiro: Associação Brasileira de Normas Técnicas - ABNT (in Portuguese).

ABNT, 2009. *NBR NM 52: Fine aggregate – Determination of the bulk specific gravity and apparent specific gravity*. Rio de Janeiro: Associação Brasileira de Normas Técnicas - ABNT (in Portuguese).

ABNT, 1991. *NBR 5733: High early strength Portland cement - Specification*. Rio de Janeiro: Associação Brasileira de Normas Técnicas - ABNT (in Portuguese).

ABNT, 2013. *NBR 9457: Hydraulic tiles to paving - Specification and test methods*. Rio de Janeiro: Associação Brasileira de Normas Técnicas - ABNT (in Portuguese).

ABNT, 2011. *NBR 9939: Coarse aggregate – Determination of total moisture content – Test method..* Rio de Janeiro: Associação Brasileira de Normas Técnicas - ABNT (in Portuguese).

ABNT, 2005. *NBR 9778: Hardened mortar and concrete - Determination of absorption, voids and specific gravity*. Rio de Janeiro: Associação Brasileira de Normas Técnicas - ABNT (in Portuguese).

ABNT, 2004. *NBR 1007: Sampling of solid waste*. Rio de Janeiro: Associação Brasileira de Normas Técnicas - ABNT (in Portuguese).

ABNT, 1997. *NBR 13818: Ceramic tiles – Specification and test methods*. Rio de Janeiro: Associação Brasileira de Normas Técnicas - ABNT (in Portuguese).

Andrade, L.C.R., 2014. *Caracterização de rejeitos de mineração, in natura e segregados, para aplicação como material de construção civil*. Doctoral dissertation, Federal University of Viçosa, Brazil (in Portuguese).

FEAM, 2015a. *Dams management 2014*. Belo Horizonte: Fundação Estadual do Meio Ambiente - FEAM (in Portuguese).

FEAM, 2015b. *Dams inventory of Minas Gerais State*. Belo Horizonte: Fundação Estadual do Meio Ambiente - FEAM (in Portuguese).

Ferreira, M. M., Varajão A. F. D. C., Morales-Carrera, A. M., Peralta-Sánchez, M. G., Da Costa, G. M. Mineralogical and crystallochemical transformations originated from thermal essays on ferruginous kaolinitic clays. *Cerâmica* 58 (2012) 105-110.

Fontes, W. C., Fontes, G. G., Costa, E. C. P., Mendes, J. C., Silva, G. J. B., Peixoto, R. A. F. (2018). Sustainable Cement Tiles produced with Iron Ore Tailings: Technical Evaluation and Value Analysis. *Ambiente Construído* (in press).

Fontes, W. C., Mendes, J. C., Silva, S. N., Peixoto, R. A. F. (2016). *Mortars for laying and coating produced with iron ore tailings from tailing dams*. *Constr. Build. Mater.* 112 (2016) 988–995. <http://dx.doi.org/10.1016/j.conbuildmat.2016.03.027>

Freedonia. *News update: huntsman to launch separate pigment business in 2017*. Disponível em <https://www.freedoniagroup.com/industry-study/world-dyes-organic-pigments-3264.htm>, acessado em 10 de setembro de 2017.

Garcia, L.C., Ribeiro, D.B., Roque, F.O., Ochoa-Quintero, J.M., Laurance, W.F., 2017. *Brazil's worst mining disaster: Corporations must be compelled to pay the actual environmental costs*. *Ecological Applications* 27, 5–9. DOI: 10.1002/eap.1461.

IBAMA, 2015. *Preliminary technical report – Environmental impacts arising from the disaster involving the rupture of the Fundão dam, in Mariana, MG*. Brasília: Instituto Brasileiro do Meio Ambiente e dos Recursos Naturais Renováveis - IBAMA (in Portuguese).

IPEA, 2012. *Diagnosis of the solid wastes of the mining activity of non-energetic substances*. Brasília: Instituto de Pesquisa Econômica Aplicada - IPEA (in Portuguese).

LUZ, A. B. et al., “Beneficiamento do Rejeito de Moscovita da Região do Seridó-Borborema (NE) para Aproveitamento Industrial”. In: *Anais do XXI Encontro Nacional de Tratamento de Minérios e Metalurgia Extrativa*, pág. 199-205, Natal - RN, 2005.

Marques, J. de S. *Estudo do processo de produção de ladrilhos hidráulicos visando à incorporação de resíduos sólidos*. 2012. 157f. Tese (mestrado em Engenharia de Edificações e Saneamento) – Universidade Estadual de Londrina, Paraná. 2012.

Peixoto, R.A.F., Oliveira, J.R., Barros, J.B., 2013. *Process for segregation of iron ore contained in rejects from mining and processing of iron ore*. Brasil, Patent No. BR 10 2012 008758 8 A2 (in Portuguese).

SHETTIMA, A. U. et al. *Evaluation of iron ore tailing as replacement for fine aggregate in concrete*. *Construction and Building Materials*, v. 120, p. 72-79, 2016.

Tango, C. E. S. *Can I use colored pigments (Xadrez) in reinforced concrete?* Available in <http://piniweb.pini.com.br/construcao/noticias/posso-utilizar-pigmentos-coloridos-tipo-po-xadrez-em-concreto-armado-83858-1.aspx>, accessed in sept. 6 2016.

Yellishetty, M., Mudd, G.M., 2014. Substance flow analysis of steel and long term sustainability of iron ore resources in Australia, Brazil, China and India. *Journal of Cleaner Production* 84, 400–410. DOI: 10.1016/j.jclepro.2014.02.046.

# Chapter 4

---

**Iron ore tailings in the production of cement tiles: a value analysis on building sustainability**

#### **4. IRON ORE TAILINGS IN THE PRODUCTION OF CEMENT TILES: A VALUE ANALYSIS ON BUILDING SUSTAINABILITY**

##### **ABSTRACT**

The present work discloses the development of a sustainable cement tile (SCT) produced with Iron Ore Tailings from tailings dams (IOT). Initially, technical evaluation and environmental analysis of IOT were performed through physical, chemical and morphological characterisation, leaching and dissolution tests. Its feasibility as pigment was also investigated. Subsequently, the value analysis was performed, starting from an empathy map to a study on environmental, social and emotional values in the relationship between people and product. As result, the IOT presented fine, crystalline particles, no toxicity, and is technically feasible to be employed as filler, aggregate and pigment in the production of SCT. The colour layer of the SCT presented more homogeneous colour and less pores than conventional ones. Thus, the design of the SCT was developed, in both technical and aesthetics aspects, incorporating intangible values such as: environmental ideology, local identity, social expression, among others. In this sense, the present work seeks to assist in the decision-making process involving IOT as construction material. This study will thus contribute to the sustainability of the built environment, new research and market opportunities, and to reducing the environmental impact and risks associated the disposal of IOT.

**Keywords:** Sustainable Building Materials; Cement Tiles; Iron Ore Tailings; Value Analysis.

#### 4.1. INTRODUCTION

Brazil is currently one of the world leaders in exploitation of mineral resources. Billions of tons of metal ores are mined in the country every year, and millions of tons of tailings and wastes are disposed of, mainly in tailing dams (FIGUEIRÔA, 2014) (IBRAM, 2015). Since the beginning of the 18th century, the mining industry is concentrated in the state of Minas Gerais, responsible for the largest production of iron ore, gold, zinc and niobium of the country (IBRAM, 2014). In Minas Gerais are accounted 445 of the 663 tailings dams in the Brazil (FEAM, 2014). As a result of the high volumes of production and poor management of residues, a dam recently failed in Minas Gerais, leading to the release of 62 million cubic meters of iron ore tailings (IOT), several casualties, and an expressive impact on the ecosystems over a 100km radius (G1, 2015). Mining operations must be conducted in sustainable, economically feasible and socially acceptable manner (FRANKS, BOGER, et al., 2011). Waste management technologies that offer improved environmental and social performance should be preferentially adopted; including opportunities for reuse of tailings (EDRAKI, BAUMGARTL, et al., 2014).

The use of tailings in construction materials implies a significant reduction in the overall carbon footprint of a building; it also mitigates the consumption of natural resources and the impacts associated with their production (PAPPU, SAXENA e ASOLEKAR, 2007) (PASSUELLO, OLIVEIRA, et al., 2014). In this sense, as examples, Fontes, et al. (2016), Shettimma, et al. (2016), Zhao, et al. (2016), Ma, et al. (2016) and Yellishetty, et al. (2008) have successfully used it as aggregate; Pereira & Bernardin (2012) as colorant; Duan, et al. (), Cheng, et al. (2016) as geopolymer and binder. Iron ore tailings are mainly composed by iron oxides, silica and alumina, resulting in a fine, dense, stable and crystalline material (BASTOS, SILVA, et al., 2016), technically feasible to be employed in civil construction.

Regarding its behaviour on the cement matrix, in a previous work, Fontes, et al. (Mortars for laying and coating produced with iron ore tailings from tailing dams, 2016), tested mortars comprising IOT in full replacement of natural aggregates. The mortars with IOT reached compressive and flexural strengths superior than the conventional ones. In a similar work, matrices developed by Sant’Ana Filho, et al. (2016), with replacement of fine aggregate by IOT in proportions up to 80%, showed lower water absorption and more resistance to abrasion than their conventional counterparts.

Therefore, in order to contribute to the reduction of the environmental and social impacts of the disposal of IOT, the present work proposes a novel application for it – as both aggregate and pigment in sustainable cement tiles (SCT).

#### *4.1.1. CEMENT TILES*

Cement tiles are cement-based composite plates with high abrasion resistance used in walls and floors, indoor and outdoor. They have a flat surface, textured or embossed, coloured or not, usually square shaped (ABCP, 2010).

Historically, by the fourth century, the tiles were made up of pieces of coloured stones, with symbolic function to express the art and religion of the territories dominated by the Byzantine Empire (WAMZER, 2011). From the second half of the nineteenth century, the composition of the tiles evolved to Portland cement composites, pressed, dried and cured by immersion in water (WAMZER, 2011). This new constitution contributed to the technological gain of the cement tiles, hence motivating its large-scale adoption around the world.

Unvalued around the 1950s, due to competition with ceramic tiles, since 1980, architects, designers and decorators began again to appreciate coatings with cement tiles (CATOIA, 2007). This is a reflex of the current trend to seek traces of memory in the past, in order

to enhance value through intangible aspects such as nostalgia and emotion. The revival of cement tiles allowed for customized designs, and creating composition with other materials (CATOIA, 2007).

A cement tile is divided in two layers. The wear/colour layer, in the surface, is approximately 3-5mm thick, and comprises a fine mixture of white cement (WC), crushed white marble (CWM) or fine sand (0.075 to 0.6 mm) and conventional pigments (CP). The quality of this layer provides the abrasion resistance, the colour and brightness of the tile. The base layer, approximately 20mm thick, consists of a mortar of cement and medium sand (0.6 to 1.18 mm), and provides the mechanical strength. Both layers are compressed into one single tile by a specific set of moulds and a hydraulic press.

The manufacture of cement tiles in Brazil is mostly scattered among craft shops in the Southeast region, where most of the population - and tailings dams – are located. The initial investment is relatively low, as is the producer's educational requirements. The incorporation of IOT does not require adaptation on the production method, based on manual hydraulic press; that is, no energy is required for either acquiring equipment nor operating it.

To achieve a good relationship between product and user, the study of interfaces is critical to the market. It involves a value analysis through the integration of technical, production, and administrative sectors, as well as environmental, social and emotional factors. Thus, by incorporating intangible attributes, the development of more effective products is attained – that is – products that meet the intended use, as well as other consumer's expectations (GONTIJO, 2008).

#### 4.1.2. VALUE ANALYSIS

Value Analysis consists in the representation of technological evolution, given its approach from the birth of a need to its final conception (VARGAS, 2013) (PEREIRA FILHO, 1994). It is a systematic application of techniques to identify the main aspects of a product or a component and to provide the desired function at the minimum cost. Consequently, it enables analysing the return on investment of a new product and thus allows for the decision whether to continue the project or not. In the economic sphere, the real value of a product, process or system comprises the combination of specific values and represents the degree of acceptance by the customer, directly depending on local and temporal conditions (VARGAS, 2013).

Regarding the Methodology of Value (CSILLAG, 1995), economic value shall be divided into:

- Use value ( $V_u$ ): monetary measure of the qualities related to the performance of use;
- Esteem value ( $V_e$ ): monetary measure of the properties that make its possession desirable;
- Cost value ( $V_c$ ): monetary measure to produce or obtain a product; and
- Exchange value ( $V_x$ ): monetary measure that enables the exchange for other goods.

From the values described, there are two ways of analysing the exchange value of a product. For the consumer, by adding the values of use and esteem:

**Equation 4.1** 
$$V_x = V_u + V_e$$

For the producer, as the sum of the cost and a differential ( $\Delta V$ ), considered the profit:

**Equation 4.2** 
$$V_x = V_c + \Delta V$$

Therefore, combining both equations:

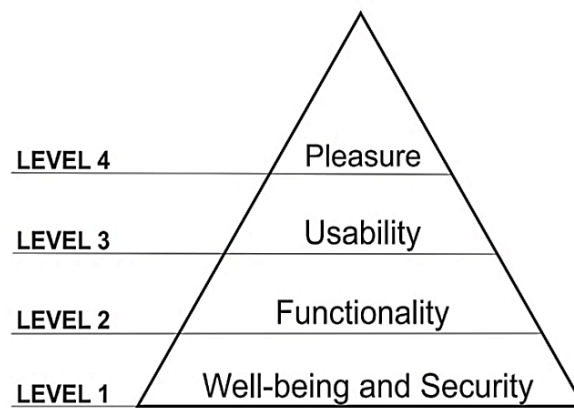
**Equation 4.3** 
$$V_u + V_e = V_c + \Delta V$$



Through this relationship, it is possible to infer that the higher the use value ( $V_u$ ) and esteem ( $V_e$ ) and the lower the cost value ( $V_c$ ), the greater the profit made on a product ( $\Delta V$ ).

#### 4.1.3. EMOTIONAL/ESTEEM VALUE

The emotion is closely linked to the relationship that people have with a product. Jordan (1999) presented a hierarchy of needs, considering that people demonstrate their experience with the product when they relate to it. This experience covers aspects of utility, functionality, ease of use, as well as sensory conceptions, as can be seen in Fig. 4.1. Hierarchy of user's needs for products (adapted from Jordan, ).



**Fig. 4.1. Hierarchy of user's needs for products (adapted from Jordan, (1999)).**

Fig. 4.1. Hierarchy of user's needs for products (adapted from Jordan, ) shows the pleasure at the top of the hierarchy of needs, representing the degree of pleasantness of people in interaction with objects. Therefore, when dealing with product design, the engineer / architect / designer can start by specifying the desired emotion as a result, such as social expression, environmental ideology, nostalgia, or sensory pleasures. Only then the professional evaluates the usability parameters, technical and safety aspects, considering whether it meets the required performance.

The esteem value of a product can be established by features that confer it beauty, prestige and admiration considering its aesthetic values, as well as connection and affection towards their symbolic values.

For a better understanding of the esteem value it is necessary to subdivide it in aesthetic value and symbolic value. The aesthetic value related to the semantics of the product, which consists of a suitable visual appearance its function. Thus, with respect to colours, shapes, textures and backgrounds, which include automatic emotional responses related to the first contact with the product (CREUSEN e SCHOORMANS, 2005). According to Kissmetrics (2010), 93% of consumers consider the appearance of the goods when shopping and 85% say the colour is the main reason they purchase a particular product.

In turn, the symbolic value of a product comprises the conception of memory and self-image, based on intrinsic and social values of each person (MIRANDA e CÂMARA, 2010). Thus, the symbolic functions are associated with socio-cultural relations, obtained through the social, historical and technological context of a country or region.

The reaffirmation of the local identity in products, to the extent that it establishes links and connections, creates a benchmark of authenticity in the midst of mass production and homogeneity that prevail since globalization. In this sense, one must unite characteristic elements of a culture: i.e. the fauna, flora, architecture, topography, religion, among others (MORAES, 2008).

In this sense, one notable example is the Lucky Iron Fish <sup>TM</sup>. In order to provide dietary supplementation of iron to underprivileged families affected by iron-deficiency anaemia in Cambodia, a group of researches distributed a rectangular iron bar for cooking. However, the women were reluctant to use the chunk of iron in the cooking pan. The solution came through design enhancement: the previous iron bars were replaced by fish-

shaped iron ingots, which carry strong cultural and historical bonds to the population. As a result, the iron fishes were received more positively by the villagers and led to immediate increases in blood iron levels amongst them. In addition, the iron fishes are cast from recycled metal, and employ the Cambodian community in the production line. Since the beginning of this project, the research group has delivered over 82,000 iron fishes around the world (LUCKY IRON FISH, 2016).

#### *4.1.4. SOCIAL VALUE*

According to the Brazilian Institute of Mining (2013), the strengthening of accountability and transparency is directly related to understanding of the mining industry's contributions to the development of the country. According to research conducted by the Ethos Corporate Social Responsibility Indicators concerning the perception of Brazilian consumers, 86% of respondents would increase their respect for a company if it became partner of a non-governmental organization or charity institution, with the purpose of solving social problems (RUSCHEL e ROSE, 2005). Therefore, the structure of the economy attributes to goods a particular social role. It is believed that the product carries an inexplicable power over the buyer, in order to satisfy their desires for attraction, ideology, identity, social expression, among others (LEDOUX, 1998).

#### *4.1.5. ENVIRONMENTAL VALUE*

Since the 1980s, intangible aspects such as image and corporate culture of companies have become their greatest asset (ESTY e WINSTON, 2009). According to Willard (2002), a company, when employing principles of social and environmental sustainability, has the potential to increase profits by up to 38%, its market value by 12% and productivity by up to 8%, due to the reduction of production costs and expenses, such as energy, water, raw materials, among others

In this scenario, customer demand for sustainable construction materials has also been boosted due to greater environmental awareness. Increased recognition of climate change is changing priorities as people remodel the way they live to reduce the impacts of their daily life on the environment. In fact, customers are seeking innovative solutions that would improve their quality of life, reduce their energy-related costs, while being environmentally-friendly (OBSERVATORY, 2014).

In conclusion, an investment in the intangibility of the product, i.e. the adoption of factors such as novelty and sustainability, is directly related to improvement in the tangibility of sales. In this sense, this work evaluates both the technical and intangible aspects of a SCT produced with IOT, aiming to develop the best possible building solution regarding design and material. Therefore, we seek to obtain an economically feasible product, whilst contributing to the reduction of the social and environmental impact of tailings dams.

## **4.2. METHODOLOGY**

Initially, an experimental program was undertaken to evaluate the technical and environmental feasibility of the use of IOT as aggregate and pigment in the production of SCT. Secondly, an empathy map was drawn based on the profile of one professional in interior design and one potential consumer seeking to identify all significant variables in the value analysis. Finally, an exploratory investigation was conducted to identify and apply intangible value on this product. Intangible aspects of this product were assessed through strategies proposed by the service design, in environmental, social and emotional levels. As a result of these studies, the SCT was developed.

### *4.2.1. TECHNICAL FEASIBILITY*

The proposed product is a sustainable cement tile (SCT), intended for use as floor tile, indoors and outdoors. In this work, IOT was employed as aggregate in the base layer and

pigment in the colour layer. The physical characterisation of IOT, CWM and sand comprised: particle size distribution by sieving and laser diffraction (Bettersize 2000 equipment), bulk specific gravity and apparent specific gravity. Tests were performed according to Brazilian standards NBR 7217 (ABNT, 1987), NBR NM 45 (ABNT, 2006) and NBR NM 53 (ABNT, 2003).

A Coleman Optical Microscope and a Scanning Electron Microscope (SEM), were used to investigate the microstructure of the tailings. Experiments and analyses involving electron microscopy were performed in the Nanolab Electronic Microscopy Laboratory, at the Redemat, UFOP; and the Materials Characterisation Laboratory, at CEFET, MG, Brazil.

Chemical characterization was carried out by a semi-quantitative energy dispersive X-ray fluorescence (XRF) in a PANalytical Epsilon 3X equipment. The DRX was carried out on a D2 PHASER from Bruker at Nanolab, Redemat, Federal University of Ouro Preto. The equipment operated with  $\text{CuK}\alpha$  radiation, 30 kV tension, 30 mA current intensity, angular velocity equal to  $0.02^\circ$ , 0.8-second step, and angular range between  $5^\circ$  and  $70^\circ$ . The analysis and refinement of results were performed using Rietveld method, on a X'Pert High Score Plus Panalytical software, aided by the Crystallography Open Database (COD) database of crystal structures. Fluorite ( $\text{CaF}_2$ ), brand VETEC, was used as internal standard, added in proportion of 10% to the IOT mass. The samples were weighed to a precision of four decimal places and homogenized in porcelain mortar.

According to the Brazilian standard, NBR 7211 (ABNT, 2009), the aggregate for cement-based composites must be an inorganic, crystalline and stable material. They must not present hazardous chemical substances, such as chlorites and sulphates (in concentrations above 0.2% and 0.1% respectively), or substances that may affect the hydration of the

cement (ABNT, 2009). Preferably, they must attend to optimum particle size distribution zones, i.e. the maximum content of material passing the #8 sieve (2.36 mm) must fall between 10% and 20% (ABNT, 2009). However, the standard states that materials with different particle size distributions may still be used, given that their applicability is proven. This is achieved by the morphological and chemical analysis.

#### *4.2.2. ENVIRONMENTAL FEASIBILITY*

Leaching and dissolution tests were performed to assess the level of contamination of the elements in the sample, according to standards NBR 10005 and NBR 10006, respectively (ABNT, 2004a) (ABNT, 2004b). These tests seek to reproduce the natural phenomena of carrier, dilution and dissolution that occur when water passes through a residue.

For the leaching test, Brazilian Standard prescribes the jar-test equipment for continuous stirring; no definite speed; and waste / deionised water ratio of 1:16. This standard uses 0.5N acetic acid as pH control (pH = 5). In turn, the dissolution test uses a waste / deionised water ratio of 4:1; 5-min stir; and 7-day rest. The leached and solubilised extracts are filtered in a 0.45 µm porous media. Subsequently, they are chemically analysed to identify several toxic organic and inorganic compounds.

According to the concentration of the substances in the leachate and solubilised extracts, the residue is classified, following the prescribed limits in standard NBR 10004 (ABNT, 2004c). Solid materials can be classified according to NBR 10004 (ABNT, 2004c) as Class I – dangerous, or Class II – non-dangerous. In addition, Class II is divided into Class II-A: non-inert and Class II-B: inert. In total, the tests evaluate 35 parameters, such as the pH, the concentration of arsenic, barium, cadmium, lead, sulphates, mercury, organic compounds, among others. The classification is based on the parameters that the samples exceed the stipulated limits.

#### 4.2.3. FEASIBILITY AS PIGMENT

The inorganic pigments used in cement tiles are fine particles, generally insoluble in water (LEE, LEE e YU, 2003). They are usually comprised of iron oxide and chromium oxide; which proportions vary according to the desired colour. In order to produce stable and aesthetically pleasing pigments, IOT was employed in 2 forms: in natura and fired. In both cases, the materials were oven-dried.

To obtain the fired IOT, the waste was initially segregated in its main components: iron ore, sand and clay; through a process performed by an outsourced company. This process involves drying, milling, density separation and magnetic separation without the use of water (PEIXOTO, BARROS e OLIVEIRA, 2014). It should also be noted that the segregation process makes it possible to recover iron ore from IOT, a material of greater economic interest.

The clay fraction was adopted in the present work. This fraction contains a higher concentration of iron oxide in the hematite and goethite phases than the raw IOT (ANDRADE, 2014). Furthermore, the sinter and calcination processes promote the conversion of goethite into hematite by dehydroxylation and, consequently, improves the pigmentation capacity of the material (TAVARES, 2012). For the preparation of the pigment, the clay from the IOT was fired at 950°C for 120 min in a muffle furnace (brand Jung JB3013), with temperature step of 3°C/min. Subsequently, it was grinded in a planetary ball mill (brand Retsch PM 100) for 10 min in rotation of 400 rpm. This fraction was adopted as pigment (P-IOT).

The SCT were fabricated according to the conventional technique called “Pastinha”, which refers to the high fluidity of the mortar in the colour layer. Specimens 5×5×2 cm were moulded in proportions 2:1 – white cement (WC):aggregate in mass (Fig. 4.2.

Sample of the colour layer with IOT as aggregate, for pigment evaluation.). Two types of aggregate were used: crushed white marble (CWM) and IOT in natura. On specimens with only CWM, contents of 5% and 10% of pigments were added – conventional and P-IOT. The conventional pigment (CP) is a brown inorganic synthetic material suitable for use in cement-based composites, produced by Lanxess and purchased directly on the market.



**Fig. 4.2. Sample of the colour layer with IOT as aggregate, for pigment evaluation.**

In all mixtures, 70ml of water was used (water/cement factor of 0.7). In total, nine mixtures were proposed using WC, CWM, CP, IOT and C-IOT both as aggregate and pigment, as shown in Figura 4.1. Mixtures T10 and T11 are dual colour, T1+T4 and T1+T8 respectively, developed seeking to access the possible mixing of colours.

**Table 4.1. Mixtures developed for the colour layer.**

	<i>WC (g)</i>	<i>CWM (g)</i>	<i>CP (g)</i>	<i>IOT (g)</i>	<i>P-IOT (g)</i>
<b>T1 - CWM</b>	100	50			
<b>T2 - 50% CWM + 50% IOT</b>	100	25		25	
<b>T3 -IOT</b>	100			50	
<b>T4 - CWM + 5% CP</b>	100	50	5		
<b>T5 - CWM + 10% CP</b>	100	50	10		
<b>T6 - CWM + 5% IOT</b>	100	50		5	
<b>T7 - CWM + 10% IOT</b>	100	50		10	
<b>T8 - CWM + 5% P-IOT</b>	100	50			5
<b>T9 - CWM + 10% P-IOT</b>	100	50			10



The colour range, surface quality and proportion of IOT as pigment were evaluated through visual inspection. As prescribed by Brazilian standard for cement tiles, NBR 9457 (ABNT, 2013), the material must present aspects such as homogeneity of colour, sharp edges, no cracks, visible burrs or flaws.

#### 4.2.4. VALUE ANALYSIS

According to the Methodology of Value (CSILLAG, 1995), when considering the use of IOT in the production of SCT, it is assumed to generate an increase in the profit of the product. This is achieved by reducing the cost, due to the replacement of natural aggregate by the recycled, IOT, and increasing the esteem value. The SCT's emotional/esteem value is related to the historical, architectural and artistic values of cement tiles, as well as the satisfaction provided to the consumer, who, when acquiring the product, contributes to the recycling of waste. On the assumption that the replacement of natural aggregate by IOT does not change the value in use of SCT, i.e. they have compatible technical aspects, we can summarize these considerations in the following equation:

**Equation 4.4** 
$$\Delta V = Ve - Vc$$

That is, reducing the cost of production and/or increasing the esteem value of cement tiles lead to higher profits.

##### 4.2.4.1. EMPATHY MAP

The Empathy Map assists on the understanding of the environment, behaviour, concerns, and aspirations that affect the users of a product (TSCHIMMEL, 2012). This method assists the design process based on the client perspectives, through a defined template and guide questions, displayed in Table 4.2 (OSTERWALDER e PIGNEUR, 2013). The empathy map in the present work was drawn based on personas representing one professional in interior design and one potential consumer. These hypothetical archetypes

of real users were evaluated in order to identify influences, needs, emotions and fears, related to the context of the SCT (FERREIRA, SILVA, et al., 2015) (ACUÑA, CASTRO e JURISTO, 2012). This tool has obtained excellent results in product development processes (RIBEIRO e SOUZA, 2014). In the present work, the user modelling technique served as a guide to understanding the intangible values associated with the SCT, through ideological mapping of feelings, thoughts, concerns and aspirations of potential consumers for the product.

**Table 4.2. Questions for developing the empathy map (Osterwalder & Pigneur (Business Model Generation, 2013)).**

Field	Guiding Questions	Field	Guiding Questions
<b>Do</b>	What is common for him / her to say?	<b>Think</b>	What are some important ideas that s/he thinks and does not say?
	How does s/he normally act?	<b>Feel</b>	How does s/he feel about life?
	What are his / her hobbies?		What bothers him / her lately? Why?
	What does he like to say?	<b>Pains</b>	What is s/he afraid of?
	How is the world in which s/he lives?		What are his / her frustrations?
	What do people around him / her do?		What has disturbed him?
	Who are his / her friends?		What would s/he like to change in his / her life?
	What is popular in his daily life?	<b>Needs</b>	What does s/he need to feel better?
	What people and ideas influence him / her?		What is success? What does s/he want to achieve?
	What do the important people in his / her life say?		What has s/he done to be happy?
	What are his / her favorite brands?		What would end his / her pain?
	Who are his / her idols?		What are some of his / her dreams?

#### 4.2.4.2. SURFACE DESIGN

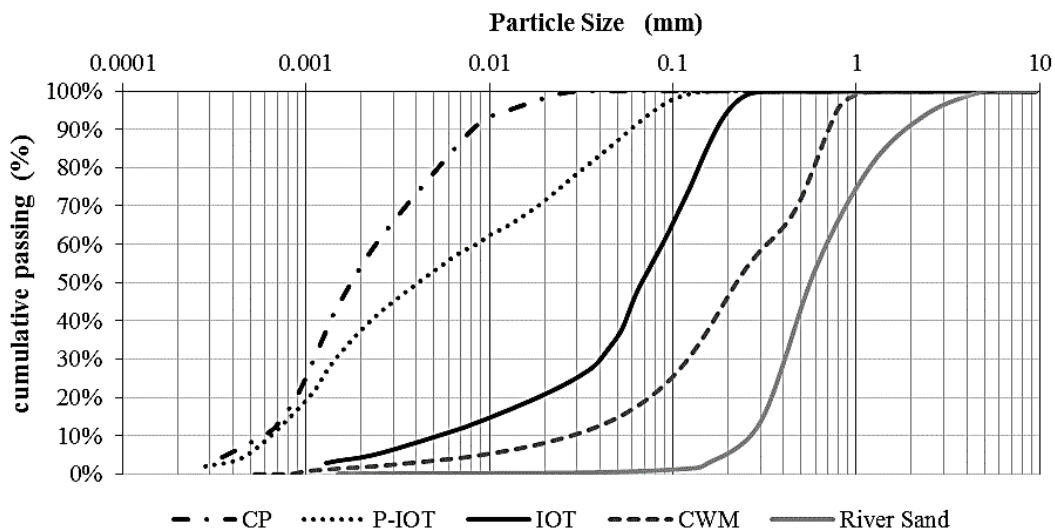
By relating the results of the Empathy Map, the colour range of IOT and a thorough investigation of the history of cement tiles, four design proposals were developed. They embrace shape, colour palette and illustration of the colour layer, seeking to incorporate value and to facilitate incorporation in the market.

### 4.3. RESULTS AND DISCUSSION

#### 4.3.1. TECHNICAL FEASIBILITY

According to Brazilian standard NBR 9457 (ABNT, 2013), aggregates for cement tiles may be natural, industrial or recycled. Therefore, the use of IOT as recycled aggregate is within the prescriptions of the standard.

Fig. 4.3 shows the particle size distribution of the materials. The characteristic dimensions, D10, D50 e D90 can be seen in Table 4. (where DN corresponds to the diameter of the sieve, in mm, above which N% passed). It is noticeable that the CP is a particularly fine material, with 90% of its particles smaller than 8  $\mu\text{m}$ . It is followed by the P-IOT, with 90% of the material smaller than 0.06 mm; IOT (0.17 mm); CWM (0.7 mm), and natural fine aggregate, river sand, with D90 of 1.8 mm.



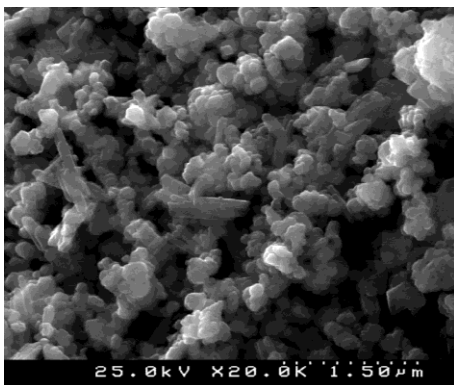
**Fig. 4.3. Particle Size Distribution of the Materials.**

**Table 4.3. Characteristic dimensions of the materials.**

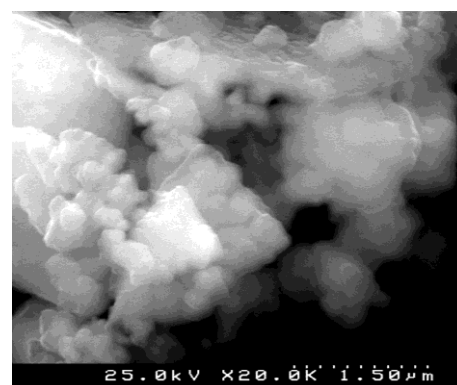
	CP	P-IOT	IOT	CWM	River Sand
<b>D10 (mm)</b>	0.0006	0.0003	0.0050	0.0300	0.3000
<b>D50 (mm)</b>	0.0020	0.0020	0.0800	0.2000	0.6000
<b>D90 (mm)</b>	0.0080	0.0580	0.1700	0.7000	1.8000

The particle size distributions of IOT and CWM are not within the optimum limits of aggregates for cement-base composites prescribed by Brazilian standard NBR 7211 (ABNT, 2009), due to their fineness. The small particle size distribution of the IOT may lead to an increase of the amount of water to obtain workability for the matrix, as is commonly observed for conventional pigments (BRUCE e ROWE, 1992). This effect will be probably more significant for CP. On the other hand, the fineness of the IOT enables it to be used as both pigment and filler on the colour layer, thus reducing the pores and enhancing its aesthetic aspects.

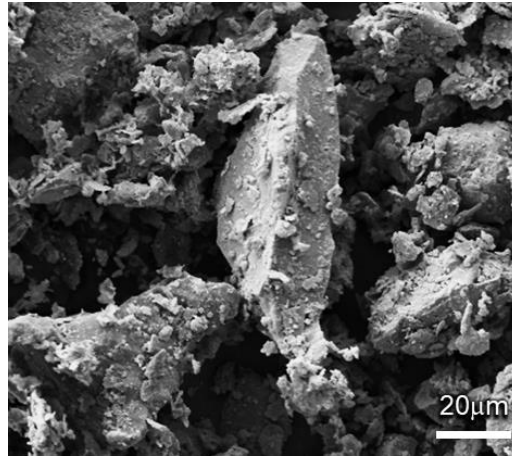
Concerning the microstructure (Fig. 4. to Fig. 4. the CP SEM predominantly presents fine, sub-rounded and tabular particles. Most of the P-IOT grains, both large and small, are also sub-rounded, due to the burning process. In the analysis, IOT particles show an irregular morphology, with a large amount of fines. Furthermore, as confirmed by the particle size distribution of the materials, river sand and CWM presented relatively larger particles, with the CWM ones slightly more angular than the others, due to its obtaining process.



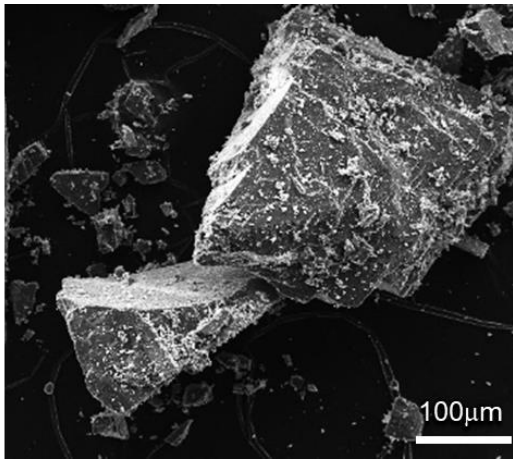
**Fig. 4.4. SEM of CP particles**



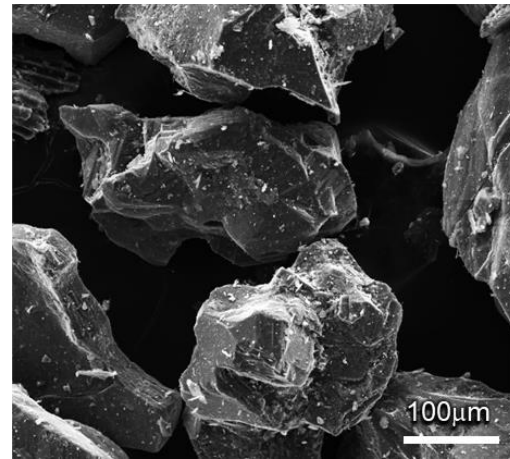
**Fig. 4.5. SEM of P-IOT particles**



**Fig. 4.6. SEM of IOT particles**



**Fig. 4.7. SEM of CWM particles**



**Fig. 4.8. SEM of River Sand particles**

Table 4.4 shows the physical characterization of the aggregates and mineral admixtures used in the present work, while Table 4.5 shows their chemical characterization. It is observable that the natural aggregate, river sand, showed lower bulk and apparent density when compared to the other aggregates. This is due to their chemical composition.

**Table 4.4. Physical Characterization of the materials.**

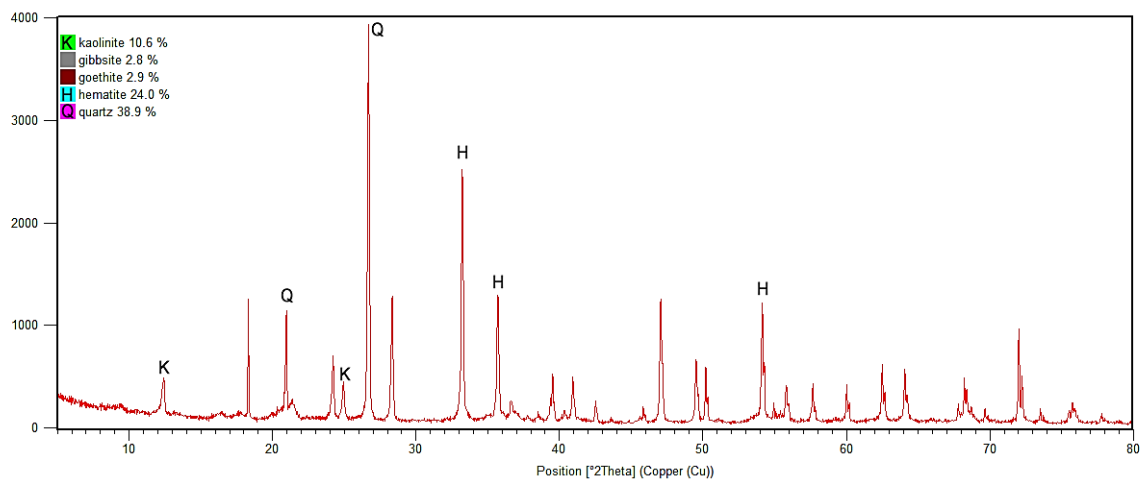
	<b>CP</b>	<b>P-IOT</b>	<b>IOT</b>	<b>CWM</b>	<b>River Sand</b>
<b>Bulk Density (kg/m<sup>3</sup>)</b>	4.26	3.88	3.37	2.88	2.69
<b>Apparent Density (kg/m<sup>3</sup>)</b>	0.56	1.13	1.42	1.70	1.54

**Table 4.5. Chemical characterisation of the Materials.**

	CP (%)	P-IOT (%)	IOT (%)	CWM (%)	River Sand (%)
<b>Fe<sub>2</sub>O<sub>3</sub></b>	92.2	66.6	49.0	0.2	4.7
<b>SiO<sub>2</sub></b>	0.0	12.6	40.1	3.1	59.6
<b>Al<sub>2</sub>O<sub>3</sub></b>	0.0	14.9	8.9	0.0	31.3
<b>K<sub>2</sub>O</b>	0.0	0.2	0.3	0.0	1.7
<b>TiO<sub>2</sub></b>	0.0	0.8	0.0	0.0	1.2
<b>SO<sub>3</sub></b>	0.5	0.3	0.1	1.0	1.0
<b>CaO</b>	4.3	0.0	0.0	63.8	0.5
<b>MnO</b>	2.5	0.3	0.1	0.0	0.1
<b>MgO</b>	0.0	3.6	0.4	31.8	0.0
<b>ZnO</b>	0.5	0.1	0.2	0.0	0.0
<b>Others</b>	0.1	0.0	0.0	0.1	0.1

Regarding the XRF, it is shown that river sand is mainly comprised by silicon and aluminium oxides; iron and silicon oxides are the predominant components of IOT, while calcium and magnesium oxides are the major constituents of CWM.

Fig. 4. shows the diffractogram of the IOT sample, with the main components highlighted in the curves: quartz, hematite and kaolinite. Therefore, the XRF and DRF analysis combined showed no deleterious or expansive substances in significant concentration, such as chlorites and sulphates (ABNT, 2009).



**Fig. 4.9. DRX diffractogram of IOT.**

As a result of the physical and chemical characterisation, the IOT is an inorganic, crystalline, innocuous and stable material, and thus a suitable aggregate for cement-based composites, according to the Brazilian standard NBR 7211 (ABNT, 2009). In addition, its fineness improves its usability as pigment and filler in the colour and base layers of the SCT.

#### **4.3.2. ENVIRONMENTAL FEASIBILITY**

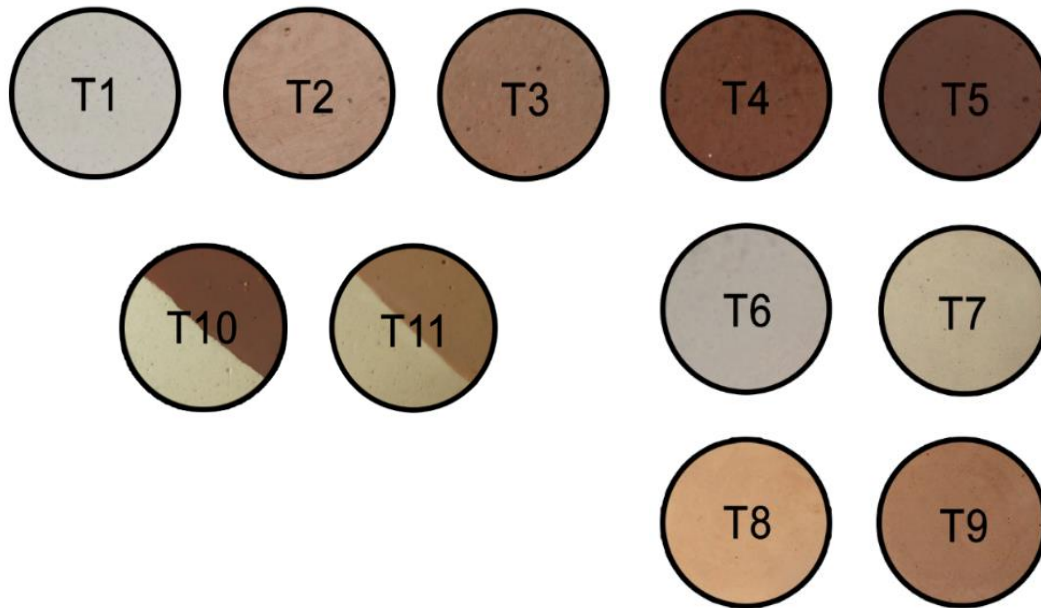
The leaching and dissolution analyses performed for the IOT confirm their environmental feasibility. The results for the dissolution parameters that exceeded the normative requirement are presented in Table 4.6. For the leaching test, the IOT presented all results within the standard limits. According to the prescriptions of standard NBR 10004 (ABNT, 2004c), the samples were classified as Class II A, non-dangerous and non-inert. Thus, it does not present hazardous characteristics such as corrosivity, reactivity, toxicity, pathogenicity or flammability (ABNT, 2004c).

**Table 4.6. Dissolution results for the raw IOT that exceeded the standard requirements**

<b>Chemical elements</b>	<b>Average concentration (mg/L)</b>	<b>Upper limit (mg/L)</b>
<b>Aluminum</b>	0.38	0,2
<b>Phenols</b>	0.53	NA
<b>Iron</b>	1.038	0.3

#### **4.3.4. FEASIBILITY AS PIGMENT**

The colour layer compositions, with IOT and conventional, are shown in Fig. 4.. The specimens showed a comprehensive variety of tones, sharp edges and a homogeneous surface – no cracks, burrs or flaws were observed. This appearance is in accordance with the visual inspection prescribed by standard (ABNT, 2013).

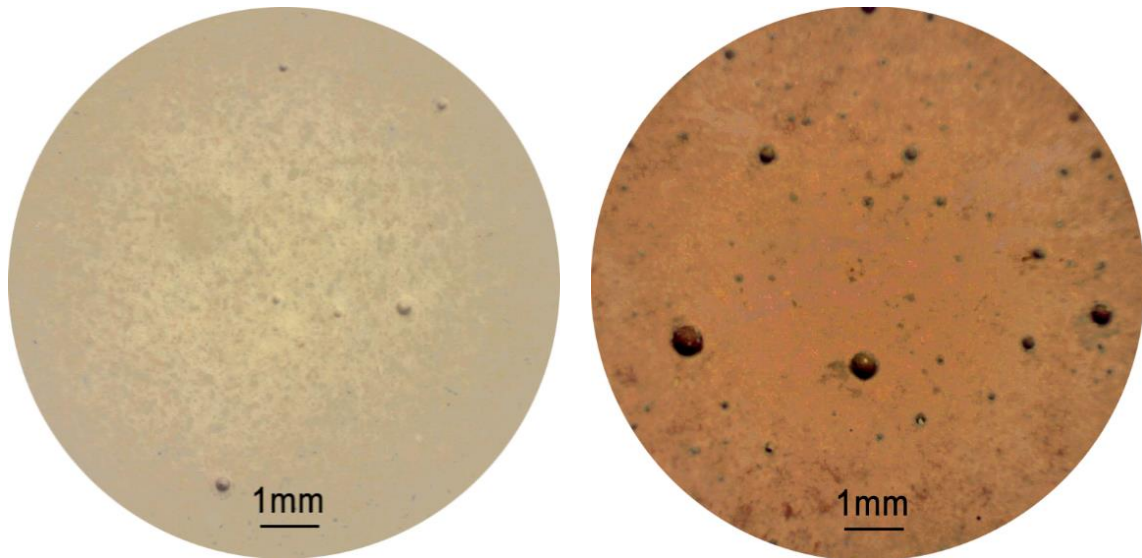


**Fig. 4.10. Colour layer mixtures: T1, T2 and T3 comprise 0%, 25% and 50% of IOT as aggregate; in T4 and T5 use CP as pigment, T6 and T7, IOT and T8 and T9, P-IOT; finally, T10 and T11 present double colours with CP and P-IOT respectively.**

In mixtures T1, T2 and T3, with increase in content of IOT as aggregate, a darker reddish/brownish tone was achieved (Fig. 4.a). In mixtures T6 and T7 (Fig. 4.b), in comparison with the same content of conventional colorant - T4 and T5 - the IOT showed slightly lower pigment properties. Mixtures with P-IOT, T8 and T9, shower better performance than those with the in natura IOT, but colours not as dark as the ones with CP.

These observations are related to the lower iron content in the IOT than in the CP. However, the lightness of tones be corrected, if wished, with an increase in IOT content, which is also more sustainable. The ones with double colours showed overall good contrast and did not present mixing, as show Fig. 4.c. Mixtures with IOT, as shown on the left of Fig. 4., presented less pores, with reduced size, in comparison with conventional ones, on Fig. 4.-right. This is a result of the filler effect of the IOT, as shown in its particle size distribution.





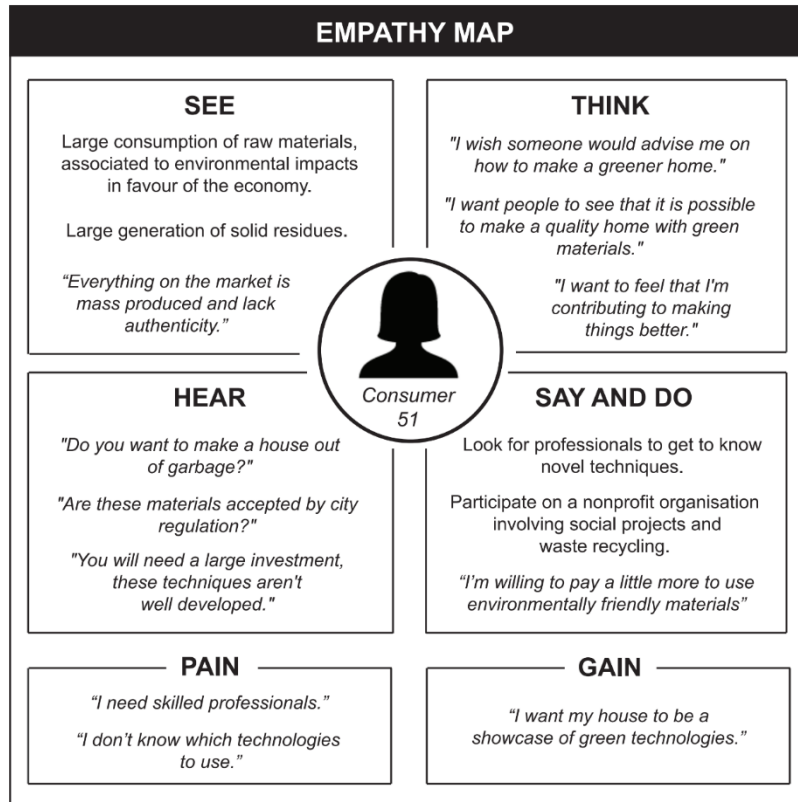
**Fig. 4.11. Surface of mixtures T5 (left) and T7 (right), magnification 10x.**

This result is in agreement with the works of Sant’Ana (2016) and Peixoto (2016), whose cement-based composites presented homogeneous colours and less pores than the conventional counterparts. In addition, the colour does not fade or stain, as observed in the work of Fontes, et al. (2016), whose coating mortars were subjected to the outdoors environment for over 3 years and showed no alteration on their surface quality.

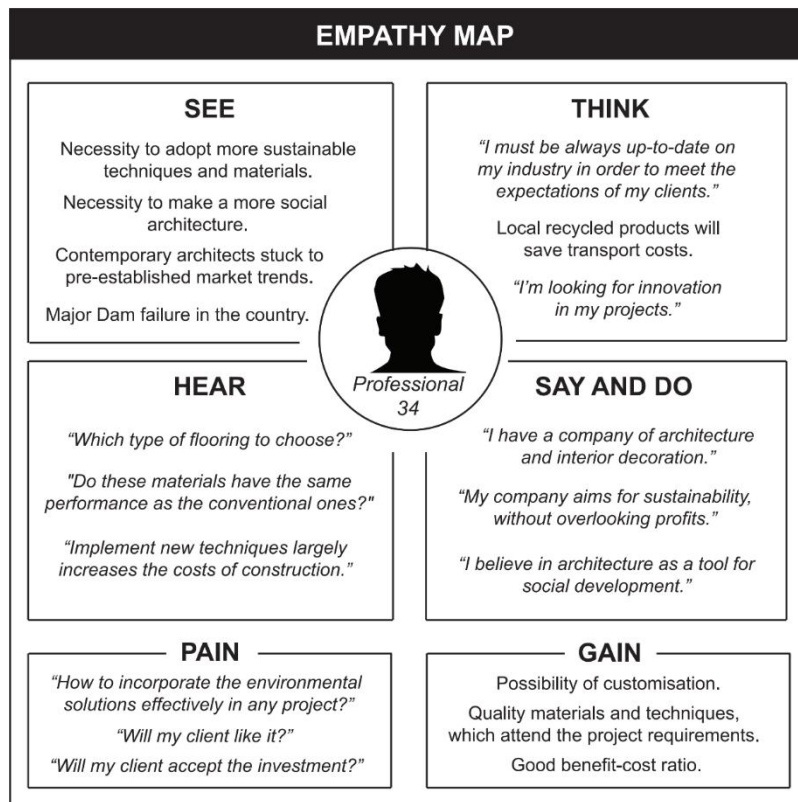
#### *4.3.4. VALUE ANALYSIS*

##### *4.3.4.1. EMPATHY MAP*

From the studies carried out, the design is presented as a fundamental tool in the conception of a link between product and user. Thus, Fig. 4. and Fig. 4. seek to trace a consumer profile for the SCT, by considering the perspective of customers, fulfilling their needs.



**Fig. 4.12. Empathy Map of a persona of a SCT consumer: end user.**



**Fig. 4.13. Empathy Map of a persona of a SCT consumer: interior designer.**

#### 4.3.4.2. ENVIRONMENTAL, SOCIAL AND ESTEEM ASSESSMENTS

In Brazil, the cement tile is responsible for creating new dimensions of the art, while acquiring national traits (WAMZER, 2011). Thus, it associated uniqueness, personal aspirations and experiences, which constituted an identity to the coating, instigating, therefore, memories and feelings in its users. Thus, this type of coating assumes an affective value able to provide well-being and pleasure when used. Furthermore, its craft process has survived in the midst of the mass-produced coatings industry.

As a result of the research, SCT prototype will be produced monochrome or coloured at up to five shades. Allied to the colours, the designs applied to the SCT will be traditional, like arabesques, floral and geometric shapes, inspired by elements that reflect local identity. Fig. 4.14 shows the surface design of the prototypes of the SCT, based on the value analysis.



**Fig. 4.14. Surface design of the prototypes of the SCT, based on the value analysis and colour palette**

The proposed SCT will also use sustainability as an intangible asset, by employing a residue in its composition. The IOT will be employed as aggregate and filler, increasing the physical-mechanical performance of the base layer. Furthermore, it will also be used as colorant in the composition of earthy tones on the colour side.

Regarding the shape, SCT will adopt the most common option, with dimensions of 200 x 200 mm and thickness of 25 mm, for ease of insertion of the market. According to the results of Empathy Map, the SCT has the potential to cover both consumers with high income, seeking for social and environmental expression, as the low-income ones, due to nostalgia aspects.

Thus, this type of coating assumes an affective value able to provide well-being when used. Its craft process has survived in the midst of the mass-produced industry, promoting labour opportunities for community craftsmen, and strengthening of the culture and local economies. In this sense, the SCT will not only contribute to the reduction of the environmental impact of IOT, but also minimize the costs with raw material, promote new business opportunities for artisans, meet the sustainability agenda of companies, and ultimately improve the quality of the built environment.

#### **4.4. CONCLUSION**

According to the physical, chemical and morphological analysis, iron ore tailings (IOT) are a stable fine material. The environmental tests resulted in a non-dangerous classification, meaning that IOT do not present hazardous characteristics such as corrosivity, reactivity, toxicity, pathogenicity or flammability. Therefore, it is technically and environmentally suitable to be used as replacement of conventional colorant and crushed marble in the colour layer; and as replacement of sand and/or filler in the base

layer. In this sense, IOT present a suitable alternative for the production of sustainable cement tiles, producing an aesthetically pleasing and potentially durable coating.

The design proposed for SCT meets the consumers' expectations regarding their desires for sustainability, ideology, social expression, nostalgia, among others. It does so by creating a product with local identity, incorporating residues in its manufacture, reducing the impacts of the disposal of IOT, promoting labour opportunities for artisans, strengthening local culture and overall improving the quality of the built environment.

Further investigation is required in order to evaluate the physical and mechanical properties of the Sustainable Cement Tile itself. However, this initial study concludes that the IOT is a technical, social and environmentally feasible alternative to the exploitation of natural resources in the production of cement-based composites. This reuse also contributes to the reduction of risks, and social and environmental impacts of tailings dams.

#### **4.5. ACKNOWLEDGMENTS**

We gratefully acknowledge the agencies FAPEMIG, CNPq, CAPES, UFOP and Fundação Gorceix for providing financial support. We are also grateful for the infrastructure and collaboration of the Research Group on Solid Wastes - RECICLOS - CNPq.

The authors would like to acknowledge the Nanolab Electronic Microscopy Laboratory, at the Redemat, UFOP; the Department of Ceramic and Glass Engineering from Universidade de Aveiro and the Materials Characterisation Laboratory, at CEFET, MG, Brazil, for providing the equipment and technical support for electron microscopy.

#### 4.6. REFERENCES

- ABCP. *Cement Tile Manual: public sidewalk*. Brazilian Association of Portland Cement. São Paulo. 2010.
- ABNT. *NBR 7217: Aggregates - Determination of Particle Size Distribution*. Brazilian Association of Technical Standards. Rio de Janeiro. 1987.
- ABNT. *NBR NM 53:2003: Coarse aggregate - Determination of the bulk specific gravity, apparent specific gravity and water absorption*. Brazilian Association of Technical Standards. Rio de Janeiro. 2003.
- ABNT. *NBR 10005: Procedure for obtention leaching extract of solid wastes*. Brazilian Association of Technical Standards. Rio de Janeiro. 2004a.
- ABNT. *NBR 10006: Procedure for obtention of solubilized extraction of solid wastes*. Brazilian Association of Technical Standards. Rio de Janeiro. 2004b.
- ABNT. *NBR 10004: Solid waste - Classification*. Brazilian Association of Technical Standards. Rio de Janeiro. 2004c.
- ABNT. *NBR NM 45:2006: Aggregates - Determination of the unit weight and air-void contents*. Brazilian Association of Technical Standards. Rio de Janeiro. 2006.
- ABNT. *NBR 7211: Aggregates - Specification*. Brazilian Association of Technical Standards. Rio de Janeiro. 2009.
- ABNT. *NBR 9457: Hydraulic tiles to paving - Specification and test methods*. Brazilian Association of Technical Standards. Rio de Janeiro. 2013.
- ACUÑA, S. T.; CASTRO, J. W.; JURISTO, N. A *HCI Technique for improving requirements elicitation*. n.12. ed. [S.l.]: Information and Software Technology, v. 54, 2012. 1357-1375 p.
- ANDRADE, L. C. R. *Characterization of iron mining tailings, in natura and segregated, for use as construction material*. Universidade Federal de Viçosa (PhD Thesis). [S.l.]. 2014.
- BASTOS, L. A. C. et al. *Using iron ore tailings from tailing dams as road material*. J. Mater. Civ. Eng., Ouro Preto, n. 10.1061/(ASCE)MT.1943-5533.0001613.04016102, 2016.
- BRUCE, S. M.; ROWE, G. H. *The influence of pigments on mix designs for block paving units*. Proc. 4th Int. Conf. Concrete Block Paving. [S.l.]: [s.n.]. 1992. p. 117-124.
- CATOIA, T. *High Performance Cement*. São Carlos. 2007.
- CHENG, Y. et al. *Test research on the effects of mechanochemically activated iron tailings on the compressive strength of concrete*. Construction and Building Materials, v. 118, p. 164-170, 2016.
- CREUSEN, M. E.; SCHOORMANS, J. P. *The different roles of product appearance in consumer choice*. Journal of product innovation management, v. 22, n. 1, p. 63-81, 2005.
- CSILLAG, J. M. *Value Analysis*. São Paulo: Atlas, 1995. 370p p.

DUAN, P. et al. *Fresh properties, compressive strength and microstructure of fly ash geopolymer paste blended with iron ore tailing under thermal cycle*. Construction and Building Materials, v. 118, p. 76-88.

EDRAKI, M. et al. *Designing mine tailings for better environmental, social and economic outcomes: a review of alternative approaches*. Journal of Cleaner Production, v. 84, p. 411-420, 1 December 2014.

ESTY, D.; WINSTON, A. *Green to gold: How smart companies use environmental strategy to innovate, create value, and build competitive advantage*. John Wiley & Sons, 2009.

FEAM. *Minas Gerais State Dam Inventory - Year 2014*. State Foundation of the Environment. [S.l.]. 2014.

FERREIRA, B. M. et al. *Designing Personas with Empathy Map*. Pittsburgh: International Conference on Software Engineering and Knowledge Engineering (SEKE 2015). 2015.

FIGUEIRÔA, S. *Mining in Brazil*. [S.l.]: Encyclopedia of the History of Science, Technology, and Medicine in Non-Western Cultures, 2014.

FONTES, W. C. et al. *Mortars for laying and coating produced with iron ore tailings from tailing dams*. Construction and Building Materials, v. 112, 2016.

FRANKS, D. M. et al. *Sustainable development principles for the disposal of mining and mineral processing wastes*. Resources Policy, v. 36, p. 114-122, 2011.

G1. *Tailings from dams reach areas up to 100km in MG*. G1, 2015. Disponível em: <<http://g1.globo.com/minas-gerais/noticia/2015/11/hidreletrica-100-km-e-afetada-por-lama-do-rompimento-de-barragens.html>>. Acesso em: 20 November 2015.

GONTIJO, L. A. *Complexity and interdisciplinarity in Interface Design*. Advanced Studies in Design: Transversality, v. 1, n. n°2, p. 79-90, 2008.

IBRAM. *Management for sustainability in mining - 20 years of history*. Brazilian Institute of Mining. Brasília, p. 168p. 2013.

IBRAM. *Information on the Mineral Economy of the State of Minas Gerais*. Brazilian Institute of Mining. Brasília, p. 14p. 2014.

IBRAM. *Information regarding the Brazilian mining economics*. Brazilian Institute of Mining. Brasília. 2015.

JORDAN, P. Inclusive design. W. S. GREEN; P. W. JORDAN (eds.). *Human factors in product design: Current practice and future trends*. London, p. 171-181, 1999.

KISSMETRICS, B. *How do colors affect purchases?*, 2010. Disponível em: <<https://blog.kissmetrics.com/colors-psychology/>>. Acesso em: 22 June 2016.

LEDOUX, J. *The emotional brain: The mysterious underpinnings of emotional life*. Simon and Schuster, 1998.

LEE, H. S.; LEE, J. Y.; YU, M. Y. *Influence of iron oxide pigments on the properties of concrete interlocking blocks*. Cement and Concrete Research, v. 33, n. 11, p. 1889-1896, 2003.

LUCKY IRON FISH. About us, 2016. Disponível em: <<http://www.luckyironfish.com/about-us>>. Acesso em: 22 June 2016.

MA, B. G. et al. *Utilization of iron tailings as substitute in autoclaved aerated concrete: physico-mechanical and microstructure of hydration products*. Journal of Cleaner Production, v. 127, p. 162-171, 2016.

MIRANDA, C. A.; CÂMARA, J. J. D. *Origin, Culture and Value Analysis in Design of products from plastic bottles*. 9° Brazilian Congress of Research and Development Design, 2010.

MORAES, D. *Design and Complexity*. Advanced Studies in Design: Transversality, v. 1, n. n°2, p. 7-23, 2008.

OBSERVATORY, B. I. *Smart Living - Advanced building materials*. European Union. 2014.

OSTERWALDER, A.; PIGNEUR, Y. *Business Model Generation*. Alta Books, 2013.

PAPPU, A.; SAXENA, M.; ASOLEKAR, S. R. *Solid wastes generation in India and their recycling potential in building materials*. Building and Environmental, v. 42, p. 2311-2320, 2007.

PASSUELLO, A. C. B. et al. *Aplicação da Avaliação do Ciclo de Vida na análise de impactos ambientais de materiais de construção inovadores: estudo de caso da pegada de carbono de clíques alternativos*. Ambiente Construído: revista da ASociação Nacional de Tecnologia do Ambiente Construído, Porto Alegre, RS, v. 14, n. n°4, p. 7-20, October/December 2014.

PEIXOTO, R. A. F. *Use of Iron Ore Tailings from Tailings Dams in Civil Construction*. Ouro Preto. 2016.

PEIXOTO, R. A. F.; BARROS, J. B.; OLIVEIRA, J. R. *Processo de extração de argila, sílica e minério de ferro através de concentração a seco*. Patent Pending - BR 10 2014 002076 4, 2014.

PEREIRA FILHO, R. R. *Value Analysis: Continuous Improvement Process*. São Paulo: Nobel, 1994. p. 186p.

PEREIRA, O. C.; BERNARDIN, A. M. *Ceramic colorant from untreated iron ore residue*. Journal of Hazardous Materials, v. 233-234, p. 103-111, 2012.

RIBEIRO, T.; SOUZA, P. *A Study on the use of personas as an usability evaluation method*. 16th International Conference on Enterprise Information Systems (ICEIS 2014), p. 168-175, 2014.

RUSCHEL, R. R.; ROSE, R. E. *The path of sustainable development: the memory of the first 5 years of the Von Martius Environmental Award*. AHK, Câmara Brasil Alemanha, 2005.

SANT'ANA FILHO, J. N. et al. *Technical and Environmental Feasibility of Interlocking Concrete Pavers with Iron Ore Tailings from Tailings Dams*. Journal of Materials in Civil Engineering, v. 29, n. 9, p. 04017104, 2016.

SHETTIMA, A. U. et al. *Evaluation of iron ore tailing as replacement for fine aggregate in concrete*. Construction and Building Materials, v. 120, p. 72-79, 2016.

TAVARES, P. H. C. P. *Obtenção de pigmentos de óxido de ferro a partir da lama gerada no beneficiamento de itabirito*. Federal University of Ouro Preto (PhD Thesis). Ouro Preto. 2012.



TSCHIMMEL, K. *Design Thinking as an effective Toolkit for Innovation*. Proceedings of the XXIII ISPIM, Barcelona, v. ISBN 978-952-265-243-0, n. Conference: Action for Innovation from Experience, 2012.

VARGAS, R. V. *Earned Value Analysis*. Brasport, n. n°6, p. 144p., 2013.

WAMZER, R. L. K. *The Cement Tile in interface with art and design in Mato Grosso*. Cuiabá. 2011.

WILLARD, B. *The Sustainability Advantage: Sever Business Case Benefits of a Triple Bottom Line*. New Society Publishers, n. Gabriola Island, 2002.

YELLISHETTY, M. et al. *Reuse of iron ore mineral wastes in civil engineering constructions: a case study - resources*. Consery, Recycl, v. 52, p. 1283-1289, 2008.

ZHAO, S.; FAN, J.; SUN, W. *Utilization of iron ore tailings as fine aggregate in ultra-high performance concrete*. Construction and Building Materials, v. 50, p. 540-548, 2016.

# Chapter 5

---

## Final considerations

Conclusions and recommendations for future research

## **5. FINAL CONSIDERATIONS**

### **5.1. CONCLUSIONS**

The results demonstrate that IOTs are suitable for use as alternative raw materials in the production of ceramic and hydraulic coating tiles.

Regarding the properties of interest for raw materials for the production of coating elements (physical, chemical and mineralogical) the following observations are listed: (I) the IOT particles have distinct forms, are predominantly fines and composed by iron, silicon and aluminum oxides; and no chlorine, vanadium or zirconium oxides were detected; (II) due to the practical absence of alkalis and oxides of alkaline-earth metals ( $\text{Na}_2\text{O}$ ,  $\text{K}_2\text{O}$ ,  $\text{CaO}$ ,  $\text{MgO}$ ), some difficulties of densification of the ceramic coatings can be anticipated; (III) on the other hand, the same absence of alkalis, particularly in sand fractions, suggests good durability performance in cement-based composites; and (IV) IOT sands showed the highest uniformity compared to raw IOT and IOT clay, both in particle size and shape, as in mineralogical and chemical composition.

The direct use of raw IOT in the production of ceramic tiles requires special care and needs to be further investigated since its coarser particles negatively affect plasticity, densification and iron-oxygen balance during firing. On the other hand, the IOT clay, obtained by the dry segregation process, can be used in the ceramic tile manufacturing process, presenting adequate plasticity and dry strength during processing, and developing mullite and glass when fired. Despite the shrinkage, which comes from the low compaction pressure used, the samples were not brittle or deformed. The ceramic obtained showed dark brown glow, compactness and of high mechanical strength.

All hydraulic tiles produced with the raw IOT and its fractions reached satisfactory physical and mechanical performance, however some particularities should be considered. Regarding the use of raw IOT as aggregate, the higher concentration of the material provides a differentiated hue to the product (brown-ocher). The higher specific surface area and its particle shape (tabular and angular with sharp edges) impairs the fluidity, requiring an increased water consumption. However, it did not impair the mechanical performance given its fineness and particle composition, favouring the composite hydration. The raw IOT, when fired and grinded, develops greater potential for pigmentation, and promising properties for use as a complementary cementing material in cement-based composites. This processing optimizes the material consumption once the addition of only 10% (by mass of cement) is possible to obtain cementitious composites with intense tones, in addition to being compact and mechanically resistant.

The IOT sand consisted of a predominantly siliceous material, with lower density (compared to raw IOT and IOT clay) and particle size and shape suitable for use as fine aggregates in cement-based composites. Such properties did not provided significant changes in the composite weight, but the better particle packing contributed to the better mechanical performance.

The IOT clay (rich in iron, silicon and aluminum), when fired, developed great potential for pigmentation, but presented the worst mechanical performance when used as mineral admixture in the composites. However, the flexural tensile strength of all tiles was higher than the minimum normative requirement (3.5 MPa).

Regarding the intangible value potential, the tiles produced with IOT are expected to meet consumers' expectations regarding their concern with sustainability, ideology and social expression. In addition, aiming at sustainability and clean production, there is enormous potential for the study and effective application of iron ore tailings in ceramic and hydraulic tiles. In this sense, this points to opportunities for job creation, greater competitiveness in the "green market" (meeting consumers' expectations); and also promotes the maintenance of the quality of the environment.

## **5.2. RECOMMENDATIONS FOR FUTURE RESEARCH**

Further investigations are required to evaluate the physical and mechanical properties of ceramic tiles and hydraulic tiles, so it is recommended to evaluate the impact resistance, cracking, staining, etching, freezing, among other properties.

The results achieved contribute to and encourage the development of these products and new technological materials using IOT. Therefore, it is also recommended to evaluate the use of IOT in the production of other types of constructive, ceramic and hydraulic elements, considering the consumer market, its function, elaboration of its design, properties of interest, composition and dosage, production conditions, among other aspects.